Final Master Thesis

Double Master's Degree in Industrial and Nuclear Engineering

Optimization of patient dose monitoring in fluoroscopically-guided interventional procedures

THESIS

Author: Álvaro Merino Canete
Director: María Amor Duch

Data: March 2018

Escola Tècnica Superior
d'Enginyeria Industrial de Barcelona

You must be the change you wish to see in the World

Mahatma Gandhi

ACKNOWLEDGMENTS

Este proyecto significa para mí la culminación de mis años universitarios, por este motivo, antes de exponerlo me gustaría dedicar unas palabras a todas aquellas personas que me han ayudado, con las que he compartido bueno y malos momentos y de las que he aprendido durante todos mis años universitarios.

En primer lugar, quiero dar las gracias a mis padres por dármelo absolutamente todo y gracias a los cuales he cumplido un sueño, nunca les estaré lo suficientemente agradecido; a mi hermano Eduardo por su apoyo incondicional, por levantarme los ánimos cuando flaqueaban las fuerzas y por mostrarme su filosofía; y a mis abuelos por su confianza ciega, incluso cuando nos las tenía todas conmigo.

Tampoco me olvido de quien, a pesar de las dificultades, siempre ha estado a mi lado y me ha apoyado de forma incansable incluso en los peores días. Capaz de comprender cuando necesitaba espacio y cuando apoyo, así como proporcionármelos, siempre le estaré agradecido.

También quiero agradecer a todos mis amigos de Madrid: Guille, Mayte, Nuria, Chechu, Sandra, Alicia, Pablo, Steven, María y a todos los demás que, aunque por la distancia no tengamos tanto contacto, siempre me han animado.

De mis primeros años en la ETSII tengo mucho que agradecer a los “Industrialitos” por hacerme el primer año mucho más llevadero de lo que a priori yo esperaba y de los cursos sucesivos es necesario mencionar a aquellos con los que he compartido silla día a día y un trabajo tras otro como Refoyo y Tere.

De mi etapa en el Máster de Ingeniería Industrial en la ETSEIB hay mucha gente con la que he trabajado y de la que he aprendido multitud de cosas y son tantas personas que aquí solo pueden estar recogidos algunos. Gracias al grupo de “Padelmania” por acogerme como uno más desde el primer día; gracias al grupo de “Blancanieves y los siete enanitos” especialmente a Esther y Miquel por trabajar como un verdadero equipo; gracias a los chicos de Girona por hacerme sentir como en casa y gracias a Cristian, Ana y David por hacerme más llevaderos estos años.

A mis compañeros del Máster de Ingeniería Nuclear les deseo lo mejor y les mando mis más sinceros agradecimientos a Alfonso, Eduard, Bartek, Miriam y Nathan, así como a todos los integrantes de “Nuclear Party”, “Spanish Mafia” y a mis predecesores del doble máster que me marcaron el camino, mención especial para Soriano.

Dentro del apartado nuclear, quiero hacer un aparte para mi querida Laura Gómez. Una persona con la que no sólo he compartido proyectos en la Universidad sino prácticamente toda la vida fuera durante el último año de máster, una persona que, en poco tiempo, se ha convertido en una de las personas más importantes de mi vida y con la que espero volverme a cruzar a nivel profesional en el futuro.

Para terminar con los agradecimientos a mis compañeros de Universidad, hay dos personas que se merecen una mención individual por lo que han significado para mí dentro de las clases, pero sobre todo por lo que han sido, son y serán fuera de ellas. Por un lado, David Arias, quien tuvo que aguantarme día tras día en Madrid y con quien estudiar, incluso las peores asignaturas, era algo que esperaba con ganas. Por otro lado, Arnau Prats, con quien he compartido mis años en Barcelona desde que salía el sol hasta que se ponía. De la mano de ambos he terminado el Grado y el Doble Máster, tal

y como se esperaba de nosotros, ambos se merecen el mayor de mis agradecimientos y les deseo lo mejor porque sé que se lo merecen.

A mis profesores, tanto a los que soy afín como a los que no, les quiero agradecer todo lo aprendido, en concreto a José María Cabanellas, mi profesor de dibujo y director del TFG; a Carlos Molpeceres, mi profesor de electromagnetismo; y a Eva Gallardo, mi profesora de recursos humanos, por hacerme sacar lo mejor de mí en cada momento y por enseñarme cosas que transcienden a la ingeniería.

Por último, quiero agradecer a Lluis Batet por facilitarme las cosas en el Doble Máster; a Mercè Ginjaume y María Amor por darme la oportunidad de trabajar en este proyecto y confiar en mí; a Sara Principi y María Rodríguez por aguantarme durante las prácticas y ayudarme siempre que lo necesitaba, incluso cuando estaban ocupadas; al INTE en general por su calurosa acogida y al CSN por su financiación para desarrollar este proyecto.

ABSTRACT

This project was developed as part of the European MEDIRAD project in the initial phase of Work package 2, Subtask 2.2.2 Real-time patient dose monitoring in fluoroscopically-guided interventional and PODIUM project. During this project, a program called MC-GPU, what is a Monte Carlo simulation code that can simulate real interventional radiological procedures conditions, was used.

The main objectives fulfilled in this project are the MC-GPU code improvement, the validation and verification of the MC-GPU results and the elaboration of a MC-GPU manual for beginner users.

The MC-GPU materials generator was updated due to a 3 %variation of the photoelectric MFPs between the materials of the versions of PENELOPE 2006 and 2014. The update was completed successfully obtaining more accurate material data files than the originals.

The computational validation phase consists of comparing the MC-GPU dose results with the obtained ones with a standard Monte Carlo simulation code, PENELOPE/penEasy. In most cases, the main MC-GPU results vary around 1 % with respect to those obtained with PENELOPE/penEasy but the simulation times are between 300 and 500 times shorter.

At the end of the computational validation, a simple comparison was made with experimental measures. This first comparison between the experimental measurements made in the Hospital and the MC-GPU simulations showed good results, giving rise to the beginning of the validation phase with real measurements. In this phase, more complex distributions in terms of materials and rotations must be used.
In the medium-long term, the validation of the new MC-GPU features as the presence of the operator, the influence of shielding materials and the us of conversion factors will be the lines of future work.

UNESCO codes: 210115, 220212, 320111, 320112, 320401, 330723

Keywords: MEDIRAD; Monte Carlo Simulation; MC-GPU; PENELOPE; PENELOPE/penEasy; CUDA; voxelized geometry; interventional radiology; patient dose monitoring; dose distribution; X-rays; validation.

1. CONTENTS

2. GLOSSARY

Following many terms used in this master thesis are shown, and all of them are explained in the context of this project.

BEAM: an X-ray beam is a stream of photons which are moving at the speed of light.

CUDA: a parallel computing platform and programming model created by NVIDIA. It allows software developers and software engineers to use a CUDA-enabled graphics processing unit (GPU) for general purpose processing.

DETECTOR: detector and image intensifier are equally used along this project. It is a rectangular plane in which the collimated beam is projected.

DOSE (TALLY): absorbed dose is a physical dose quantity representing the mean energy imparted to matter per unit mass by ionizing radiation. This quantity may be referred to materials or a voxel. It depends on the material and particle energy.

ENERGY DEPOSITION (TALLY): is the energy absorbed by a material or a voxel. This quantity depends on the material and particle energy.

HISTORIES: In Monte Carlo simulation of radiation transport, the history (track) of a particle is viewed as a random sequence of free flights that end with an interaction event where the particle changes its direction of movement, loses energy and, occasionally, produces secondary particles.

MASS: the masses of each material are calculated by knowing the number of voxels that make up each material, the voxel volume and the density of the material.

MASS ATTENUATION COEFFICIENT: mass attenuation coefficients of the volume of a material characterizes how easily it can be penetrated by a beam of particles. In addition, mass attenuation coefficients can be defined for electromagnetic radiation (such as X-rays).

MC-GPU: is a Monte Carlo simulation code that can generate synthetic radiographic images and computed tomography scans of realistic models of the human anatomy using the computational power of commodity Graphics Processing Unit cards. The code implements a massively multi-threaded Monte Carlo simulation algorithm for the transport of x rays in a voxelized geometry. The x ray interaction models and material properties have been adapted from PENELOPE.

MEAN FREE PATH: is the average distance travelled by a particle between successive interactions which modify its direction or energy or other particle properties.

MONTE CARLO SIMULATIONS: of a given experimental arrangement consists of the numerical generation of random histories. To simulate these histories, an “interaction model" is need. i.e., a set of differential cross sections (DCS) for the relevant interaction mechanisms. The DCSs determine the probability distribution functions (PDF) of the random variables that characterise a track; 1) free path between successive interaction events, 2) type of interaction taking place and 3) energy loss and angular defection in a particular event (and initial state of emitted secondary particles, if any). Once these PDFs are known, random histories can be generated by using appropriate sampling methods. If the number of generated histories is large enough, quantitative information on the transport process may be obtained by simply averaging over the simulated histories.

OPERATOR: in the context of this thesis, the word operator refers to the sanitary personal, physicians and nurses, who work in operating rooms in which interventional radiology procedures are developed.

PENEASY: is a general-purpose main programme for PENELOPE. It provides users with a set of source models, tallies and variance reduction techniques that are invoked from a structured code. Users need only to input all the required information through a simple configuration file and through the usual PENELOPE data files (geometry and materials).

PENELOPE: is a computer code system which performs Monte Carlo simulation of coupled electron-photon transport in complex geometries and arbitrary materials for a wide energy range, from a few hundred eV to about 1 GeV. Photon transport is simulated by means of the standard, detailed simulation scheme. It is freely distributed by the OECD Nuclear Energy Agency Data Bank (http://www.nea.fr). The core of the system is a set of Fortran subroutines that deal with the intricacies of the transport process.

PHANTOM: Computational human phantoms are models of the human body used in computerized analysis. The radiological science community has developed and applied these anthropomorphic models for ionizing radiation dosimetry studies. This term is also used for all the voxelized geometries that are not anthropomorphic.

PMMA: Poly methyl methacrylate, also known as acrylic or acrylic glass as well as by the trade names Crylux, Plexiglas, Acrylite, Lucite, and Perspex, is a transparent thermoplastic often used in sheet form as a lightweight or shatter-resistant alternative to glass.

QUALITY OF X-RAY BEAMS: characterization of x-ray beams in terms of its ability to penetrate materials of known composition.

REGION OF INTEREST: a user determined part of a phantom, which contains information of interest.

SPECTRUM: an energy spectrum of a particle is the number of particles or intensity of a particle beam as a function of particle energy.

STANDARD DEVIATION: A measure of the variability of a series of measurements about the mean.

VOXEL: a voxel represents a value on a regular grid in three-dimensional space. As with pixels in a bitmap, voxels themselves do not typically have their position (their coordinates) explicitly encoded along with their values. Each voxel is a rectangular prism with a homogeneous material composition.

VOXELIZED GEOMETRY: A voxelized geometry is a geometry model in which the object to be simulated is described in terms of a (usually large) collection of (usually small) voxels.

X-RAY: or X-radiation is a form of electromagnetic radiation. Most X-rays have a wavelength ranging from 0.01 to 10 nm and energies in the range of 100 eV to 100 keV. The X-radiation used in conventional and digital X-ray equipment is characterized by low energy photons, lower than 150 keV.

2.1 SYMBOLS AND UNITS

Symbol	Quantity	Unit	Unit Name	Equivalence
E	Energy	J	Jule	1 $kg \cdot m^2 / s^2$
	Energy	eV	Electron volt	$1.602 \cdot 10^{-19}$ J
D	Absorbed dose	Gy	Gray	1 J/kg
	Absorbed dose	eV/g	-	-
V	Voltage	kVp	Volts	-
s	Standard deviation or sigma	various	-	-
μ/ρ	Mass attenuation coefficient	cm^2/g	-	-
ρ	Density	g/cm^3	-	-
H	Equivalent dose	Sv	Sievert	1 J/kg

Table 1: Symbols and units

2.2 ABBREVIATIONS AND ACRONYMS

Abbreviation / Acronym	Meaning
AP	Anterior – Posterior projection
CAUD	Caudal projection
CRAN	Cranial projection
CT	Computed Tomography
ICRP	International Commission on Radiological Protection
IC	Interventional Cardiology
IR	Interventional Radiology
LAO	Left Anterior Oblique projection
MC-GPU	Monte Carlo power on Graphics Processing Unit
MFP	Mean Free Path
PA	Posterior – Anterior projection
PMMA	Polymethylmethacrylate
RAO	Right Anterior Oblique projection
ROI	Region Of Interest
TRL	Technology Readiness Level
WP	Work Package

Table 2: Abbreviations and acronyms

3. PREFACE

The project explained in this thesis is encompassed in a European project named MEDIRAD[1][2][3]. The **Horizon 2020 MEDIRAD** project on implications of medical low dose radiation exposure aims to enhance the scientific bases and clinical practice of radiation protection in the medical field and thereby addresses the need to understand and evaluate the health effects of low dose ionising radiation exposure from diagnostic and therapeutic imaging and from off-target effects in radiotherapy.

MEDIRAD pursues three major operational objectives:

- First, it will improve organ dose estimation and registration to inform clinical practice, optimise doses, set recommendations and provide adequate dosimetry for clinical-epidemiological studies of effects of medical radiation.
- Second, it aims to evaluate and understand the effects of medical exposures, focusing on the two major endpoints of public health relevance: cardiovascular effects of low to moderate doses of radiation from radiotherapy in breast cancer treatment incl. understanding of mechanisms; and long-term effects on cancer risk of low doses from CT in children.
- Third, it will develop science-based consensus policy recommendations for the effective protection of patients, workers and the general public.

INTE-UPC work is included in one of the six work packages, the **WP2**. The main objective of this work package is to develop novel methodologies to reduce patient and staff radiation dose and potential radiation-related risks of cancer and non-cancer outcomes from chest imaging while maintaining or improving diagnostic information from existing and emerging techniques. Work will focus on state-of-the-art CT, fluoroscopically-guided interventional procedures and hybrid systems. Detailed dosimetry data will be produced, which will be valuable for optimising RP of patients from high-dose diagnostic and interventional procedures, as well as for input to epidemiological RP research studies and development of models of radiation induced risk.

To be more precise, the subtask in which INTE-UPC is working is the **Subtask 2.2.2 Real-time patient dose monitoring in fluoroscopically-guided interventional procedures**. Following a brief explanation of this subtasks:

A state-of-the-art method has been described for real time patient dose monitoring for interventional cardiology procedures based on the freely available accelerated Monte Carlo (MC) code, MC-GPU. The system uses two independent computer codes, for the simulation of the X-ray transport including detailed voxelized phantoms and for the virtual X-ray control console where the operator manually introduces the relevant acquisition parameters. The programme has not yet been benchmarked against standard simulation codes such as EGSnrc, MCNP or PENELOPE, nor tested in the clinical environment. The objective of this Subtask will be to validate and improve MC-GPU to determine skin dose distribution for specific realistic clinical set-up. First the X-ray transport will be validated by simulating a realistic clinical set-up with PENELOPE and MCNP MC codes. Corresponding measurements will be carried out using a Rando anthropomorphic phantom and passive dosimeters in an interventional cardiology suite in Belgium. Validation will be performed first for single projections and then for a complete treatment. In a second step the virtual X-ray source console module will be reviewed and improved, so that acquisition conditions can be read automatically from the console. The prototype performance will further be assessed in patients undergoing interventional procedures.

[1] Official webpage: http://www.medirad-project.eu/#about-medirad
[2] Brief explanation on: http://www.eibir.org/projects/h2020-projects/medirad/
[3] Project members on: https://cordis.europa.eu/project/rcn/211042_en.html

Clinical tests will be performed at least in two hospitals (Barcelona and Belgium). Systems able to accurately monitor the dose to the patient in real time are the state-of-the-art solutions to the issue of minimizing the likelihood of radiogenic skin injuries and estimating organ doses from fluoroscopically-guided procedures. The real time dose monitoring system developed in this Subtask will fulfil the requests of recent EU Council Directive 2013/59/EURATOM Basic Safety Standards[4], Articles 60 and Article 63.

The extract of this Council Directive that concerns in this project and thesis is the following:

> *THE COUNCIL OF THE EUROPEAN UNION,*
>
> *Having regard to the Treaty establishing the European Atomic Energy Community, and in particular Articles 31 and 32 thereof,*
>
> *Having regard to the proposal from the European Commission, drawn up after having obtained the opinion of a group of persons appointed by the Scientific and Technical Committee from among scientific experts in the Member States, and after having consulted the European Economic and Social Committee,*
>
> *Having regard to the opinion of the European Parliament,*
>
> *Having regard to the opinion of the European Economic and Social Committee,*
>
> *Whereas:*
>
> *(28) In the medical area, important technological and scientific developments have led to a notable increase in the exposure of patients. In this respect, this Directive should emphasise the need for justification of medical exposure, including the exposure of asymptomatic individuals and should strengthen the requirements concerning information to be provided to patients, the recording and reporting of doses from medical procedures, the use of diagnostic reference levels and the availability of dose-indicating devices.*

Also, the mentioned article number 60 refers to Equipment and the number 63 refers to accidental and unintended exposures.

To summarize, the project explained in this thesis is part of the Horizon 2020 MERIRAD project in the framework of WP 2, Subtask 2.2.2 Real-time patient dose monitoring in fluoroscopically-guided interventional.

Additionally, another European project named PODIUM[5] has begun concurrently to MEDIRAD project. The acronym PODIUM stands for *Personal Online Dosimetry Using Computational Methods*, which main objective is to improve personal dosimetry by using an innovative tool based on an on-line application. The validation and verification of results and user manual developed during this project will be also used in this new project.

[4] https://ec.europa.eu/energy/sites/ener/files/documents/CELEX-32013L0059-EN-TXT.pdf
[5] Some additional information on: http://www.irrs.eu/documents/IRRS2017Programme.pdf

3.1 ORIGIN OF PROJECT

Optimization of patient dose monitoring in fluoroscopically-guided interventional procedures project takes place at the beginning of the work requested to INTE-UPC. It is its first task.

Before using the MC-GPU code for real-time monitoring, is necessary validate the code in static situations. The validation and verification of the results is done in ascending order of difficulty, starting with the most basic modules of the programme and ending with the most realistic simulations.

3.2 MOTIVATION

The main purpose of this project is to explain in detail the validation and verification process of the MC-GPU code.

The motivation and choice of this topic responds to two different circumstances: one institutional and other personal.

First, the ultimate goal of the subtask 2.2.2 of MEDIRAD and PODIUM projects is the obtaining of a software capable of monitor the dose received by patients and medical personnel in fluoroscopically-guided interventional procedures. The motivation of this WP is fulfilling the European regulation of dose monitoring, in order to protect workers and general public.

Second, the personal motivation to get involved in this project is the remarkable social character of it. The last beneficiaries of the project will be the patient who must pass through this kind of procedures. The development of a final commercial product is also one of the main attractive of the project.

3.3 STATE-OF-THE-ART

As previously mentioned, this project is the first work developed in the INTE-UPC as part of MEDIRAD project and it starts few months after the beginning of MEDIRAD project.

At this point, the programme is completely written and some test had been already made. The documentation about the main features of the code and how to compile the codes were provided by the coder. A folder full of materials files usually used in this kind of simulations and some spectra were also provided. Last modifications of the codes are dated in 2014 as the provided documentation. Few papers in which the code and test made are published during the last years before the project.

About the MEDIRAD project, the budget, objectives, scope and WPs are clearly defined.

4. INTRODUCTION

Previous section of this thesis provides a global picture in which this project and this thesis are framed. In this part, the main challenges and objectives of the project are highlighted as well as an overall view of the project.

The project has been developed at the Institut de Tècniques Energètiques of the Universitat Politècnica de Catalunya with partial funding support of the Consejo de Seguridad Nuclear, the Spanish Nuclear Regulatory Body.

The project includes Monte Carlo simulations of different scenarios carried out by two different programmes, MC-GPU and PENELOPE/penEasy, the comparative between them and with experimental data measured in Vall d'Hebron Hospital of Barcelona.

This project may be considered as a concept validation of the MC-GPU programme. For this reason, this project can be included between TRL 3, experimental proof of concept, and TRL 4, technological validity in a laboratory.

4.1 PROJECT OBJECTIVES

The aforementioned code was developed few years ago, and some test were developed with it. However, a most exhaustive use of it must be done, mainly validation the results of the code with already tests codes as PENELOPE/penEasy and with experimental measurements.

Within the before explained framework, this thesis has the following main aims:

1. Analyse, understand, improve and update to the extent possible the MC-GPU code and all the complementary codes and files, in order to obtain more realistic and accurate simulations.

2. Validation and verification of the MC-GPU and MC-GPU Beta, an extended version not yet publicly released, results. A comparative of simulations run by them and with PNELOPE/penEasy must be included. Moreover, a comparative of the results obtained by simulations with experimental data measured in a laboratory. This is the main objective of the project.

3. Elaboration of a MC-GPU user manual during the first months of this project to allow other users to use the programme and future personnel who will be involved in the MEDIRAD and PODIUM projects. This handbook must include information complementary to the code, explanation of the code and how to use it.

4.2 SCOPE OF THE PROJECT

The European project in which this project is included will last 4 years, but the duration of this project is shorter. This project and the members in charge of it are the responsible of the validation and verification of the results, that is, the pre-project of what will be a commercial product.

The scope of this project and thesis finishes in the experimental data validation phase. At this stage measured results obtained in an operating room will be compared with computational results obtained in the MC-GPU simulations.

4.3 CONTEXTUALIZATION

As it is explained in previous sections, the project is based on the validation of a code which simulates real fluoroscopically-guided interventional procedures.

An interventional radiological (IR) procedure is any procedure using radiological imaging equipment in order to guide a therapeutic/invasive procedure on a patient. Examples of such procedures include angiography, angioplasty, embolization, biopsy and drainage, dilations and stent placements. Fluoroscopy is predominantly used, which is a way of working in real time. Currently almost exclusively fluoroscopy is used.

Interventional procedures are complex and generally involve the use of long fluoroscopy times. Consequently, there is a potential for high radiation doses to patients and staff as compared to other X-ray examinations.

Because fluoroscopy involves the use of X-rays, an ionizing radiation, fluoroscopic procedures pose a potential for increasing the patient's risk of radiation-induced cancer. Radiation doses to the patient depend on the size of the patient as well as duration of the procedure. Exposure times vary depending on the procedure being performed. Because of the long duration of some procedures, additionally to the cancer risk and other stochastic radiation effects, deterministic radiation effects have also been observed ranging from mild erythema, equivalent of a sun burn, to more serious burns.

While deterministic radiation effects are a possibility, radiation burns are not typical of standard fluoroscopic procedures. Most procedures sufficiently long in duration to produce radiation burns are part of necessary life-saving operations.

Moreover, some procedures are very complex and they can lead to relatively high doses to the medical staff, henceforth the operators, who stand close to the primary radiation field if they do not protect themselves with the appropriate shield. Moreover, as the procedures performed in IC/IR require the interventional cardiologists and radiologists stand close to the patient, the patient represents the main source of scattered radiation.
From a radiation protection point of view, under-couch (x-ray tube) operation is preferable as it reduces the amount of scattered radiation on operators.

Following figure shows a real interventional radiological procedure using a radiological imaging equipment.

Figure 1: Photo of a IC/IR procedure using Phillips Allura

Next figure shows a real radiological imaging equipment to provide a better idea of the equipment and environment which are simulated during this project.

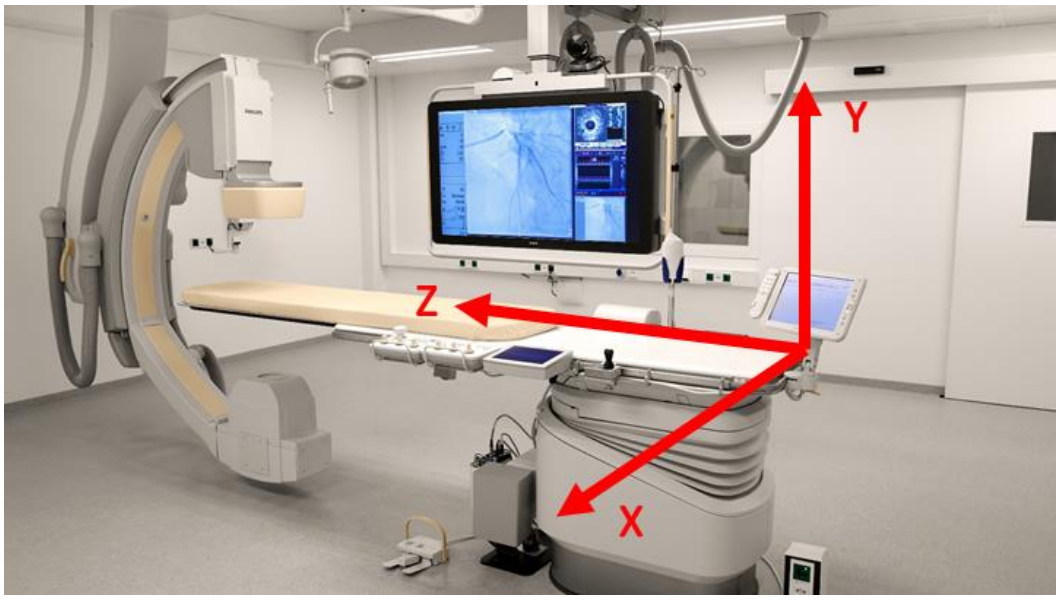

Figure 2: Real radiological imaging equipment (Philips Allura)

The photo is taken from the side where the medical staff usually works. The picture shows the couch where the patient lies down, the screen in which the image appears and the machine C-arm, which has the X-ray source at the bottom and the image intensifier (detector) at the top. This image also includes the coordinate axis employed in the MC-GPU simulations.

All information related to MC-GPU simulation may be consulted in the MC-GPU User Manual at the end of this thesis.

4.4 TECHNOLOGY CHALLENGES

In this section, two different topics are explained. On the one hand, the technologies necessaries in which this project is based on and its state of art. On the other hand, possible activities with which the project may transfer technology bidirectionally.

The code in which the software is based on is written in CUDA language CUDA 5.0. MC-GPU was developed using the CUDA programming model from NVIDIA to achieve maximum performance on NVIDIA GPUs. The code can also be compiled with a standard C compiler to be executed in a regular CPU.

However, the code that creates the material files necessary in the simulations is written in Fortran, the same programming language in which PENELOPE and penEasy are written.

At the beginning of the project the MC-GPU software and the material generator code were completed but their last modifications were made in 2014.

The PENELOPE/penEasy [4] and PENELOPE [5] version employed in this project are the latest version published by their authors.

Complementary to these four codes, some other programmes are necessary to analyse the results and do the comparatives:

- MATLAB[6] : some scripts to read the data obtained in MC-GPU and PENELOPE/penEasy simulations need to be run on it.
- IMAGEJ[7] : programme used to visualize the raw binary files, which is the format in what the code reports the results. It is mainly used to obtain images but also to obtain some numerical results.
- GNUPLOT[8] : this programme is used to visualize the tallies obtained in penEasy.
- XCOMP5r[9] : this software is employed to create the X-ray spectrum files.

Most of these programmes are public and free for student and research personnel.
All are tested programmes and belong to different users' communities.

Although this project is based on code simulations and all stuff related to the computational framework, experimental data is also needed, thus and for these activities dosimeters and real x-ray tubes are need. In this case, the relation between the discipline of medicine and computing is clear.

Regarding to the possible activities related to this project, it is important to point out that this programme is focused on interventional procedures in which X-rays are employed. Nevertheless, this programme and technology have two possible paths:

- The objective which this programme was created for, the real on-time monitoring of patient and medicine personnel during the interventional procedures taken place in an operating room using tracking cameras. In this case, the relation is between the software (code) and hardware (cameras) disciplines.
- Parallel to the main path, the technology could be transferred to other activities (mainly medical procedures) in which radiation is used. The programme (and materials) would need some modifications but it could be employed.

[6] Source: https://es.mathworks.com/products/matlab.html
[7] Source (free): https://imagej.nih.gov/ij/
[8] Source (free): http://www.gnuplot.info/download.html
[9] This is an old DOS programme and very difficult to find, it is in possession of the INTE personnel.

4.5 BUSINESS AND COMMERCIAL OPPORTUNITIES

The ultimate aim of the European projects is the developing of a commercial product which monitor the doses received by patients and medical personnel in interventional procedures.

The idea for the final product is a software connected to tracking cameras to track the personal and to the x-ray tube to know the energy and time of the pulses generated.

At the moment this thesis is written, there is not a commercial product which provides the required information (doses and maximum dose location) in a reasonable time using Monte Carlo methods, but there are ones that use other methods. These estimations are required by physicians for two different reasons:

- Patient doses: in patients who undergo lot of procedures or lot of projections of different energies is important to know the received dose to avoid deterministic effects, mainly on the skin where the maximum dose is usually located.
- Personnel doses: personnel who usually work with radiation equipment must wear passive dosimeters to monitor the received dose. The problem is that the passive dosimeters do not give a rapid measure and there exist some limitations on their use.

Moreover, the directive[10] about the dose received is changing and the collection of this information will not be optional but compulsory.

The interest shown by the medical personnel who has been consulted by the project member joined to the lack of commercial products with the mentioned characteristics creates a commercial opportunity with possible profitable results in medium to long term.

[10] EU Council Directive 2013/59/EURATOM Basic Safety Standards

5. METHODOLOGY

The methodology followed to meet the main objectives was to update the codes and perform the validation phase of the code with one already known. This validation phase consisted on simulate different scenarios, different spectra, geometry and materials with both programmes.

To achieve this, the MC-GPU, the PENELOPE/penEasy and a cluster of computers have been used. These are explained below.

5.1 MC-GPU

Project first stage is the understanding of the code and all the complementary information and executables to run simulations properly. In this section, the main concepts of the code are explained to understand the following steps of the project.

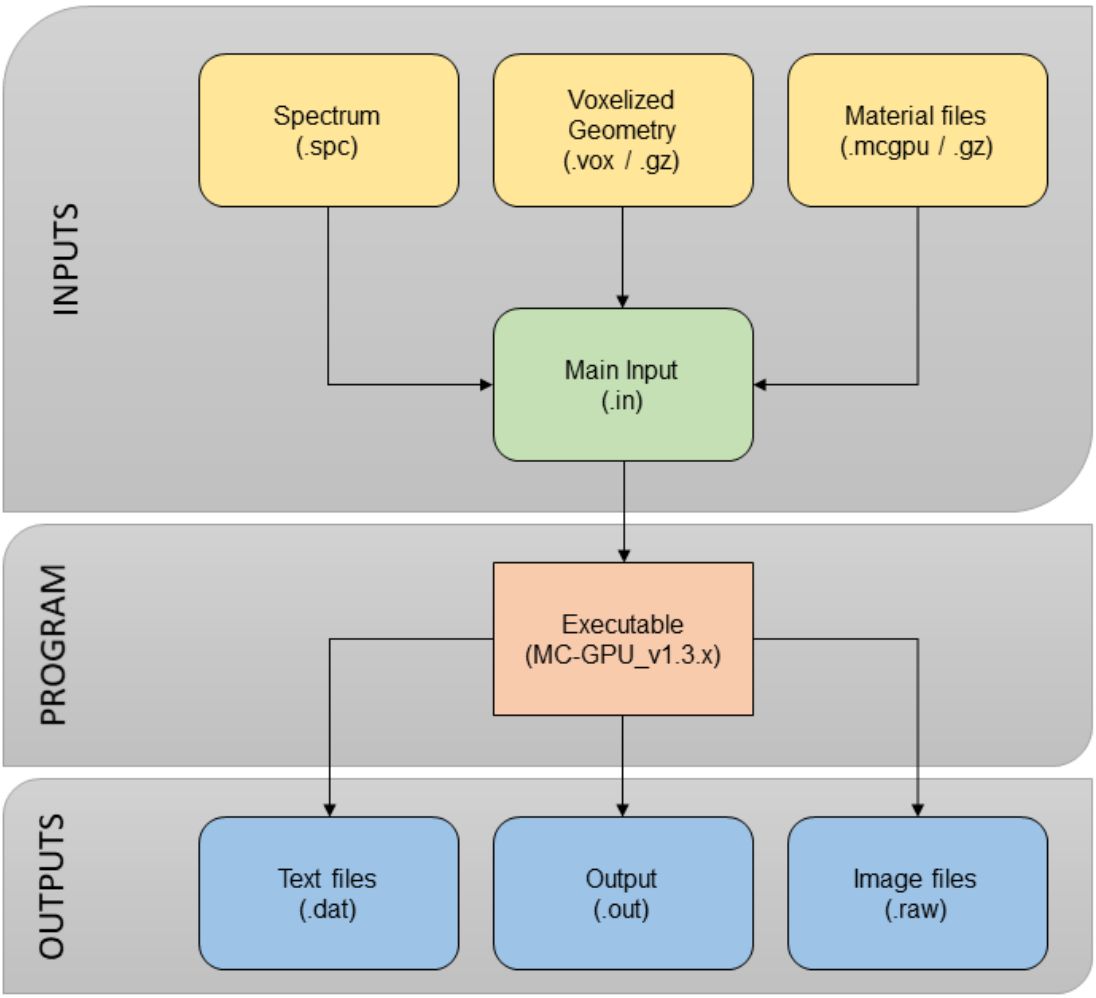

Figure 3: MC-GPU operating scheme

The latest version of this software was released in 2012.

The package of files needed to compile de MC-GPU executable (**MC-GPU_v1.3.x**) is formed by the kernel and the main code, both are CUDA codes, and a library written in C.

- **MC-GPU_v1.3.cu**: initializes the simulation environment, launch the GPU kernels that perform the x ray transport and report the final results. This function reads the description of the simulation from an external file given in the command line. This input file defines the number of particles to simulate, the characteristics of the x-ray source and the detector, the number and spacing of the projections (if simulating a CT), the location of the material files containing the interaction mean free paths, and the location of the voxelized geometry file.
- **MC-GPU_kernel_v1.3.cu**: definition of the CUDA GPU kernel for the simulation of x ray tracks in a voxelized geometry. This kernel has been optimized to yield a good performance in the GPU but can still be compiled in the CPU without problems. All the CUDA specific commands are enclosed in pre-processor directives that are skipped if the parameter "USING_CUDA" is not defined at compilation time.
- **MC-GPU_v1.3.h**: this file declares all the host and device functions and structures, the library files to include in the compilation, various constants parameters of the simulation, pre-processor macro functions, etc.

However, to simulate the atomic interactions, MC-GPU uses a database of material properties based on the database from PENELOPE. A PENELOPE 2006 material file can be converted into an MC-GPU material file using the auxiliary utility **MC-GPU_create_material_data.f** provided with the MC-GPU package. Pre-defined material files for a set of materials typically used in medical imaging simulations are already provided in the MC-GPU package.

The **MC-GPU_create_material_data.f** is based on PENELOPE's subroutine **tables.f**. Compiling this Fortran file the executable **MC-GPU_create_material_data.x** is obtained. This programme reads a PENELOPE 2006 material file (.mat) and outputs a table with photon interaction mean free paths (MFP), and data for Rayleigh and Compton interaction sampling. It should be pointed out that while in PENELOPE the material data is interpolated in a LOG-LOG scale, for fast calculations on GPU's, the MC-GPU code needs a material data file in which MFPs and Rayleigh and Compton data should be listed for each energy in a linear grid. This code that generates the material files in the necessary format to run simulations in MC-GPU (.mcgpu) is written in Fortran and divided in two parts:

- Main programme: this section reads data from keyboard, performs some calculations and prints the results both onto the output screen and the new material file. This is also divided in four parts:
  - Initialization: the code receives the energy parameters, the PENELOPE 2006 material data file and the name of the output data file. PENELOPE is initialized with the material information.
  - Mean Free Paths: those are obtained calling the PENELOPE's function PHMFP, a function which returns the MFP [cm] for the input energy, kind of particle, material number and kind of interaction. Only Rayleigh, Compton, Photoelectric and total MFPs are written in the output file. The Rayleigh cumulative probability is computed calling the subroutine GRAaI.
  - Rayleigh Sampling Data.
  - Compton Sampling Data.

- Subroutine GRAaI: the inputs are the material, number of bins required, minimum energy of spectrum and energy step, the output is the re-calculated maximum

Rayleigh cumulative probability for each linear energy bin instead of the PENELOPE grid.

This version of the materials generation code is not independent, version 2006 Penelope's main code (penelope.f) must be included.

In addition to the MC-GPU code, there is a new and extended version of the software created in 2015 and henceforth named MC-GPU Beta which has not been released to the public yet. This code is explained more detailed in the APPENDIX A: USER MANUAL.

The MC-GPU Beta code is based on the MC-GPU version 1.3 code. In this new version the name of some of the utilities has been changed and the features extended. The main change is the inclusion of an operator in the simulation that allows the user to run simulations using a voxelized phantom as operator or the use of depth-cameras to track operator's movements. This project is only focus on the non-real time use, without cameras.

5.2 PENELOPE/penEasy

PENELOPE/penEasy[11] is a general-purpose main programme for PENELOPE. It provides users with a set of source models, tallies and variance reduction techniques that are invoked from a structured code. Users need only to input all the required information through a simple configuration file and through the usual PENELOPE data files (geometry and materials).

The PENELOPE/penEasy is a Fortran general-purpose main programme for PENELOPE. Its main features are:

- To provide a set of ready-made source models and tally schemes applicable to a variety of practical situations. Users must provide a configuration data file; no programming is required.
- To supply a structured and modular code that, if needed, facilitates its adaptation by end users, reducing the programming effort to a minimum.
- It extends PENELOPE's variance reduction and introduces voxelized geometries.

The election of this programme is because of its modular structure is easier to use and its use does not require programming. The chosen version of PENELOPE/penEasy was the latest, penEasy for PENELOPE 2014.

5.3 THE CLUSTER

To run simulations with MC-GPU and PENELOPE/penEasy, the Argos Cluster located into the INTE/SEN facilities (Barcelona) was used. Depending on the programme, two different ports were used:

- MC-GPU uses CUDA to access NVIDIA GPUs. Simulations were run in a Geforce GTX 780 graphics card (12 multiprocessors, 2304 cores) @ 0.94GHz.

- PENELOPE/penEasy simulations were run in a CPU Intel(R) Core(TM) i7-3820 CPU @ 3.60GHz.

[11] It is an open software available on http://www.upc.es/inte/downloads/penEasy.htm

6. RESULTS AND DISCUSSION

6.1 THE USER MANUAL

Since its release in 2012, the MC-GPU v1.3 code has not been modified and just few users have been simulating with it. All the users who use the code had to learn to use the code with the only support of the documentation provided by the coder, the comments inside the code and using the programme.

As mentioned at the beginning, one of the main objectives of this project is to learn to use the programme, acquire as much knowledge as possible and transmit it to future users of the code. This goal was the main reason why the User Manual was elaborated.

MC-GPU User Manual is attached at the end of this thesis.

The manual was written while the programme was being taught, performing the first simple simulations and improved after acquiring good management of the programme. For this reason, it is useful for beginner users to learn how to use the programme, but also for common users. This handbook is a complementary information to those provided in the MC-GPU package.

This manual may be considered as divided in three main sections:

- Contextualization: the first sections of the manual explain some concepts about physics, interventional radiology, X-rays tubes and more relevant information necessary to understand the code and the results of the simulations. Also, some tips about the simulations and most likely errors are included.
- MC-GPU: this is the core of the handbook; its main purpose is to teach to the readers how to run simulations and how to interpret the results. Also, the pre-processing and post-processing of data are included.
- MC-GPU Beta: the final section includes an explanation of the extended version of the code, how to use and how to obtain the results.

The MC-GPU User Manual v 1.0 attached to this thesis is the first version, it will be necessary to be revised, extended and improved by future users. This information is totally open and will be available in INTE-UPC.

6.2 MC-GPU UPDATE

6.2.1 Materials generator code

Once the initial stage of learning was considered as finished, the code update process started. MC-GPU codes were modified to the newest version possible.

As mentioned before, the latest version of MC-GPU code was released in 2012 and it has not suffered any modification since then. However the programme in which is based on, PENELOPE, has been updated as well as the materials that it uses. The latest version of PENELOPE and which is used for PENELOPE/penEasy simulation in this project is PENELOPE 2014[12].

There have been few changes between the PENELOPE versions of 2006 and 2014, one of them what concerns to this project is that, as the NEA announces in its webpage, programmes for the calculation of mass energy-absorption coefficients for photons, and linear energy transfers for charged particles have been included in the distribution package. Therefore, the cross sections and the mean free paths of both versions are not the same.

From material data files the MFP's have been obtained and the relative differences between both versions, 2006 and 2014, are plotted below. Analysing the plots, it may be concluded:

- Compton MFP difference is high at low energies but rapidly decreases at high energies.
- Rayleigh MFP difference is also high at low energies and although decrease at high energies, it does slower.
- Photoelectric MFP difference is roughly constant in all the energy range between 2 and 3 %.
- Total MFP difference may be considered medium values at low energies but at high energies decreases. Above 60 keV, the difference is almost negligible.

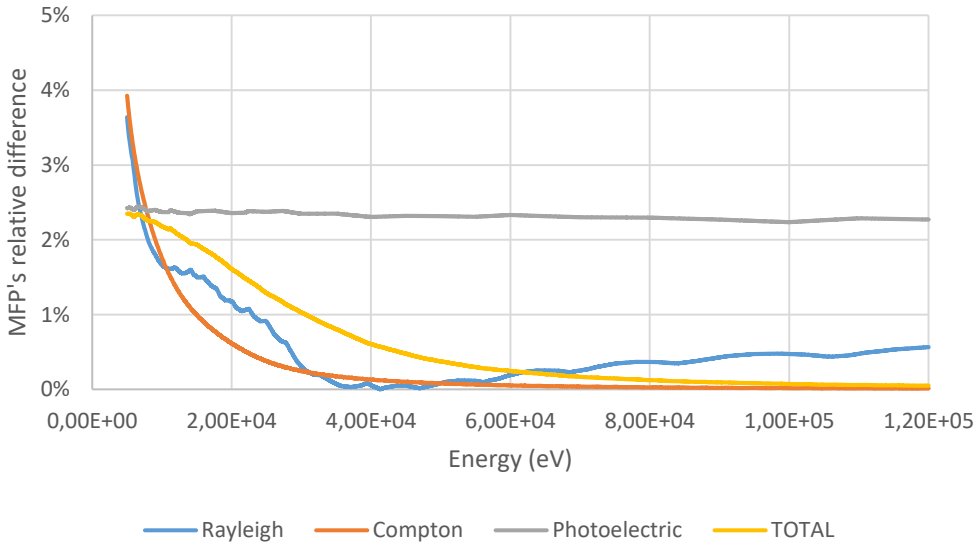

Figure 4: MFP's PENELOPE 2006 and 2014 comparative for Dry Air

[12] Available on https://www.oecd-nea.org/tools/abstract/detail/nea-1525

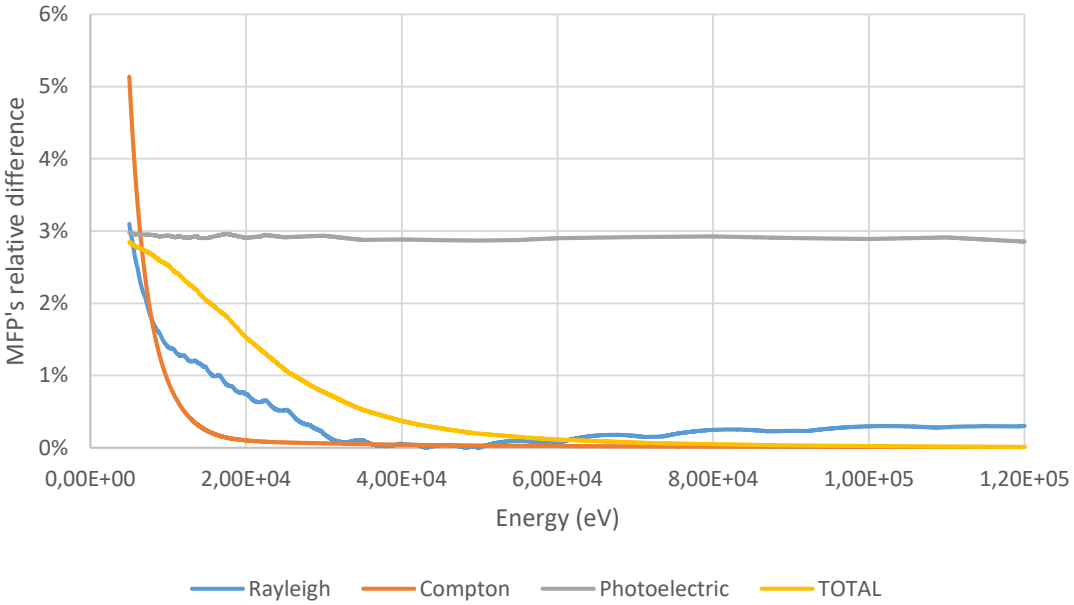

Figure 5: MFP's PENELOPE 2006 and 2014 comparative for PMMA

As it has been concluded before, the difference in the total MFP's is small at low energies and almost negligible at high energies. These variations between versions could have disregarded if the simulations used a broad energy range of spectrum. Figure 4 and Figure 5 just show the MFP's relative difference for dry air and PMMA.

However, the IR energy range of spectra is 60 to 120 keV, range in which the most probable interaction is the photoelectric effect and as it has shown before the variation of this interaction is roughly constant of 2 - 3 % depending on the material of interest.

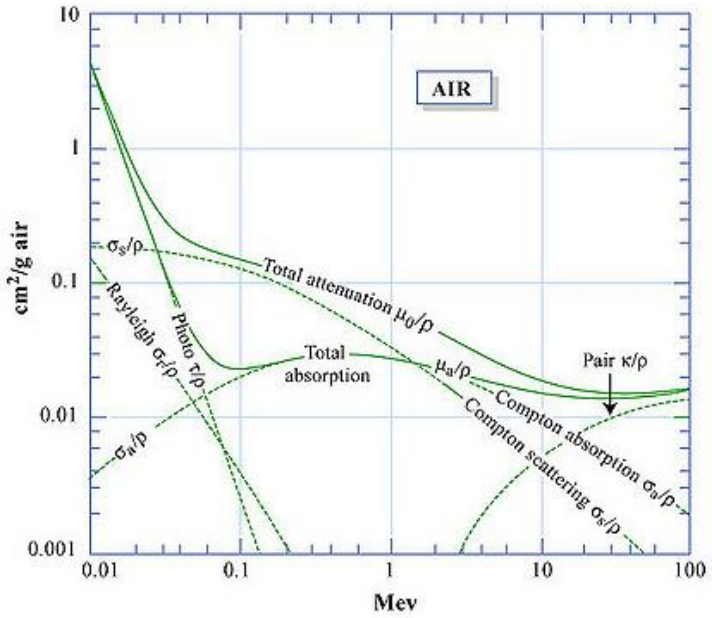

Figure 6: Mass attenuation coefficient for Dry Air[13]

[13] Source: MIT open course ware: https://ocw.mit.edu/courses/nuclear-engineering/22-101-applied-nuclear-physics-fall-2006/

To sum up, as the MFP's of materials used in the MC-GPU simulations are based on PENELOPE 2006 data and the MFP's of materials used in the penEasy simulations are based on latest version of PENELOPE, and also the interaction most important in this kind of simulations has the larger variations thus the provided material files for MC-GPU simulations cannot be used to validate the code comparing with penEasy.

For these reasons, the code which creates the materials in MC-GPU format (.mcgpu) from PENELOPE material data files (.mat) was updated.

All the steps and of this process and all the modifications made in the code are in the APPENDIX B: UPDATED CODE AND NEW FILES.

6.2.2 MC-GPU library modification

Due to the modifications explained in the previous section and the difference in the size and number of data included in the new PENELOPE material file, the MC-GPU library in where the variables are declared, named **MC-GPU_v1.3.h**, had little modifications.

- The maximum number of shells for materials has been enlarged from 30 to 52.
- The maximum number of energy bins has been enlarged from 25005 to 26005.

6.3 MATERIALS VALIDATION

After updating the materials generator code and modifying the MC-GPU variables library, it was necessary to check if the material data files generated by the new executable were the same as in PENELOPE 2014. Also, to check that all the tables and variables were correctly written.

The new MC-GPU material file (.mcgpu) looks like this:

Air_5_120keV.mcgpu

```
#[MATERIAL DEFINITION FOR MC-GPU: interaction mean free path and sampling data from PENELOPE 2014]
#[MATERIAL NAME]
# AIR, DRY (NEAR SEA LEVEL)  (104)
#[NOMINAL DENSITY (g/cm^3)]
#   0.00120479
#[NUMBER OF DATA VALUES]
#  23001
#[MEAN FREE PATHS (cm) (ie, average distance between interactions)]
#[Energy (eV)      | Rayleigh        | Compton         | Photoelectric   | TOTAL (+pair prod) (cm) | Rayleigh: max cumul prob F^2]
  5.0000000000E+03  1.5383521825E+03  8.8214400008E+03  2.1475099122E+01  2.1128710234E+01  3.3697163820E-01
  5.0050000000E+03  1.5401633560E+03  8.8156226766E+03  2.1539780758E+01  2.1191628750E+01  3.3721959472E-01
  5.0100000000E+03  1.5419748502E+03  8.8098149914E+03  2.1604591935E+01  2.1254669497E+01  3.3746753094E-01
  5.0150000000E+03  1.5438046817E+03  8.8040169199E+03  2.1669532782E+01  2.1317836015E+01  3.3771542679E-01
  5.0200000000E+03  1.5456456294E+03  8.7982284364E+03  2.1734603426E+01  2.1381127065E+01  3.3796326216E-01
  5.0250000000E+03  1.5474869364E+03  8.7924495156E+03  2.1799803996E+01  2.1444540706E+01  3.3821101695E-01
  5.0300000000E+03  1.5493286024E+03  8.7866801322E+03  2.1865134620E+01  2.1508077045E+01  3.3845867109E-01
  5.0350000000E+03  1.5511706272E+03  8.7809202610E+03  2.1930595428E+01  2.1571736186E+01  3.3870620448E-01
  5.0400000000E+03  1.5530130104E+03  8.7751698769E+03  2.1996186546E+01  2.1635518233E+01  3.3895359702E-01
```

Figure 7: MC-GPU material file: MFP's and Rayleigh max cumul prob table

Air_5_120keV.mcgpu

```
#[RAYLEIGH INTERACTIONS (RITA sampling  of atomic form factor from EPDL database)]
#[DATA VALUES TO SAMPLE SQUARED MOLECULAR FORM FACTOR (F^2)]
#    128
#[SAMPLING DATA FROM COMMON/CGRA/: X, P, A, B, ITL, ITU]
  0.0000000000E+00  2.7555440646E-03 -6.4004091321E-03  5.7900082577E-04    1    4
  1.0561873956E-06  5.4815488904E-03 -5.5002750093E-03 -3.0777036093E-06    3    5
  2.1123747912E-06  1.0844503752E-02 -1.0884079932E-02 -3.7647908999E-06    4    6
  4.2247495824E-06  2.1226352931E-02 -2.1623884185E-02  2.0464725546E-04    5    7
  8.4494991649E-06  3.1175453162E-02 -2.0631249493E-02 -2.7668683039E-04    6    7
  1.2674248747E-05  4.0712482354E-02 -2.0827873675E-02  1.5080196585E-04    6    8
  1.6898998330E-05  4.9868818971E-02 -1.9917169991E-02  1.2285842525E-04    7    9
  2.1123747912E-05  5.8670888394E-02 -1.9197591483E-02 -2.0111762273E-04    8   10
  2.5348497495E-05  7.5266357449E-02 -3.8429153864E-02 -2.5829331890E-05    9   10
  3.3797996659E-05  1.0492119585E-01 -7.1042563969E-02  2.6059866825E-04    9   11
  5.0696994989E-05  1.3066230523E-01 -6.5937329122E-02 -1.6159298318E-04   10   11
  6.7595993319E-05  1.5319976692E-01 -6.2354446443E-02  1.8005411540E-05   10   11
  8.4494991649E-05  1.7310217604E-01 -5.8473669749E-02  2.4570488877E-04   10   11
  1.0139398998E-04  2.0673451058E-01 -1.0388765051E-01  8.3893712754E-04   10   12
  1.3519198664E-04  2.3415718387E-01 -9.2307963964E-02  5.8726992301E-04   11   12
  1.6898998330E-04  2.5702910821E-01 -8.3224261823E-02  9.6154170598E-04   11   12
  2.0278797996E-04  2.7649234534E-01 -7.4465194983E-02  8.1753123540E-04   11   13
  2.3658597662E-04  2.9334142093E-01 -6.7418375037E-02  1.1662130820E-03   12   13
  2.7038397328E-04  3.2137066486E-01 -1.1382074096E-01  3.5726405956E-03   12   13
  3.3797996659E-04  3.4411307351E-01 -9.4704770431E-02  3.3655763589E-03   12   14
```

Figure 8: MC-GPU material file: Rayleigh interactions table

Air_5_120keV.mcgpu

```
#[COMPTON INTERACTIONS (relativistic impulse model with approximated one-electron analytical profiles)]
#[NUMBER OF SHELLS]
#     11
#[SHELL INFORMATION FROM COMMON/CGCO/: FCO, UICO, FJ0, KZCO, KSCO]
   0.30037400E-03   0.11260000E+02   0.66924682E+02    6   30
   0.32246090E+01   0.14303508E+02   0.53767140E+02    0   30
   0.15688600E+01   0.20330000E+02   0.92073666E+02    7   30
   0.43083822E+00   0.28496480E+02   0.79406063E+02    0   30
   0.18684440E-01   0.24850000E+03   0.14217622E+02   18    4
   0.93422200E-02   0.25060000E+03   0.14139237E+02   18    3
   0.30037400E-03   0.28800000E+03   0.20977471E+02    6    1
   0.93422200E-02   0.32650000E+03   0.27055428E+02   18    2
   0.15688600E+01   0.40300000E+03   0.17833454E+02    7    1
   0.42149600E+00   0.53800000E+03   0.15510145E+02    8    1
   0.93422200E-02   0.32063000E+04   0.66727076E+01   18    1
```

Figure 9: MC-GPU material file: Shell information table

These figures correspond to the material Dry Air, in the energy range 5 – 120 keV. The columns are written correctly and in their places. Also, the Rayleigh and Compton tables are updated to the new materials.

Following a comparative between the MFP's generated with the new executable and in PENELOPE 2014 is shown:

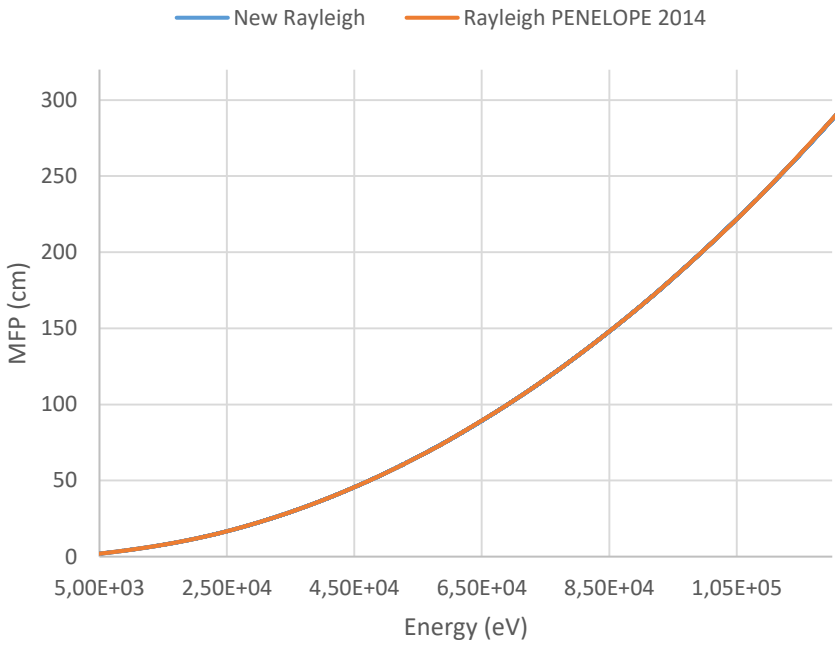

Figure 10: Rayleigh MFP comparative

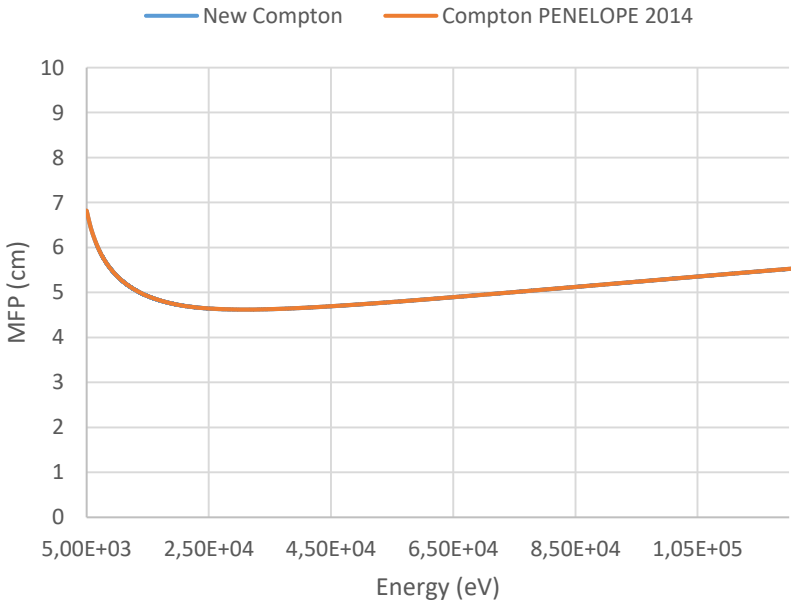

Figure 11: Compton MFP comparative

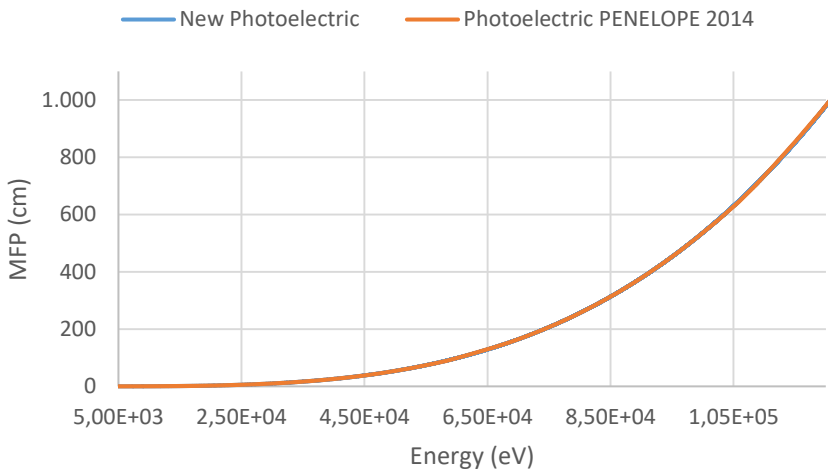

Figure 12: Photoelectric MFP comparative

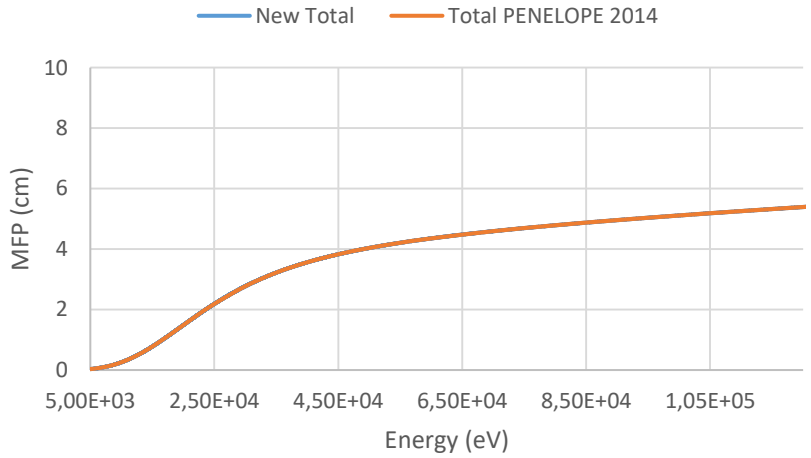

Figure 13: Total MFP comparative

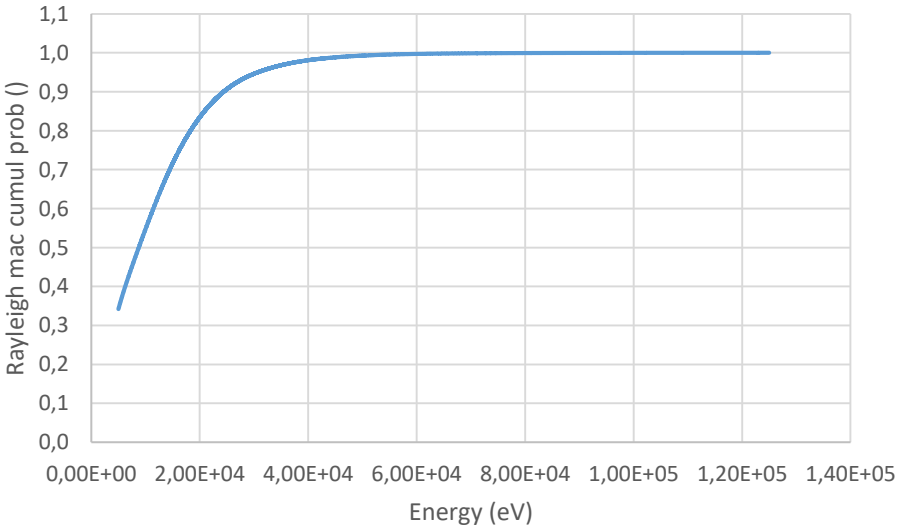

Figure 14: MC-GPU material file Rayleigh cumulative probability

In this thesis, only the comparative between PENELOPE 2014 and the new material generator for Dry Air is shown, but the same process was made for different materials.

As the graphs show, the results obtained with the new executable are the same obtained in PENELOPE 2014.

In the light of these results, new materials may be considered as updated but the complete validation of the materials is made by running simulations with them.

6.3.1 Simulation 1: Air voxel

The simulation run in the first place was the simplest possible, one voxel of air. The features what MC-GPU demands for run a simulation are shown in the following table:

SIMULATION 1		
Phantom	Nº Voxels	1 x 1 x 1
	Voxel size (cm^3)	10 x 10 x 10
	Dimensions (cm^3)	10 x 10 x 10
	Material	Dry air (ρ = 0.001205 g/cm^3)
Source	Focal position (cm)	5 -15 5
	Spectrum	Monoenergetic spectra (60 – 120 keV)
	Histories	1.0E9
Detector size (cm^2)		20 x 20
Source-to-detector distance (cm)		30

Table 3: Simulation 1

This simulation consists on irradiate a voxel of air perpendicularly to the XZ plane. The simulation is run for only one projection but repeated for the photon range of energies used in the interventional radiology (60 – 120 keV).

The number of simulated histories was high in order to reduce as much as possible the uncertainties of the dose and energy deposited in the phantom but having in mind the simulation time.

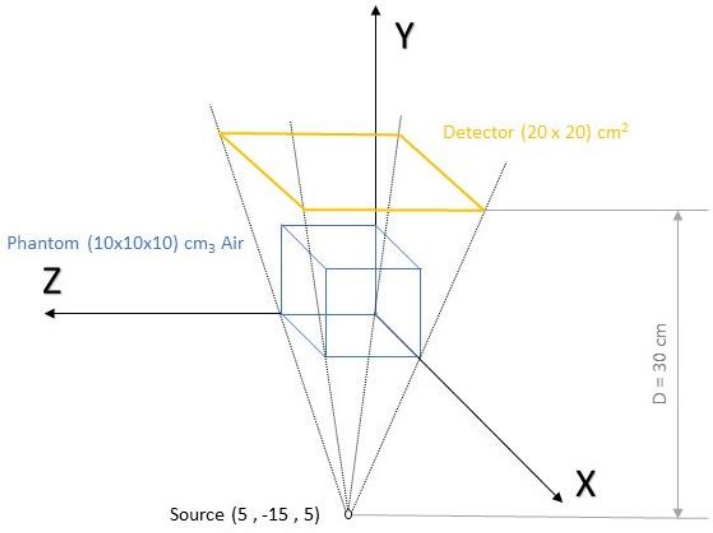

Figure 15: Simulation 1 scheme

From these simulation characteristics, a package of simulations was run with PENELOPE/penEasy simulating exactly the same elements.

The results obtained from the simulations using the same inputs with new and old material data files, and the comparative with the PENELOPE/penEasy 2014 are shown below.

	Energy Spectrum (keV)	MC-GPU	NEW MC-GPU	penEasy	Old Difference	New Difference	Old Relative error	New Relative error
DOSE (eV/g·hist)	60	11.61226	11.47738	11.436	0.176	0.042	1.543%	0.364%
	70	11.54258	11.44943	11.418	0.124	0.031	1.088%	0.273%
	80	12.22802	12.15716	12.115	0.113	0.042	0.935%	0.350%
	90	13.34371	13.28865	13.256	0.087	0.032	0.659%	0.244%
	100	14.75085	14.71027	14.650	0.100	0.060	0.686%	0.409%
	110	16.36093	16.32939	16.252	0.109	0.077	0.668%	0.474%
	120	18.08912	18.06191	17.984	0.105	0.078	0.582%	0.431%
	200		33.94609	33.830		0.116		0.344%
	300		54.81751	54.566		0.252		0.462%

	Energy Spectrum (keV)	MC-GPU	NEW MC-GPU	penEasy	Old Difference	New Difference	Old Relative error	New Relative error
ENERGY DEPOSITION (eV/hist)	60	13.99	13.83	13.780	0.210	0.050	1.523%	0.362%
	70	13.91	13.80	13.759	0.151	0.041	1.097%	0.297%
	80	14.73	14.65	14.598	0.132	0.052	0.903%	0.355%
	90	16.08	16.01	15.974	0.106	0.036	0.664%	0.226%
	100	17.77	17.73	17.654	0.116	0.076	0.659%	0.432%
	110	19.71	19.68	19.584	0.126	0.096	0.643%	0.490%
	120	21.80	21.76	21.671	0.129	0.089	0.594%	0.410%
	200		40.91	40.765		0.145		0.356%
	300		66.06	65.752		0.309		0.469%

Table 4: Simulation 1 new comparative

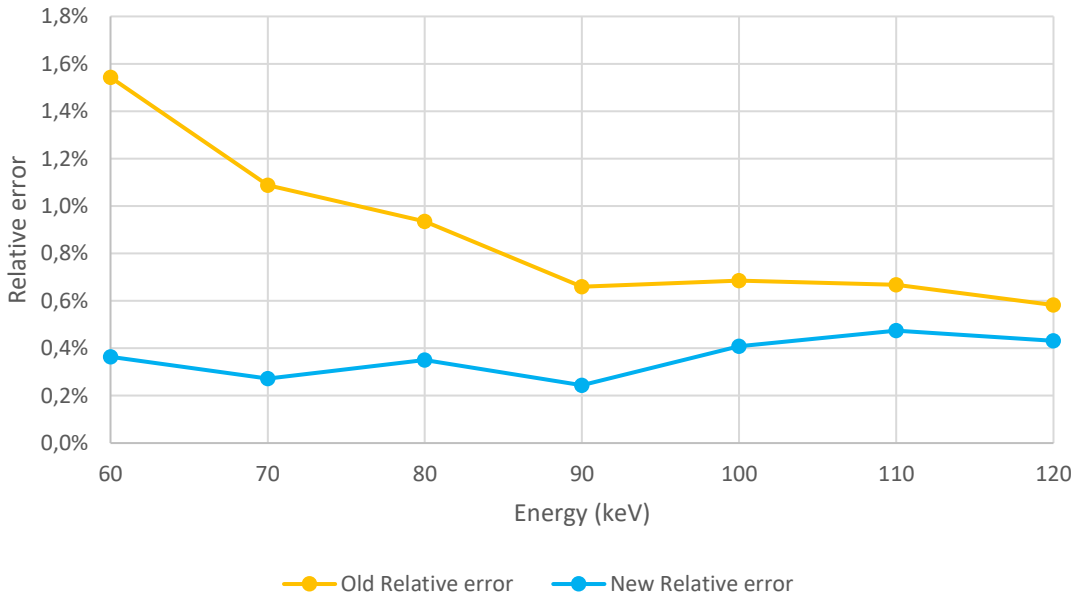

Figure 16: Simulation 1 dose relative errors

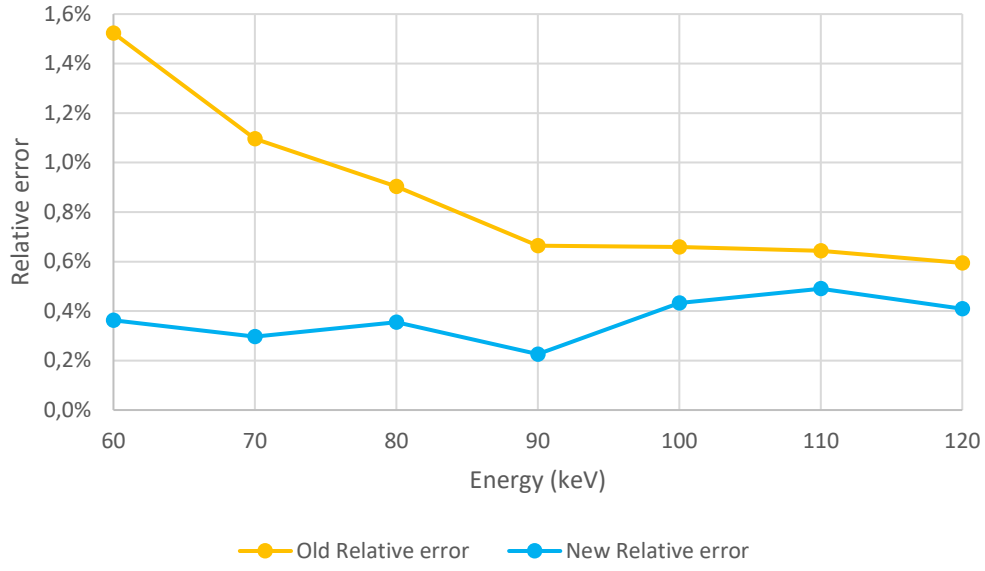

Figure 17: Simulation 1 energy deposition relative errors

In light of these results, a little more complex simulation was proposed.

6.3.2 Simulation 2: PMMA block

For the second simulation, a PMMA block was chosen. The parallelepiped phantoms used in experimental measurements in dosimetry laboratories are usually made of this material. Moreover, the dimensions of the block are similar to a thick person's chest.

SIMULATION 2		
Phantom	Nº Voxels	6 x 3 x 6
	Voxel size (cm^3)	5 x 10 x 5
	Dimensions (cm^3)	30 x 30 x 30
	Material	PMMA (ρ = 1.19 g/cm^3)
Source	Focal position (cm)	15 -45 15
	Spectrum	Monoenergetic spectra (60 – 120 keV)
	Histories	1.0E9
Detector size (cm^2)		54 x 54
Source-to-detector distance (cm)		81

Table 5:Simulation 2

Some features are different between first and second simulation but the most important are the change in the material and that in this second simulation the voxel dimensions are not equal in the three axes.

Using the same inputs but with the new and old material data files, the results obtained from the simulations and the comparative with the penEasy/PENELOPE 2014 are shown below.

	Energy Spectrum (keV)	MC-GPU	NEW MC-GPU	penEasy	Old Difference	Old Relative error	New Difference	New Relative error
DOSE (eV/g·hist)	60	0.808	0.801	0.802	0.0053	0.666%	0.0009	0.116%
	70	0.888	0.882	0.883	0.0049	0.555%	0.0011	0.124%
	80	0.983	0.978	0.979	0.0045	0.456%	0.0011	0.114%
	90	1.090	1.085	1.086	0.0041	0.378%	0.0011	0.100%
	100	1.206	1.201	1.202	0.0038	0.318%	0.0010	0.086%
	110	1.328	1.324	1.325	0.0036	0.273%	0.0010	0.074%
	120	1.456	1.452	1.453	0.0033	0.231%	0.0009	0.065%
	200		2.591	2.592			0.0008	0.030%
	300		4.114	4.115			0.0006	0.015%

	Energy Spectrum (keV)	MC-GPU	NEW MC-GPU	penEasy	Old Difference	Old Relative error	New Difference	New Relative error
ENERGY DEPOSITION (eV/hist)	60	25947.550	25745.970	25776.000	171.550	0.666%	30.030	0.117%
	70	28540.420	28347.670	28382.900	157.520	0.555%	35.230	0.124%
	80	31596.950	31417.570	31453.500	143.450	0.456%	35.930	0.114%
	90	35020.840	34854.070	34888.900	131.940	0.378%	34.830	0.100%
	100	38732.970	38577.050	38610.300	122.670	0.318%	33.250	0.086%
	110	42673.680	42526.050	42557.500	116.180	0.273%	31.450	0.074%
	120	46793.210	46655.240	46685.500	107.710	0.231%	30.260	0.065%
	200		83241.110	83266.300			25.190	0.030%
	300		132191.460	132211.000			19.540	0.015%

Table 6: Simulation 2 new comparative

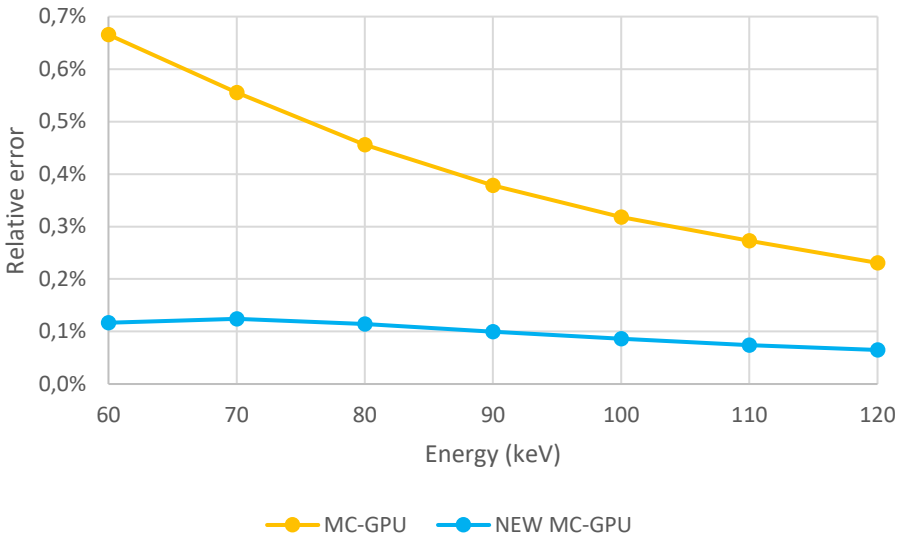

Figure 18: Simulation 2 dose relative errors

6.3.3 Conclusions

As the figures show, the dose and energy deposition relative errors between the MC-GPU and the penEasy/PENELOPE 2014 were clearly reduced after the code update.

It can be easily checked that the relative errors of dose and energy deposition vary depending on the materials, this is due to the materials have different absorption coefficients at different energies. However, as expected, the maximum difference between relative errors appears always for low energies.

In real interventional procedures, the used spectra are not monoenergetic but the range of energies, in which the intensity is considerable, is between 30 and 90 keV with the mean energy of photons approximately on 60 keV, where the precision improvement is significant. Moreover, in both cases the new maximum relative errors are lower than the old minimum relative errors.

Even though the relative errors between MC-GPU and PENELOPE/penEasy exist due to the algorithms used by MC-GPU and the simple pre-fabricated material data files used on it, the new relative differences are lower enough to consider the new materials as suitable to make the code validation.

To sum up, the conclusion was that the update of the code reduced discrepancies between MC-GPU and PENELOPE/penEasy results and the code validation process using the new material data files began.

6.4 LIBRARIES

The programme MC-GPU was designed to simulate fluoroscopically-guided interventional procedures. These processes differ mainly from each other in patients and X-ray machines. To be able to carry out diverse and varied simulations it is necessary to have a library of voxelized geometries, materials and spectra.

After the updating of the materials to the latest available version of PENELOPE, next stage is to create a library of materials and spectra to facilitate the work to the next users who want to carry out simulations.

6.4.1 Materials library

As well as the Manual, INTE-UPC has available the new materials generator programme, both the Fortran code (.f) and the executable (.x).

Using the new executable, a library in which the main materials needed to simulate human in the programme was created.

PENELOPE 2014 already has included pre-defined materials. Some materials were created just converting the .mat files into .mcgpu.

Other materials were created with the executable material.x (provided in PENELOPE 2014 package) from their element composition, information obtained in ICRP publication 110[14], and later converting it into mcgpu format.

Materials library includes four types of materials:

- Elements.
- Compounds and mixtures.
- Materials from ICRP.
- ICRU materials.

Most of material data files have been created with 23001 values for the MFP's table and the energy range usually employed in IR, 5 – 120 keV. Also, the materials in format .mat are included in the library in case of someone wants to generate a different energy range and different energy steps.

6.4.2 Spectra library

A similar case of the materials is the case of the spectra, to carry out simulations spectrum files are necessary, for this reason a library of them was created.

This library contains a spreadsheet in which all the generated spectra are referred. The spectra most important included in this library are the monoenergetic, the RQR series and the N series[15].

With the exception of monoenergetic spectra, the rest of them were generated with a programme called Xcomp5r changing the main parameters of an X-ray tube.

The lecture of the User Manual is highly recommended before using these spectra.

[14] ICRP Annals of the ICRP publication 110: Adult Reference Computational Phantoms.
[15] ISO 4037-4:2004 X and gamma reference radiation for calibrating dosimeters and dose rate meters and for determining their response as a function of photon energy

6.5 MC-GPU VALIDATION

Once the materials generator was updated and validated, the programme validation process began. Many simulations were carried out, but only the most representatives are included in this thesis. The complexity in voxelized geometry, materials and spectra is increasing with the simulations.

The parameters, in which this thesis focus, are the relative error in the results (dose and energy deposition), maximum dose (location and magnitude) and real simulation time. About the simulation time, it is important to point out that all simulations were launched in a cluster, using different computational machines for the simulations.

Most of the results tables are included in the APPENDIX C: SIMULATIONS' RESULTS for a better visualization.

6.5.1 Simulation 3: One air voxel in PMMA block

For this simulation, a phantom of 3 x 3 x 3 voxels of PMMA with one central voxel of dry air is used. Just one projection parallel to Y axis is simulated.

SIMULATION 3		
Phantom	Nº Voxels	3 x 3 x 3
	Voxel size (cm^3)	10 x 10 x 10
	Dimensions (cm^3)	30 x 30 x 30
	Materials	PMMA and Dry Air (1voxel)
Source	Focal position (cm)	15 -45 15
	Spectrum	N100
	Histories	1006720000
Detector size (cm^2)		54 x 54
Source-to-detector distance (cm)		81

Table 7: Simulation 3

Results of this simulation lay bare the idea of the MC-GPU is amply faster than PENELOPE/penEasy, the results are pretty much precise and the maximum location is also the correct one. Nevertheless, absorption influence of certain materials is shown.

	MC-GPU original	MC-GPU updated	PENELOPE/penEasy	Original Relative Error	Updated Relative Error
Total Energy Absorbed (eV/hist)	32322.85	32144.36	32180.97	0.441%	0.114%
Maximum voxel dose (ev/g·hist)	2.851025	2.831048	2.8371	0.493%	0.212%
Sigma	0.000845	0.000838	0.00060		
Coordinates	(1,0,1)	(1,0,1)	(2,1,2)=(1,0,1)		
PMMA					
Dose ROI (ev/g·hist)	1.057630	1.05179	1.05299	0.441%	0.114%
Sigma	<< 1%	<< 1%			
E dp (ev/hist)	32321.29	32142.82	32179.40	0.441%	0.114%
Sigma	-	-	1.90		
Mass (g)	30560.000010				
Dry Air					
Dose ROI (ev/g·hist)	1.292280	1.28424	1.301278008	0.691%	1.309%
Sigma	0.011590	0.01153			
E dp (ev/hist)	1.56	1.55	1.5680	0.513%	1.150%
Sigma	-	-	0.014		
Mass (g)	1.205				
Real simulation time (s)	49.30	59.72	20357.19		

Table 8: Simulation 3 results

6.5.2 Simulation 4: Three materials phantom

In order to perform more realistic simulations a phantom that resembles a human body was used. Simulations of three layers of human material, basic[16] and realistic[17], were carried out. The second one is what is explained following because is more realistic due to the size of the material layers.

The phantom in this case is composed by 10 equal layers of three different materials arranged as the figure shows. The adjacent layers of same materials, are included in the same block so that the phantom is made by 5 blocks. The beam is perpendicular to XZ plane.

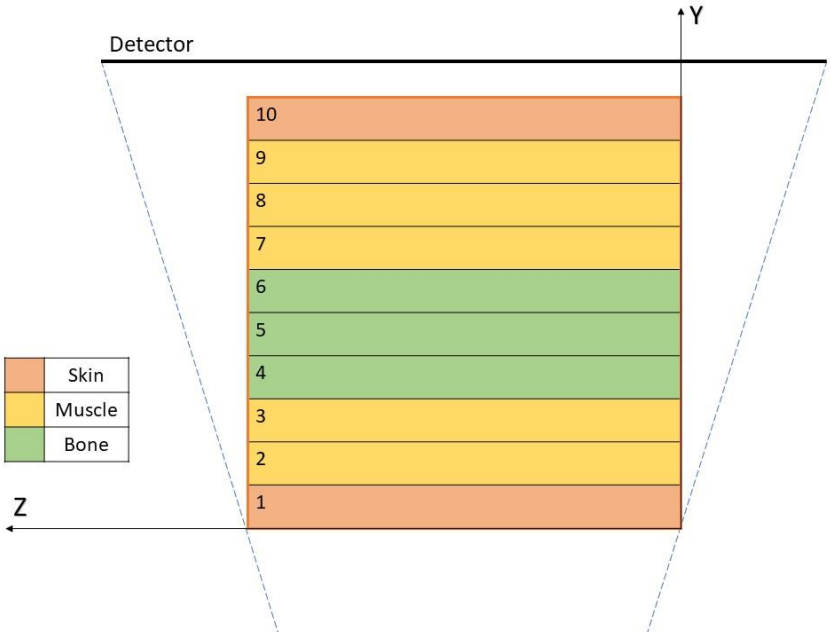

Figure 19: Simulation 4 scheme

As the materials employed in this simulation are realistic, the spectrum is also real.

SIMULATION 4		
Phantom	Nº Voxels	3 x 10 x 3
	Voxel size (cm^3)	10 x 1 x 10
	Dimensions (cm^3)	30 x 10 x 30
	Materials	Skin, Muscle and Bone
Source	Focal position (cm)	15 -30 15
	Spectrum	90 kVp 4 mm Al
	Histories	1006720000
Detector size (cm^2)		50 x 50
Source-to-detector distance (cm)		50

Table 9: Simulation 4

[16] Results at: Basic Layers Block
[17] Results at: SIMULATION 4

In this case, the standard deviations (sigmas) obtained in the simulations are not included because in both cases (MC-GPU and penEasy/PENELOPE) are below the 1 % of the obtained value.

	MC-GPU original	MC-GPU updated	PENELOPE/penEasy	Original Relative Error	Updated Relative Error
Total Energy Absorbed (eV/hist)	30525.70	30415.65	30406.04	0.394%	0.032%
Sigma					
Maximum voxel dose (ev/g·hist)	8.659510	8.687543	8.7034	0.504%	0.182%
Sigma	0.001915	0.001915	0.00290		
Coordinates	(1,3,1)	(1,3,1)	(2,4,2)=(1,3,1)		
E dp Maximum voxel dose (ev/hist)	1602.009384	1607.195447	1610.12	0.504%	0.182%
E deposition (eV/hist)					
1 (Skin)	4066.19	3867.54	3893.75	4.429%	0.673%
2 (Mucle)	6056.99	5983.71	6024.76	0.535%	0.681%
3 (Bone)	19560.43	19715.85	19653.70	0.475%	0.316%
4 (Muscle)	697.48	704.93	693.30	0.603%	1.678%
5 (Skin)	144.62	143.62	140.54	2.906%	2.194%
Dose (eV/g·hist)					
1 (Skin)	4.10727	3.90661	3.93	4.429%	0.673%
2 (Mucle)	3.23557	3.19643	3.22	0.535%	0.681%
3 (Bone)	3.916	3.94712	3.93	0.475%	0.316%
4 (Muscle)	0.24839	0.25104	0.25	0.603%	1.677%
5 (Skin)	0.14608	0.14507	0.14	2.905%	2.194%
E deposition (eV/hist)					
Skin	4210.81	4011.16	4034.29	4.376%	0.573%
Muscle	6754.47	6688.64	6718.06	0.542%	0.438%
Bone	19560.43	19715.85	19653.70	0.475%	0.316%
Dose (eV/g·hist)					
Skin	2.13	2.03	2.04	4.376%	0.573%
Muscle	1.44	1.43	1.44	0.542%	0.438%
Bone	3.92	3.95	3.93	0.475%	0.316%

Real simulation time (s)	43.1	66.43	24704.07

Table 10: Simulation 4 results

In first place, simulation performed with MC-GPU obtains results of total energy absorbed and maximum voxel dose almost equal, less than 0.2 % of relative error, to the PENELOPE/penEasy obtained ones and the coordinates of the maximum dose is the same.

Secondly, the energy deposition or dose are analysed in two different ways: one focusing on the material and other focusing on the layer. It is important to highlight that the phantom's layers are numbered from the closest point to the source.

Comparing only the updated MC-GPU results with the PENELOPE/penEasy ones and attending to the materials' dose, the relative errors are within the 0.3 and 0.6 %, what can be considered as acceptable. However, if the results comparison is made layer by layer of different materials, the precision is much higher in the layers closer to the source than in the remote ones, in which the relative errors reach the 2.2 %.

In the face of these discrepancies, two ideas are concluded. One the one hand, the presence of high absorbent materials as bone, between the source and other materials, conditions the dose results in farther points from the source. On the other hand, as the code provides a mean dose in all voxels of the same material, when the fact that the relative errors of a number of voxels are low and the others high occurs, the result is unrealistic.

In addition, it also important emphasise the improvement of the results using the new materials with respect the old ones and the huge difference in simulation time using MC-GPU instead of PENELOPE/penEasy.

6.5.3 Simulation 5: Zubal chest[18]

To verify the conclusions previously mentioned, a human body phantom was used to carry out the simulation, the Zubal original phantom was used. This is the original head/body torso phantom with no arms or legs attached. The number of materials was reduced to 15 in order to simplify the results. The simulation is a PA projection.[19]

SIMULATION 5		
Phantom	Nº Voxels	128 x 128 x 243
	Voxel size (cm3)	0.4 x 0.4 x 0.4
	Dimensions (cm^3)	51.2 x 51.2 x 97.2
	Materials	Human body materials
Source	Focal position (cm)	25.6 -51.2 48.6
	Spectrum	N100
	Histories	1006720000
Detector size (cm^2)		110 x 110
Source-to-detector distance (cm)		110

Table 11: Simulation 5

Dose (eV/g·hist)	MC-GPU original	MC-GPU updated	Relative difference	PENELOPE/penEasy	Original Relative Error	Updated Relative Error
Air	0.23407	0.23338	0.295%	0.2324	0.701%	0.405%
Muscle	0.27855	0.27903	0.172%	0.2781	0.153%	0.326%
Soft tissue	0.20116	0.20262	0.726%	0.2011	0.019%	0.745%
Bone	0.71376	0.70083	1.812%	0.6992	2.085%	0.236%
Cartilage	0.33987	0.33960	0.079%	0.3408	0.258%	0.338%
Adipose	0.08942	0.08954	0.134%	0.0897	0.320%	0.186%
Blood	0.42861	0.42304	1.300%	0.3977	7.759%	6.358%
Skin	0.32297	0.31833	1.437%	0.3350	3.589%	4.974%
Lung	0.36786	0.37012	0.614%	0.3562	3.269%	3.904%
Glands	0.45867	0.45600	0.582%	0.4471	2.581%	1.984%
Brain	0.03322	0.03391	2.077%	0.0338	1.771%	0.269%
Red Marrow	0.20604	0.20856	1.223%	0.2077	0.812%	0.401%
Liver	0.51752	0.51760	0.015%	0.5169	0.122%	0.137%
Stomach	0.61291	0.61117	0.284%	0.6082	0.770%	0.484%
Water	0.42900	0.42847	0.124%	0.4268	0.522%	0.398%
Maximum dose point	6.125987	5.989736		5.8445		
Sigma	0.002147	0.001928		4.5		
Sigma/mean	0.035%	0.032%		77.00%		
Coordinates	(72,2,116)	(72,15,106)		(91,25,173)		
Real simulation time (s)	87.25	128.32		41570.21		

Table 12: Simulation 5 results

Some extracted conclusions were: dose precision improvement between MC-GPU versions, simulation time reduction between MC-GPU and PENELOPE/penEasy, and debatable high dose relative errors in materials distributed throughout the whole phantom or very absorbent. Nevertheless, the maximum dose point and its location is not as precise as in the previous simulations mainly due to the large standard deviation of the result in PENELOPE/penEasy, about 77 %.

The same PENELOPE/penEasy simulation was repeated with $2 \cdot 10^{10}$ histories in order to reduce the voxel dose uncertainties to less than 0.1 %[20]. The doses and maximum dose precision do not improve significantly due to the large number of materials, voxels' size and the presence of very absorbent materials but the real simulation time increases exponentially.

[18] Source: http://noodle.med.yale.edu/zubal/info.htm
[19] Results at: SIMULATION 5
[20] Results at: SIMULATION 5 LONG

6.5.4 Simulation 6: Duke tests[21]

These simulations were carried out in order to avoid the discrepancies due to a large number of materials. In this case, the entire Duke voxelized by 0.5 x 0.5 x 0.5 cm^3 voxels was used. Although the phantom is a representation of a whole human body, the radiation field is focus on the chest. Same simulation was repeated with a 100 keV monoenergetic and with a realistic RQR 6 spectrum, both simulated a PA projection.

The first simulation used a 100 keV monoenergetic in which the results are also compared with the obtained with the MC-GPU original. In the second one, the spectrum was the RQR 6 and only the comparison between the updated MC-GPU and PENELOPE/penEasy is shown[22].

SIMULATION 6		
Phantom	Nº Voxels	122 x 62 x 372
	Voxel size (cm^3)	0.5 x 0.5 x 0.5
	Dimensions (cm^3)	61 x 31 x 186
	Materials	Human body materials
Source	Focal position (cm)	30.5 -30.5 130
	Spectra	100 keV monoenergetic and RQR 6
	Histories	1006720000
Detector size (cm^2)		143 x 143
Source-to-detector distance (cm)		71.5

Table 13: Simulation 6

Dose (eV/g·hist)	MC-GPU updated	PENELOPE/penEasy	Updated Relative Error
Air	0.13787	0.1379	0.029%
Muscle	0.22679	0.2269	0.053%
Soft tissue	0.13792	0.1371	0.572%
Bone	0.63196	0.6299	0.332%
Cartilage	0.06394	0.0634	0.923%
Adipose	0.16574	0.1661	0.228%
Blood	0.10704	0.1067	0.309%
Skin	0.26648	0.2677	0.439%
Lung	0.29497	0.2930	0.667%
Maximum dose point	7.232274	7.3318	1.357%
Sigma	0.001633	0.067	
Sigma/mean	0.02%	0.91%	
Coordinates	(58,5,271)	(58,5,271)	
Real simulation time (s)	112.96	33641.11	

Table 14: Simulation 6 with RQR6 results

[21] Source: https://www.itis.ethz.ch/virtual-population/virtual-population/overview/
[22] Results of both simulations at: SIMULATION 6

Regarding to the simulation that uses a monoenergetic spectrum, it can be appreciated that blood and skin have relative errors above 1 % when the old materials are used but when the new materials are employed, all relative errors are below 0.17 %. Maximum dose point is also obtained accurately even with almost 60 % sigma in PENELOPE/penEasy results.

When the energy deposition standard deviations obtained in PENELOPE/penEasy for each material are taken into account, the higher maximum relative error is 0.18 % and the higher minimum relative error is 0.14 % (air is neglected). These results may be considered as accurate enough.

As the updated MC-GPU results are more precise, the simulation using RQR 6 spectrum is just carried out with this code. The comparative between the MC-GPU and PENELOPE/penEasy results are, one more time, below 1 %. In this case, the maximum dose sigma for PENELOPE/penEasy simulation is approximately 1 % and the relative error in the maximum dose between codes are 1.4 % being the same coordinates.

It is easy to check that when the obtained PENELOPE/penEasy sigmas are taken into account the relative errors improve.

In the lights of all these results, it may be concluded that the updated MC-GPU provides results as good as the PENELOPE/penEasy ones but in much less time.

The simulation which uses 100 keV monoenergetic is repeated with PENELOPE/penEasy simulating $1.8 \cdot 10^{10}$ histories and dose and maximum dose precision do not improve significantly, however the real simulation time increases exponentially[23].

Figure 20: Simulation 6 dose distribution using RQR 6

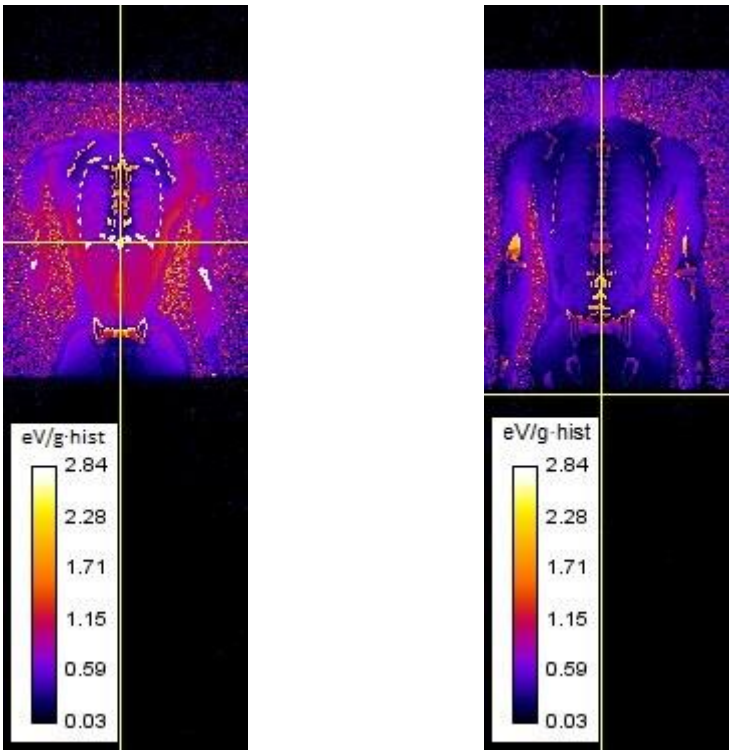

[23] Results at: SIMULATION 6 LONG

6.5.5 Simulation 7: Duke's chest tests

This section explains the last package of simulations carried out by MC-GPU programme that were performed in order to analyse the influence of voxels' size and different spectra on the dose and simulation time. For this analysis, the phantom employed was only the Duke's chest, formed by 0.1 x 0.1 x 0.1 cm^3 voxels.

The performance of the programme in a realistic range of energy spectrum wanted to be test so that the spectra used were 100 keV monoenergetic and a bunch of RQR spectra from 80 kVp (RQR 6) to 120 kVp (RQR 9). In all simulations X-ray beams are parallel to Y axis, PA projection.

SIMULATION 7		
Phantom	Nº Voxels	580 x 260 x 300
	Voxel size (cm^3)	0.1 x 0.1 x 0.1
	Dimensions (cm^3)	58 x 26 x 30
	Materials	Human body materials
Source	Focal position (cm)	29 -32.65 15
	Spectra	100 keV monoenergetic and RQRs 6 - 9
	Histories	1006720000
Detector size (cm^2)		122.8 x 61.4
Source-to-detector distance (cm)		68.65

Table 15: Simulation 7

The simulation which uses a monoenergetic spectrum is also repeated with PENELOPE/penEasy using $1.2 \cdot 10^{10}$ histories. In this case, dose and maximum dose precision do not improve significantly, however the real simulation time increases. These results are at SIMULATION 7 LONG.

All the results tables obtained in this package of simulations are included in the APPENDIX C: SIMULATIONS' RESULTS because the tables which include the values and the comparison between programmes are too large[24]. The following tables and plots summarize the most important results.

	Dose Relative Errors				
	100 keV Monoenergetic	RQR 6	RQR 7	RQR 8	RQR 9
Air	0.17%	0.18%	0.14%	0.08%	0.20%
Muscle	0.09%	0.15%	0.16%	0.16%	0.17%
Soft tissue	0.09%	0.88%	0.72%	0.54%	0.36%
Bone	0.12%	0.26%	0.19%	0.14%	0.06%
Cartilage	0.11%	1.12%	0.75%	0.69%	0.50%
Adipose	0.02%	0.30%	0.28%	0.24%	0.18%
Blood	0.10%	0.19%	0.10%	0.19%	0.02%
Skin	0.03%	0.45%	0.42%	0.36%	0.28%
Lung	0.17%	0.65%	0.51%	0.42%	0.21%

Table 16: Simulation 7 dose relative errors

[24] Results at: SIMULATION 7

Real Simulation Time (s)		
Spectra	MC-GPU	PENEASY
100 keV Monoenergetic	128.54	61326.63
RQR 6	108.12	49790.51
RQR 7	110.86	51640.70
RQR 8	113.65	51355.24
RQR 9	116.13	54053.39

Table 17: Simulation 7 real simulation times

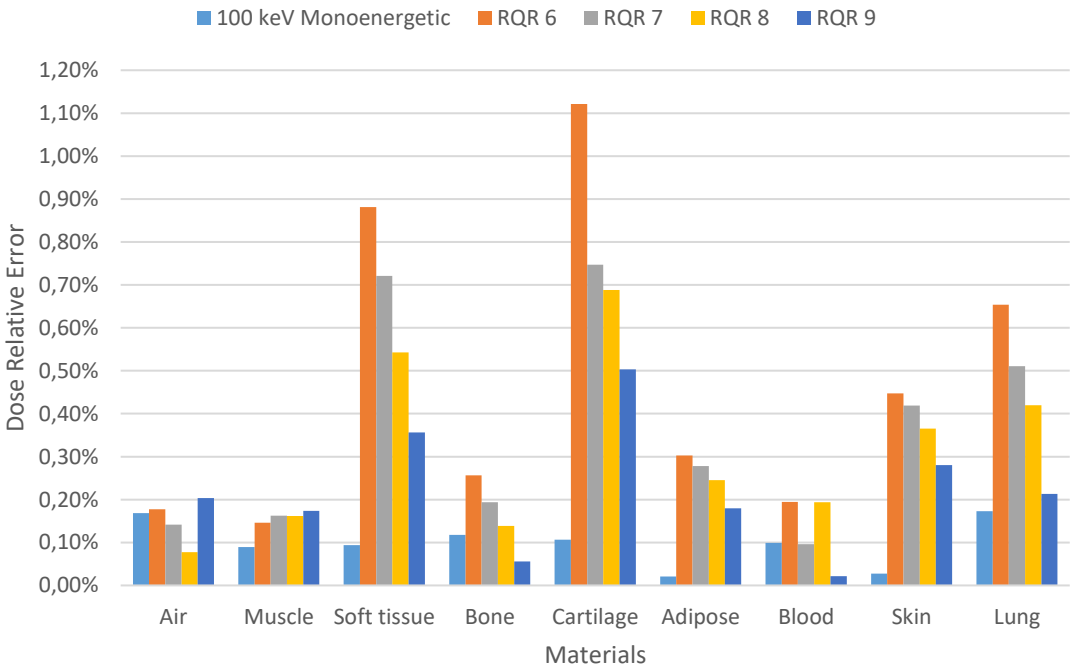

Figure 21: Simulation 7 dose relative errors

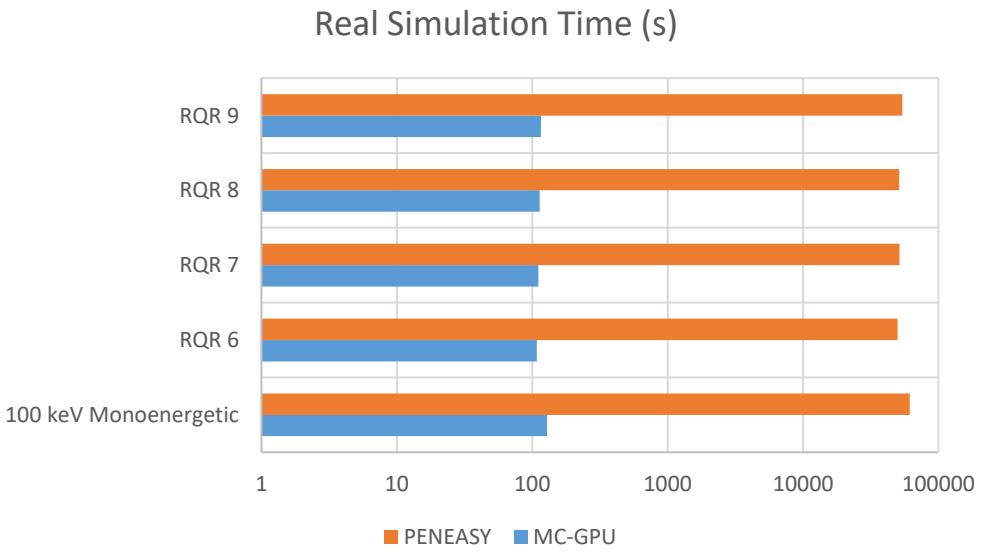

Figure 22: Simulation 7 real simulation time

Analysing the graphs, some conclusion can be extracted:

- The widely distributed materials (skin) are materials with large relative errors.
- All materials have low dose relative errors for a 100 keV monoenergetic spectrum.
- For most of materials, the higher the mean energy of the spectrum, the lower dose relative error.
- The used spectrum has not influence in the simulation time. The ratio between the MC-GPU and PENELOPE/penEasy simulation times is within 400 and 500.

In spite of everything mentioned before, the maximum relative error is approximately 1.1 %, what highlights the precision of the MC-GPU code in terms of dose calculations.

The repetition of the 100 keV monoenergetic spectrum simulation using a larger number of histories does not provide a significate results due to the large standard deviation in the maximum dose point in PENELOPE/penEasy. The dose relative errors of the materials are as precise as the simulations explained above.

Once few simulations are carried out and the obtained results are satisfactory, the MC-GPU Beta validation begins. At this point, the new material files were considered correct and the algorithm that compute the dose in MC-GPU validated.

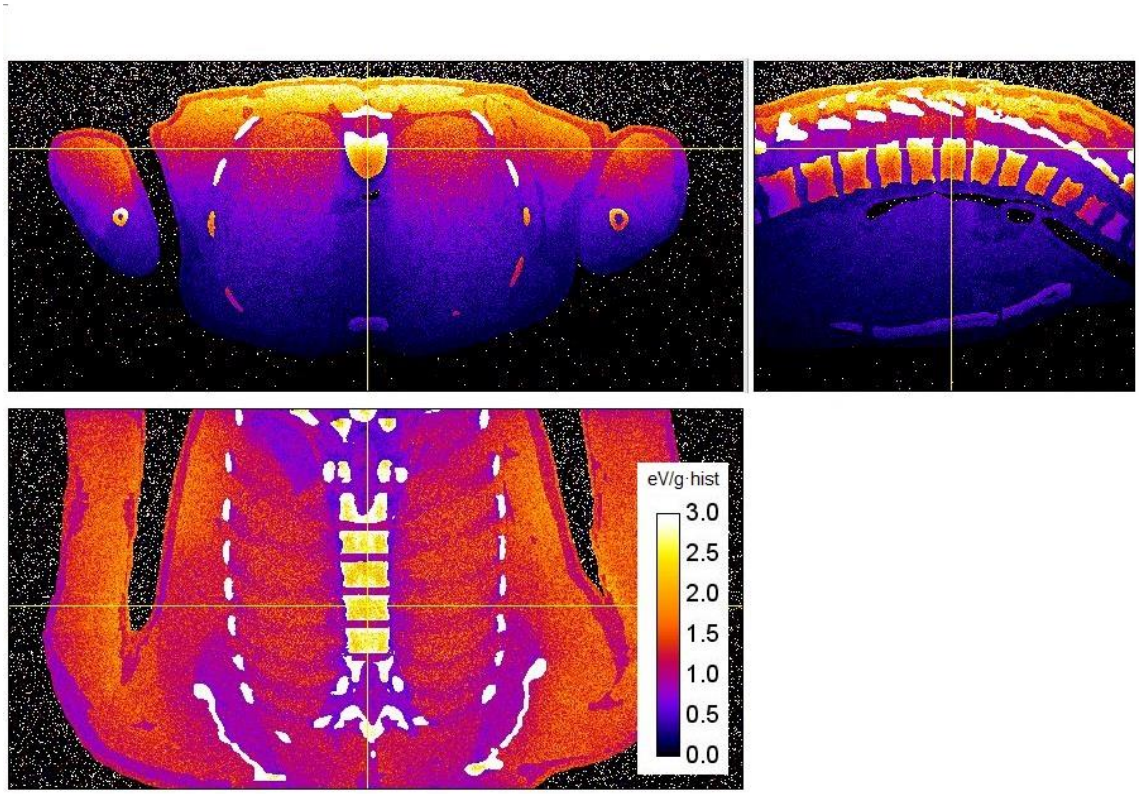

Figure 23: Simulation 7 using RQR 9 dose distribution

6.6 MC-GPU BETA VALIDATION

MC-GPU Beta is an extended version of the basic programme and includes a lot of new features as operator inclusion, shielding and one spectrum for each projection. However, this project is only focused on the validation of patient dose calculation and the source rotation is included. In this section, the Duke phantom, new materials and realistic spectra were used.

The complexity of this version are the angles and the rotations. Once the results obtained in MC-GPU were considered as enough accurate, the results obtained with MC-GPU Beta were compared to MC-GPU results and experimental measurements.

6.6.1 Simulation 8: Two projections

The first simulation run with MC-GPU Beta had two projections, PA and AP, with the Duke's phantom and focusing the beam to the chest. The simulation was repeated with MC-GPU to compare the results.[25]

SIMULATION 8		
Phantom	Nº Voxels	122 x 62 x 372
	Voxel size (cm^3)	0.5 x 0.5 x 0.5
	Dimensions (cm^3)	61 x 31 x 186
	Materials	Human body materials
Source	Initial focal position (cm)	30.5 -30.5 130
	C-arm radius (cm)	46
	Spectra	RQR 8 (PA) and RQR 9 (AP)
	MC-GPU Beta Simulation time (s)	150
	MC-GPU histories per simulation	1006720000
Detector size (cm^2)		143 x 143
Source-to-detector distance (cm)		71.5

Table 18: Simulation 8

Dose (eV/g·hist)	MC-GPU 1	MC-GPU 2	MC-GPU Total	MC-GPU Beta	Relative Error
Air	0.12815	0.18678	0.31493	0.32	0.174%
Muscle	0.23431	0.19600	0.43031	0.43	0.005%
Soft tissue	0.16054	0.20567	0.36621	0.37	0.003%
Bone	0.68175	0.46335	1.1451	1.15	0.000%
Cartilage	0.07868	0.18722	0.2659	0.27	0.101%
Adipose	0.17586	0.16412	0.33998	0.34	0.000%
Blood	0.13217	0.34773	0.4799	0.48	0.023%
Skin	0.25623	0.20848	0.46471	0.46	0.026%
Lung	0.33691	0.31644	0.65335	0.65	0.009%

Table 19: Simulation 8 dose results

The energy deposition relative errors for each material are all below 0.1 % (excluding air). Moreover, even with a higher standard deviation in the maximum point dose, the relative errors are less than 0.7 %. The coordinates of the maximum are the same in both codes.

[25] Results at: SIMULATION 8

6.6.2 Simulation 9: Main projections

After the outstanding results, a simulation with eight projections was performed. This simulation is more complex because the rotation angles gain importance. The position of each projection is shown in the figure. For this simulation the Duke's phantom is also used focusing the beam into the chest[26].

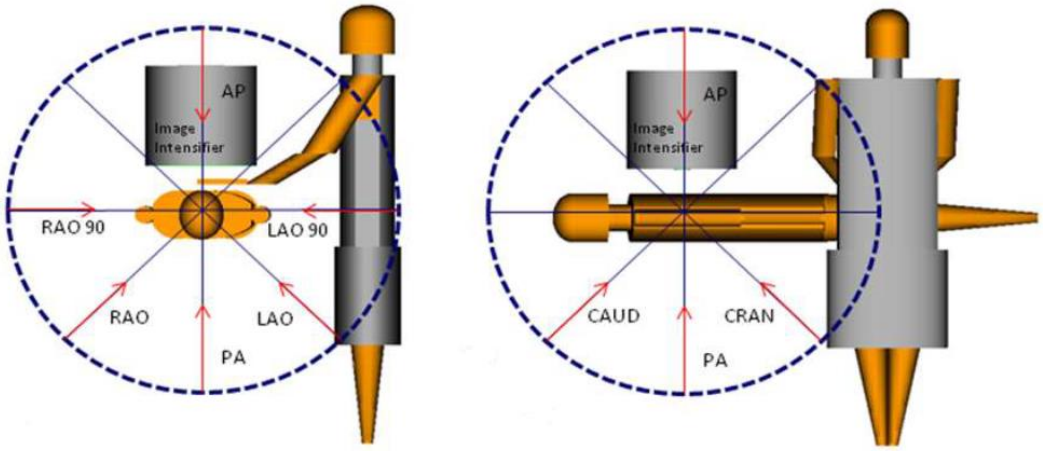

Figure 24: Projections and patient orientation (stylized phantoms)[27]

SIMULATION 9		
Phantom	Nº Voxels	122 x 62 x 372
	Voxel size (cm^3)	0.5 x 0.5 x 0.5
	Dimensions (cm^3)	61 x 31 x 186
	Materials	Human body materials
Source	Initial focal position (cm)	30.5 -29.5 124
	C-arm radius (cm)	45
	Spectra	RQR 6 and RQR 7
	MC-GPU Beta Simulation time (s)	150
	MC-GPU histories per simulation	1006720000
Detector size (cm^2)		55 x 55
Source-to-detector distance (cm)		81

Table 20: Simulation 9

The rotations of the projections are referred to the patient reference system and the PA initial position. The election of these projections is because they are the most common on interventional procedures.

Projections PA, AP and the rotated around Z axis used the RQR 6 spectrum and the projection caudal and cranial used the RQR 7 spectrum. This was to check the automatic change of spectrum in different projections, one of the MC-GPU Beta new features.

[26] Results at: SIMULATION 9
[27] EURADOS Report 2012-02 ORAMED: Optimization of Radiation Protection of Medical Staff

The obtained MC-GPU results for different projects were added and averaged to be compared with the MC-GPU Beta which does not sum the values automatically but it averages them.

All the obtained results are included in SIMULATION 9 in the appendices section.

The comparison generates exceptional results, the dose and energy deposition obtained in each projection are almost the same, the individual differences between them are below 0.1 %.

Total energy deposition relative error is a little higher (0.2 %) than the individual ones but it is an outstanding result. It is important to point out that the Air relative error is 100 % due to the MC-GPU Beta eliminates automatically the energy deposited in materials with such low density.

The conclusion is that the rotation of the source around the reference system axis are the expected and the results are incredible even when the spectra are not as simple as a monoenergetic one.

In this case, the simulation time comparison cannot be performed because in MC-GPU Beta the simulations are configured by time and not by the number of histories.

6.7 EXPERIMENTAL MEASUREMENTS

This is the last part of the validation and it includes the preparation of the experimental measurements, the simulations and the comparative between them.

6.7.1 Experiment preparation

Before the experimental measurement a preparation process was carried out. In this process the different experiments were established and the thermoluminescent dosimeters (TLDs) were selected and treated at the INTE's TLD Laboratory.

With the available slabs of the equivalent materials (bone, lung and plastic water) and different thickness, some phantoms were designed. This project only focuses on plastic water phantom whose dimensions are 30 x 15 x 30 cm^3.

Regarding the TLDs, they were erased by a thermal treatment and calibrated.

6.7.2 Experimental measurement

The photo shows the real set up of the plastic water sheets at the Vall d'Hebron Hospital. The image intensifier, the plastic supports and the couch also appear in the photo.

As it may be appreciated, the couch is without the mattress.

Below the phantom there was an ionization chamber to measure the air kerma and the irradiation time for each projection.

All data referred to the distance source-to-detector and the spectrum was provided by the computer (DICOM).

After the experiments, some irradiation where performed allocated the ionization chamber below and over the couch to compute the attenuation due to the couch.

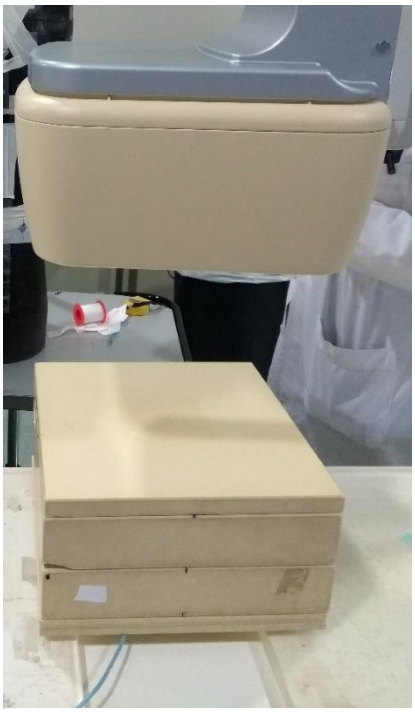

Figure 25: Experimental measurement assembly

DATA		
Floor-phantom	84.5	cm
Floor-source	29.5	cm
Intensifier	25x25	cm2
FDD	100	cm
Phantom	30*15*30	cm3
Phantom-source	55	cm

Table 21: Experimental measurement geometry data

Following image show a schematic draw of the whole assembly for a better visualization of the experiment.

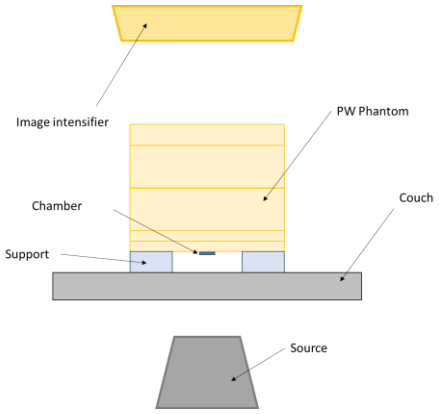

Figure 26: Experimental measurement scheme

With this configuration, different irradiations were performed:

- PA and TLD's at 1 cm depth within the plastic water phantom, central axis
- PA and TLD's at 7 cm depth within the plastic water phantom, central axis
- PA and TLD's at 13 cm depth within the plastic water phantom, central axis

6.7.3 Simulation 10

Before carry out the simulations, some additional tasks were performed:

- Material creation: knowing the chemical composition and the density of the plastic water the slabs are made of, the material was generated in PENELOPE 2014 (.mat) and converted into MC-GPU material data file format (.mcgpu).
- Couch thickness estimation: knowing the air kerma for a spectrum below and above the couch without and knowing the inherent and added filtration of the x-ray tube employed, the XCOMP5r was used to estimate the thickness of equivalent aluminium, it was 0.8 mm Al.
- Voxelized geometry creation: this was created taking into account the 0.8 mm Al, 2 cm air and the real dimensions of the phantom. The result was a 9 x 453 x 9 voxels phantom whose unitary dimensions are 3.33 x 0.04 x 3.33 cm^3.

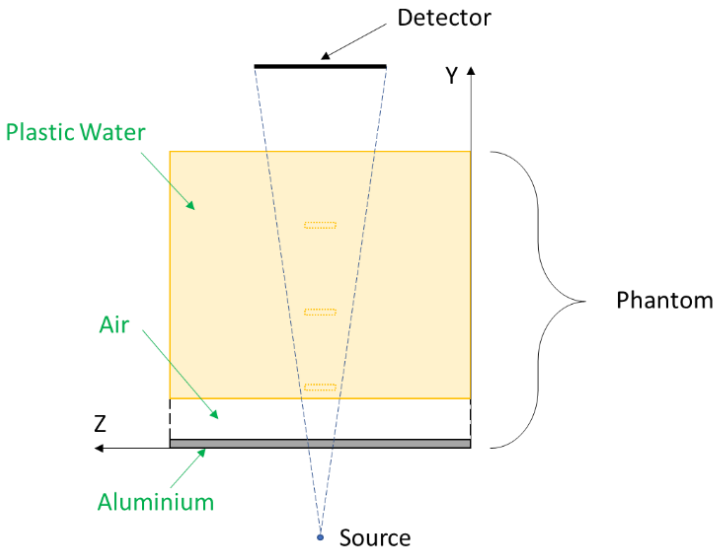

Figure 27: Simulation 10 scheme

In order to compare results of simulations and measured by the detectors, it was needed to locate some air voxels at the defined distances.

To obtain the simulated air kerma where the ionization chamber was allocated, the simulation was made changing the plastic water into air.

6.7.4 Comparative

The conversion factor to transform eV/g·hist into mGy is computed dividing the air kerma measured with ionization chamber and the air kerma resulted in the simulation with air phantom.

Projection	Depth (cm)	TLDs (mGy)	Kair (mGy)
PA	1	3.6204	3.618
PA	7	1.0608	5.474
PA	13	0.1459	3.807

Projection	Depth (cm)	Simulation (eV/g·hist)	Kair (eV/g·hist)
PA	1	25.466	24.823
PA	7	5.327	24.823
PA	13	1.109	24.823

Projection	Depth (cm)	Simulation mean (mGy)	Factor (mGy/(ev/g·hist))
PA	1	3.712	0.146
PA	7	1.175	0.221
PA	13	0.170	0.153

Projection	Depth (cm)	MEAN Relative Error
PA	1	2.52%
PA	7	10.74%
PA	13	16.62%

Table 22: Simulation 10 and experimental measurement results

The comparative shows good results but the accuracy gets worse as the depth increases. The possible causes of discrepancies may be the absorption coefficient of materials, the disregarded standard deviation of calibrated dosimeters, other sources of uncertainties as the simulated spectrum or the couch thickness and fine air layers between plastic water sheets.

It was also checked that the dose measured by TLDs has a high dependency on the spectrum used to calibrate them.

This experiment is just one of those that took place at the Vall d'Hebron Hospital. The end of this project constitutes a good starting point for the experimental phase in which more complex phantoms and geometries will be compared to MC-GPU simulations.

7. CONCLUSIONS

This thesis is aimed at analysing the MC-GPU code in order to find some possible improvements and validating the MC-GPU results with other Monte Carlo simulation code. Other additional objective is the elaboration of a user manual of the programme. The main conclusions of this thesis are the following:

1. **This thesis includes updating the code to the most current version possible.**

   Once the original version of the code was analysed the code that generates the MC-GPU material files was updated and subsequently the new results were validated. The results were the expected ones and from this moment the new materials were used for all simulations.

2. **The results collected in this thesis validate the code for the calculation of doses in patients.**

   All the simulations carried out in this thesis aimed to analyse the doses in patients. The simulations performed with MC-GPU and PENELOPE / penEasy show very low relative errors, mainly due to the approximations used by the MC-GPU to perform the dose calculations with a much higher speed than PENELOPE/penEasy. The results obtained with different voxelized geometries, materials, spectra and layouts are sufficiently precise to validate the algorithm used by the MC-GPU.

3. **One of the appendix of this thesis provides the first version of the MC-GPU user manual.**

   The user handbook developed during this project, in parallel with other activities, constitutes a first useful version for future users of the programme. This manual helps beginner users, explains how to perform simulations with MC-GPU and how to do the data post-processing. This version will need continuous improvement and it is expected that future updates will be made by future users.

4. **This thesis highlights the strength and weaknesses of the MC-GPU and MC-GPU Beta programme as well as the future work to do in order to improve them.**

   The simulations performed show the outstanding precision and speed compared with standard codes. However, there are points of improvement in topics such as voxelized geometries or automation.

The conclusions of this thesis could be used to continue the work in the short-term to improve the programme and achieve the objectives of the MEDIRAD project.

8. FUTURE WORK

In the introduction of this thesis, it is explained that this project is just the first work of the requested works to INTE-UPC in the MEDIRAD project. For this reason, the studies and the research in this topic and the main project will continue.

8.1 MEDIRAD/PODIUM

Regarding the MEDIRAD project, the term of the completion of the project is four years. The research will continue until the consecution of its three major operational objectives.

Another European project named PODIUM[28] has begun concurrently to MEDIRAD project. The acronym PODIUM stands for *Personal Online Dosimetry Using Computational Methods*, which main objective is to improve personal dosimetry by using an innovative tool based on an on-line application. The validation and verification of results and user manual developed during this project will be use in this new project.

For its part, INTE-UPC group in which this project has been developed is also working in both projects, MEDIRAD and PODIUM. Moreover, this group is involved in other projects and collaborations with hospitals and research centres, so the studies will continue.

To continue this project in the short-term, some tasks and work must be done in the following areas:

- Improve the precision of the phantoms. Using smaller voxels, more materials and segmented phantoms. All these tasks should be done to reduce the uncertainties.
- Automatization of the program. It is important to work in programmes which connect the MC-GPU Beta with DICOMs and depth cameras.
- Automatic conversion factors from eV/g·hist to Gy using experimental data.

8.2 COMMERCIAL PRODUCT

At the beginning of this thesis, it was expounded that this project consisted just in a proof of concept or technology testing, but the final aim of the main project is the achievement of a commercial software.

Currently, in the medical equipment market there is not an alternative which the characteristics and performance that MC-GPU software offers.

The following steps are divided in two ways:

- The technical path: all modules' software must be validated and tested. The compatibility study with the tracking cameras and the X-ray tubes to connect all. Additionally, x-ray tube manufacturers must be consulted.
- The commercial path: the medical personnel consulted before the project showed their interest in a product like this, but a more exhaustive market analysis will be necessary. Also, the patents analysis and request the appropriate one to the relevant entities must be done.

The initial results were promising, but efforts would have to continue over the long term if definite and sustainable results were to be achieved.

[28] Some additional information on: http://www.irrs.eu/documents/IRRS2017Programme.pdf

9. EXPECTED IMPACT AND SUSTANABILITY

9.1 ENVIRONMENTAL IMPACT

As a research project the environmental impact is certainly not relevant. Most of the project is made by a computer, simulations and documentation. The only impact may be considered is the electricity cost of the computers, but it is negligible. At the end of the project when the final product will be finished, this impact will be more relevant.

9.2 ECONOMIC IMPACT

This kind of impact is similar to the previous one, the most important costs are the referred to human resources, those concepts are included in the project budget. At the end of the MEDIRAD project, when the final product will be commercialized, this impact will be the most important one.

9.3 TECHNOLOGICAL IMPACT

Besides the main aims, the knowledge and technology transfers are direct consequence of the project. All the technology developed and improved during the project may be used in other no related fields with this topic. For example, NDT procedures.

9.4 INSTITUTIONAL IMPACT

This project is part of MEDIRAD, project brings together 33 partner institutions from 14 European countries. The multi-disciplinary consortium includes clinical experts, scientists and policy makers in the fields of medical, radiation protection and nuclear research from hospitals, universities and major research centres across Europe. In close interaction with European medical associations (EANM, EFOMP, EFRS, ESR and ESTRO), MELODI, EURADOS and EURAMED.

The collaboration among different disciplines groups of different countries reinforces the relations of the EU members and the people who work in various fields.

9.5 SOCIAL IMPACT

The project has a noticeable social character since the final users of the software will be the patients and the medical workers. The final purpose of the projects is monitoring and controlling the doses received by both, patients and operators, to avoid any kind of harm.

9.6 EPISTEMOLOGICAL IMPACT

As this project is a research project, the epistemological impact is one, if not, the most important impact. All worked developed during this project will be used by the collaborators who continue the research and the MEDIRAD and PODIUM projects.

One of the main tasks of this project is the elaboration of the user manual, which will be use by all the future users of the programme and will help them if any new updating of the code will be necessary.

In addition, the libraries of spectra and material files are prepared so that future users can use them easily.

10. PROJECT EXECUTION

This part of the thesis shows the scheduling of the project, its budget and the work packages in which the project is divided.

It is important to note that this section explains how the real project was carried out, which is different from what was originally planned.

10.1 WORK SCHEDULE

Following the work packages are explained. Those are separated in six stages chronologically organized.

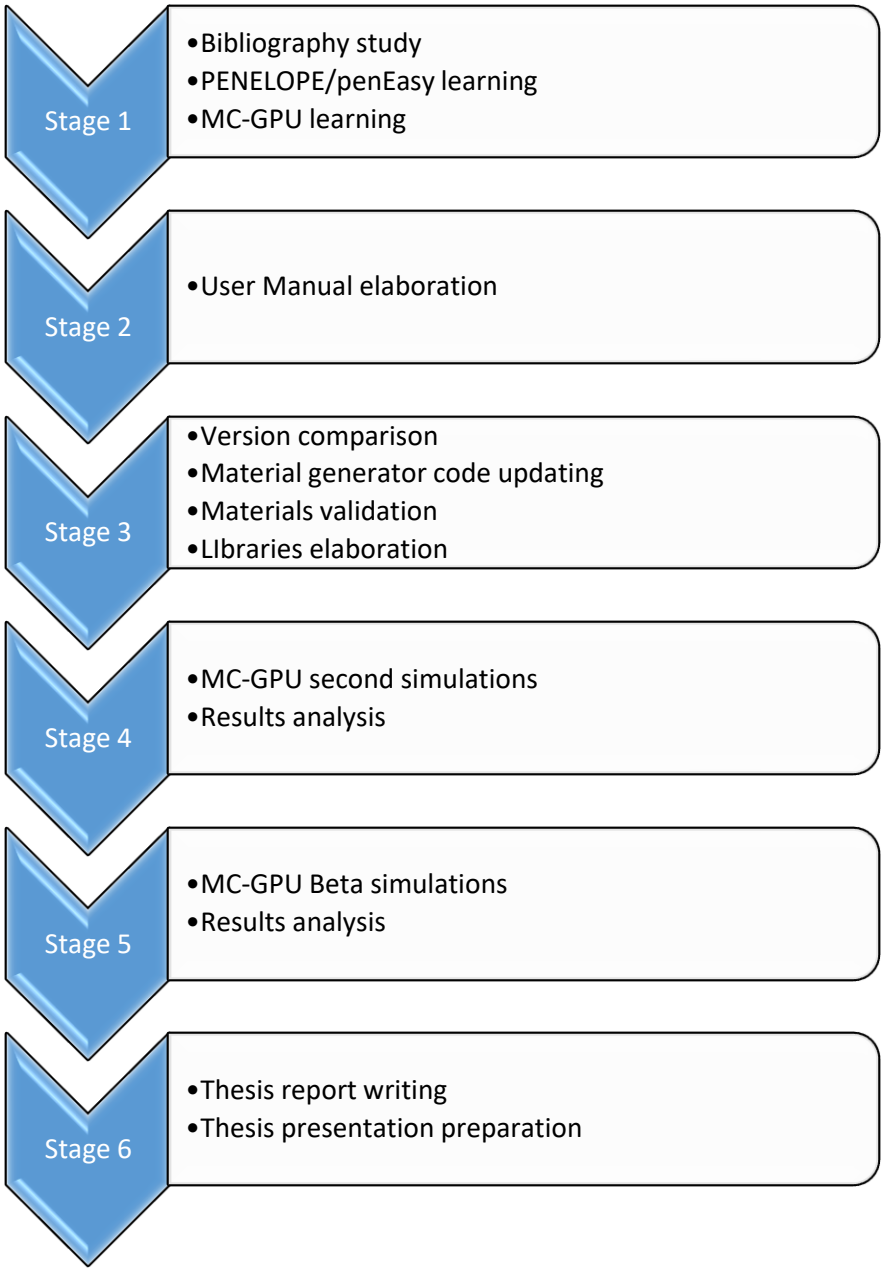

Figure 28: Work Packages

STAGE 1

- Bibliography study: the project begins with a learning stage through the reading of books and articles on physics and computation, related papers and the documentation provided by the MC-GPU code author.
- PENELOPE/penEasy learning: since this programme is used during the project it is necessary to know how to use it. Reading of the bibliography provided by the authors and some explained examples were carried out. Also, learning how to create geometries and materials.
- MC-GPU learning: understand the necessary inputs to carry out the simulations and the output files as well as learn how to obtained are the tasks included in this step.

STAGE 2

- User Manual elaboration: the preparation of the user manual takes place during the whole stage, as the initial tests were carried out.

STAGE 3 (Delayed. It was not executed as planned)

- Version comparison: the comparison of the PENELOPE's versions.
- Material generator code updating: once the option to update the material generator code is chosen, the study of the code takes place. Since the code is written in Fortran, learning basic concepts of this programming language is necessary.
- Materials validation: material files are generated using the updated code. These materials are used to repeat the simulations carried out in the previous stage and the results are compared.
- Libraries elaboration: a materials library is generated with the updated material generator code and a spectra library with the XCOMP5r.

STAGE 4

- MC-GPU second simulations: this stage was planned but delayed by the tasks not initially planned. Simulations with more complex geometries and spectra are carried out. Same simulations are done with PENELOPE/penEasy.
- Results analysis: results of both programmes are compared to validate de results.

STAGE 5

- MC-GPU Beta simulations: this stage was also delayed. The most complex simulations emulating a real procedure are carried out in this stage.
- Results analysis: results are compared with some experimental measurements.

STAGE 6

- Thesis report writing: documentation of all the project in the Final Master Thesis.
- Thesis presentation preparation: preparation of the audio-visual support used in the presentation of the project.

10.1.1 GANTT DIAGRAM

ACTIVITY	PLANNED BEGINNING	PLANNED DURATION	REAL BEGINNING	REAL DURATION	COMPLETED PERCENTAGE
STAGE 1					
Bibliography study	1	4	1	4	100%
PENELOPE/penEasy learning	2	3	2	3	100%
MC-GPU learning	3	2	3	2	100%
STAGE 2					
User Manual elaboration	5	11	5	11	100%
STAGE 3					
Version comparison	5	9	5	9	100%
Material generator code updating	0	0	7	7	100%
Materials validation	0	0	14	1	100%
Libraries elaboration	0	0	15	1	100%
Christmas Holidays	16	2			
STAGE 4					
MC-GPU second simulations	0	0	18	4	100%
Results analysis	0	0	22	1	100%
STAGE 5					
MC-GPU Beta simulations	0	0	18	4	100%
Results analysis	0	0	22	1	100%
STAGE 6					
Thesis report writting	23	4	23	4	100%
Thesis presentation preparation	27	1	27	1	100%
Holy Week Holidays	28	1			

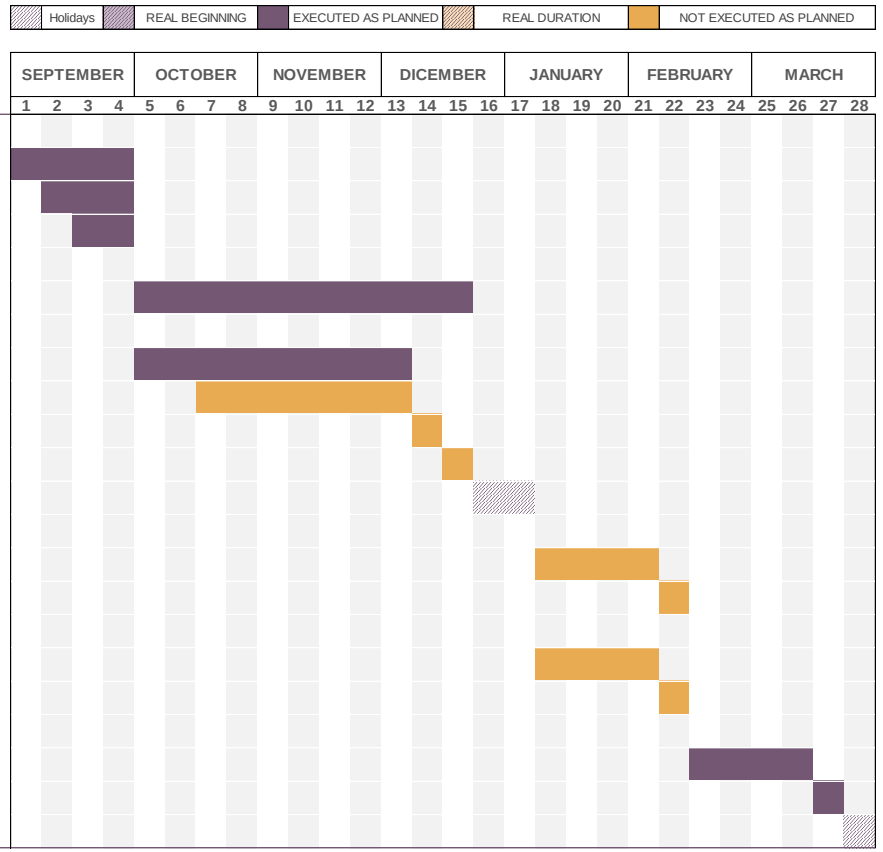

Figure 29: Gantt Diagram

ETSEIB

10.1.2 PERT DIAGRAM

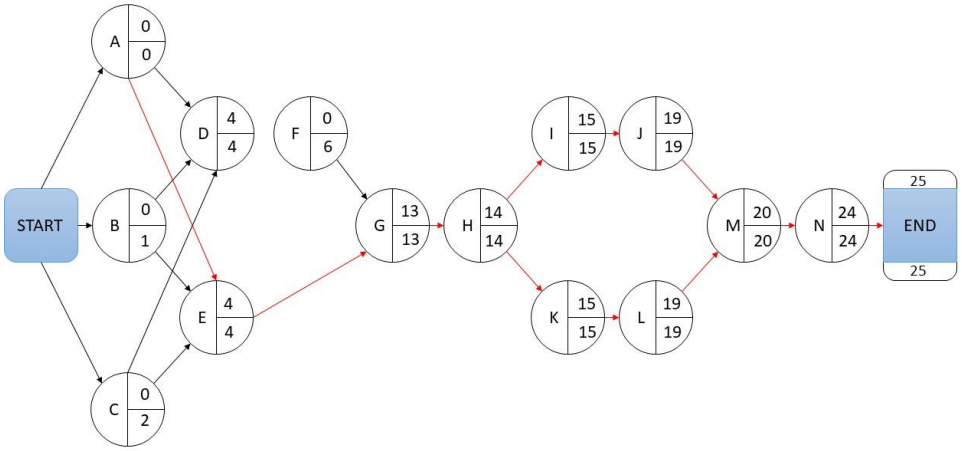

Figure 30: Pert Diagram

Task		Duration	Precedent
STAGE 1			
A	Bibliography study	4	-
B	PENELOPE/penEasy learning	3	-
C	MC-GPU learning	2	-
STAGE 2			
D	User Manual elaboration	11	A,B,C
STAGE 3			
E	MC-GPU first simulations	9	A,B,C
F	Material generator code updating	7	-
G	Materials validation	1	E,F
H	Libraries elaboration	1	G

Task		Duration	Precedent
STAGE 4			
I	MC-GPU second simulations	4	H
J	Results analysis	1	I
STAGE 5			
K	MC-GPU Beta simulations	4	H
L	Results analysis	1	K
STAGE 6			
M	Thesis report writing	4	J,L
N	Thesis presentation preparation	1	M

Table 23: Work Packages

10.1.3 CRITICAL RISKS IN THE IMPLEMENTATION

As mentioned at the beginning of this section, the scheduling showed in this thesis (Gantt and PERT diagrams) are the real and the executed ones. For this reason, the critical path and the critical tasks that delay the projects are known.

First of all, the stage of learning, stage one, is one of the most important due to it is in the critical path of the project whose duration depends on it. This step is important because huge volume of information has to be analysed.

The version comparison took more time than the expected This incident changed the original schedule delaying the following tasks.

Once that problem was solved, the simulation package was carried out, and this is one of the most important points. The time of simulations preparation, the simulation time with PENELOPE/penEasy and the number of simulations is the third key parameter which was critical in the project duration.

To avoid problems due to these three factors, the simulations are carried out in the INTE-UPC cluster Argos2, which allows running simulations in parallel. Moreover, as the simulations duration are too large, the simulations are launched to run during the nights.

On the other hand, as MC-GPU and PENELOPE/penEasy simulations are run in different ports of the cluster, they are prepared and run in parallel.

Last steps about results analysis and documentation do not show complexity.

10.2 TIME AND COST ANALYSIS

This section includes the used equipment during the project and tables of costs and dedication time.

This is a seven months' project, from September 2017 to March 2018. The diary dedication is of 4 hours. The total number of hours is approximately 560 hours. The labour cost of this project is summered in the following table:

CONCEPT	COST (€)
Junior Engineer	6720
Senior / Advisors	4200
TOTAL	10920

Table 24: Human Resources costs

The budget of this project is very simple due to the most of the project is based on computer simulations.

CONCEPT	UNITARY COST (€/unit)	UNITS (unit)	TOTAL COST (€)
PC	800	1	800
Pack of 500 sheets	3	1	3
TOTAL			803

Table 25: Equipment costs

Complementary costs of consumption of the project are approximately:

CONCEPT	UNITARY COST	UNITS	TOTAL COST (€)
Electricity[29]	0.13 €/kWh	1 kW · 560h	72.80
Computer electricity	0.13 €/kWh	0.5 kW · 560 h	36.40
Water[30]	0.00166 €/L	50 L/d · 140 d	11.62
TOTAL			120.82

Table 26: Complementary costs

The estimated cost of the whole project is 11843.82€

[29] Electricity mean price obtained from ENDESA webpage.
[30] Data provided by OCU. The Price is the Spanish mean Price.

11. APPENDICES

In this section, three different appendices are included. Each appendix corresponds to a stage of the project and they are organized chronologically.

Appendix A: MC-GPU User Manual v1.0

Appendix B: This appendix includes the updated material generator code as well as part of a material data file and entire spectrum file. The original versions of codes and materials may be found in the download package provided by the MC-GPU coder.

Appendix C: Results of all simulations, included or not in this thesis, carried out during the project are collected in different Excel files, most of the results are attached in this appendix.

11.1 APPENDIX A: USER MANUAL

The User Manual elaborated during the project is a completely independent document with its own cover, index and bibliography, for this reason, it is a document attached to and not included in this thesis.

11.2 APPENDIX B: UPDATED CODE AND NEW FILES

11.2.1 Code update process

The first matter to take into account before modify Fortran codes based on PENELOPE code is to know that in the latest version of PENELOPE, 2014 version, the RITA initialization functions are in a separate subroutine package called rita.f.

Attending to the code **MC-GPU_create_material_data.f** itself, it may be noticed that the variables used on it are the same which were used in PENELOPE 2006 and they have been named different in PENELOPE 2014, even some of them also have changed its meaning. For this reason, the first task is identifying in the new PENELOPE code the variables necessary in the materials generator code.

Following the modifications and additions in the new MC-GPU materials generator code are showing. Also, some comparative screenshots between the old and new codes are presented.

- At the beginning, the Fortran files penelope.f and rita.f files (both 2014 version) are included.

- The penelope.f (2014 version) had been previously modified:
  - PENELOPE_mod and TRACK-mod are disabled
  - MAXMAT and NEGP parameters are added manually and also few COMMON blocks.

- Variables initialization

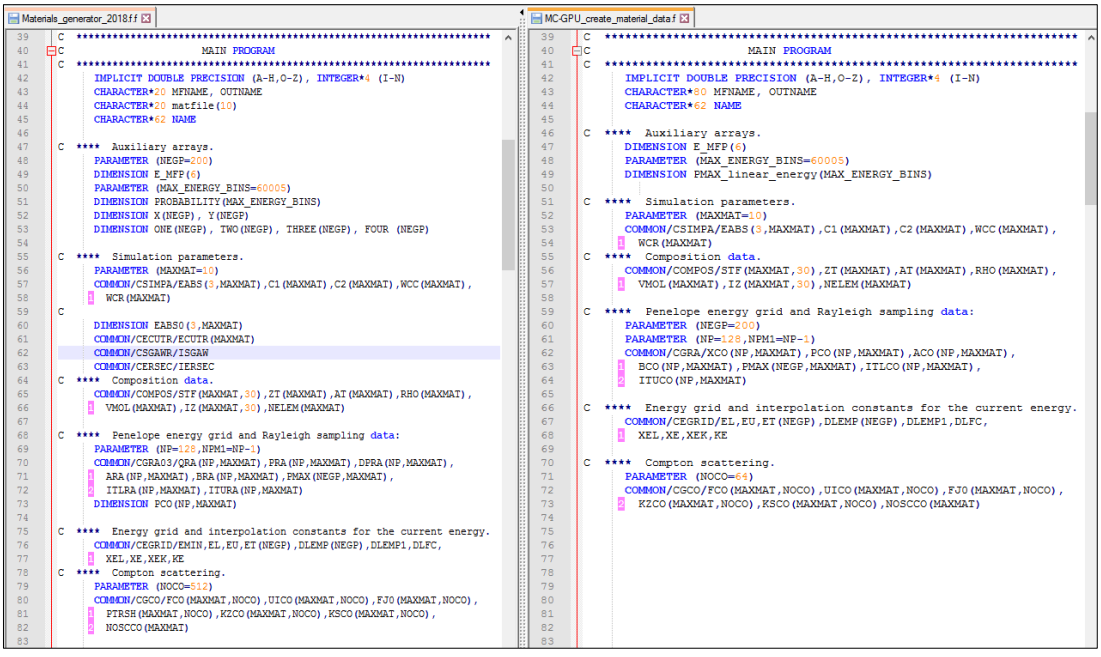

Figure 31: Variables initialization

- The main modifications are made in the COMMON blocks which depends directly of the penelope.f file.

- Moreover, few new variables are added in the auxiliary array section.

- Inputs demand: the part in which the user must introduce the variables and the name of the input and output files has not been modified with the only exception of names format.

Figure 32: Inputs demand

- PENELOPE initialization with material information: the parameters which initialize PENELOPE are the same. In both cases the Fortran code calls the PENELOPE subroutine PEINIT to get the material information.

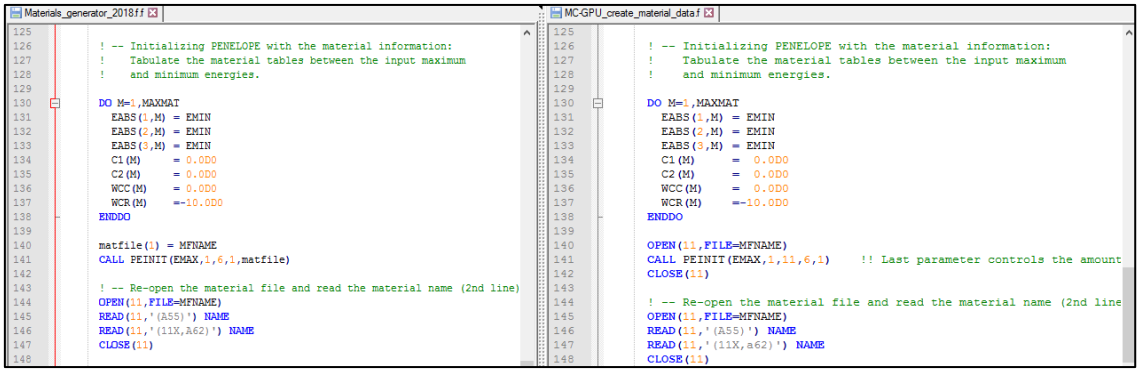

Figure 33: PENELOPE initialization with material information

- Next part of the code has not suffered any modification because is just the part in which the material (the only one) and the type of particle (photon) are chosen and also the header of the output file is written.

- MFP loop: as the figure shows this part is which has suffered more modifications.

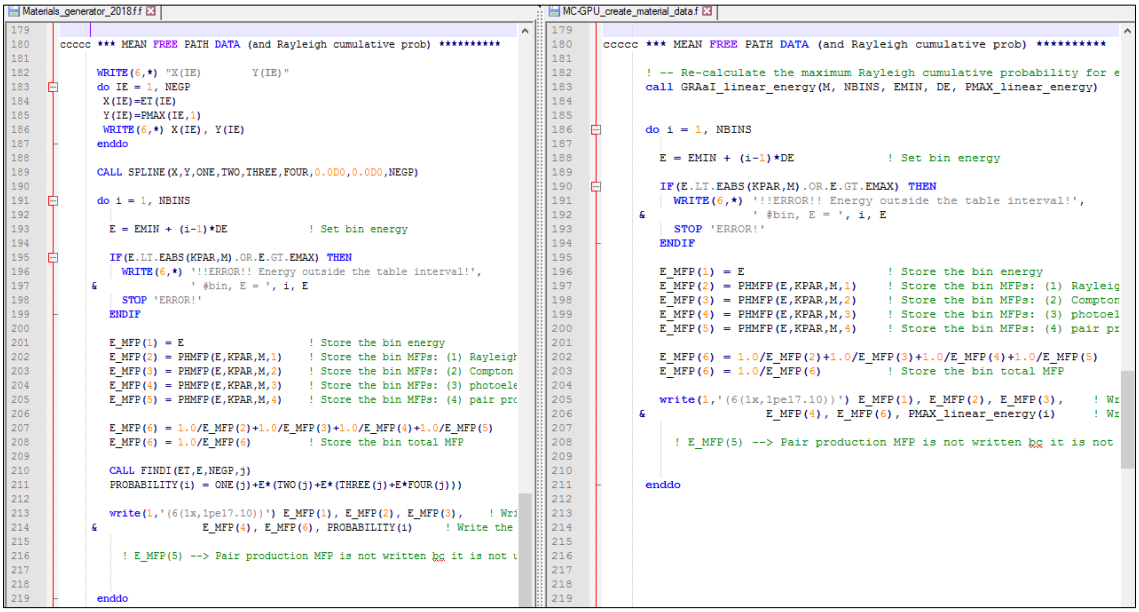

Figure 34: MFP loop

First, it is important to notice that the subroutine GRAaI_linear_energy, which was part of the programme itself, is totally erased in the new version of the code. This subroutine re-inited random sampling for Rayleigh scattering using the input linear energy scale. In order words, it re-calculated the maximum Rayleigh cumulative probability for each linear energy bin instead of the PENELOPE grid.

Instead of using this subroutine, the decision was to use PENELOPE variables like ET(IE) and PENELOPE functions like SPLINE and FINDI.

The arrays X and Y stores the logarithmical energy steps and the maximum Rayleigh cumulative probability from PENELOPE respectively. All this data is used later in the function SPLINE, which makes a cubic spline interpolation of tabulated data, getting the spline coefficients of the interpolating cubic polynomial in each interval.

Then, the function FINDI is used to find the interval that contains the value of the new lineal energy grid points.

Once the coefficients of the polynomial for each stretch have been obtained and the stretch in where all the lineal energy grid points are located, the array PROBABILITY stores the maximum Rayleigh cumulative probability for each linear energy bin.

Attending to the MFP for the different interactions, the values are obtained using the PENELOPE subroutine PHMFP which stores the MFP in centimetres. Only the MFP for Rayleigh, Compton, Photoelectric and total are included in the output file.

- Rayleigh Data: modifications in this section are divided in two.
  - Related to name. As the figure shows, the most of variables of this section changed their names from one version to other.
  - Cumulative probability PCO. The CUDA codes need to have in the second column (variable PCO) the accumulative probability. This is the reason of the do loop in which variables from PENELOPE are used.

- Compton Data: in this section of the code, no modifications were made. The variables are named in the same way in both PENELOPE versions. This part just takes the necessary variables from PENELOPE material fil (.mat) and write them in the output file (.mcgpu).

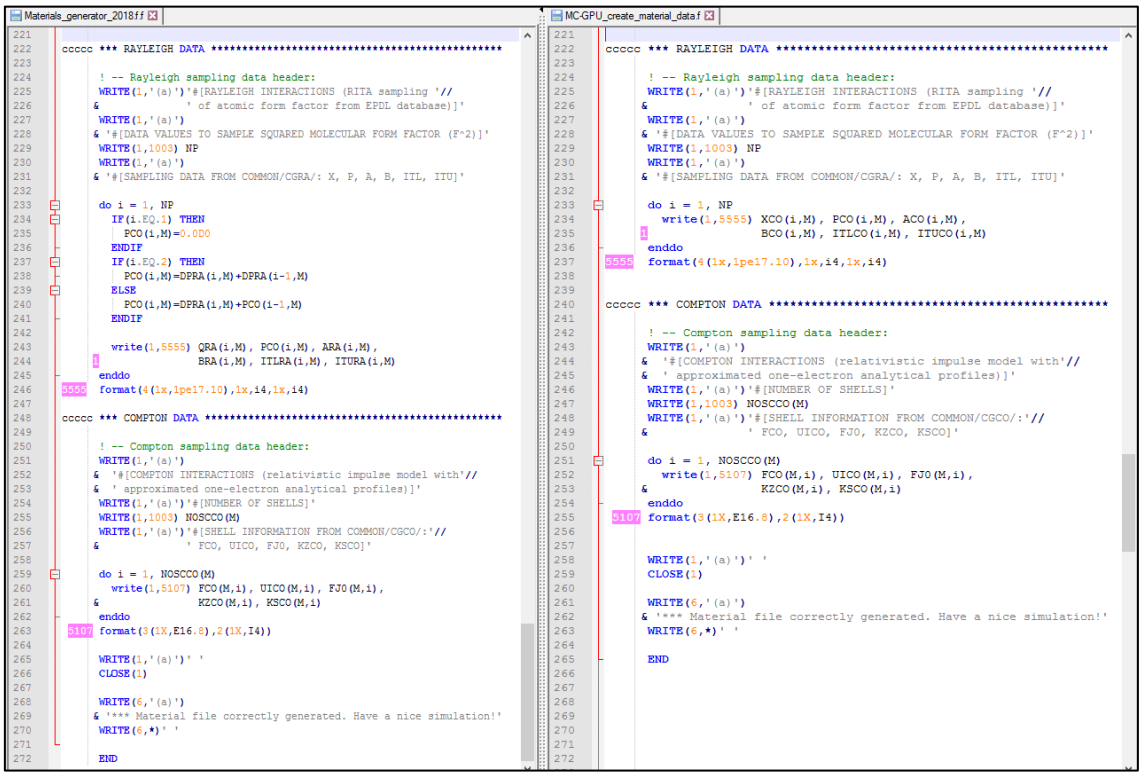

Figure 35: Rayleigh and Compton Data

No modifications in CUDA codes were required.

11.2.2 Material_generator_2017.f

Figure 36: Material generator 2017 code

```
C  ****  Files included to simplify compilation.
      INCLUDE 'penelopeDICIEMBRE.f'
      INCLUDE 'rita.f'

CCCCCCCCCCCCCCCCCCCCCCCCCCCCCCCCCCCCCCCCCCCCCCCCCCCCCCCCCCCCCCCCCCCCCCCCCC
C                                                                      C
C   This program reads a PENELOPE 2014 material file and outputs a     C
C   table with photon interaction mean free paths (MFP), and data for  C
C   Rayleigh and Compton interaction sampling.                         C
C                                                                      C
C   While the PENELOPE database is linearly interpolated in LOG-LOG,   C
C   the energy grid in the output table is a linear, ie, has equally   C
C   spaced energy bins. A small bin width is required to allow direct  C
C   linear interpolation of the MFP, avoiding the LOG computation.     C
C                                                                      C
C   This source code is based on PENELOPE's "tables.f".                C
C                                                                      C
C                      Andreu Badal, 2009-03-31/ Álvaro Merino, 2017   C
CCCCCCCCCCCCCCCCCCCCCCCCCCCCCCCCCCCCCCCCCCCCCCCCCCCCCCCCCCCCCCCCCCCCCCCCCC

CCCCCCCCCCCCCCCCCCCCCCCCCCCCCCCCCCCCCCCCCCCCCCCCCCCCCCCCCCCCCCCCCCCCCCCCCC
C --Copyright notice from tables.f and penelope.f:                     C
C                                                                      C
C  PENELOPE/PENGEOM (version 2014)                                     C
C  Copyright (c) 2001-2014                                             C
C  Universitat de Barcelona                                            C
C                                                                      C
C  Permission to use, copy, modify, distribute and sell this software  C
C  and its documentation for any purpose is hereby granted without     C
C  fee, provided that the above copyright notice appears in all        C
C  copies and that both that copyright notice and this permission      C
C  notice appear in all supporting documentation. The Universitat de   C
C  Barcelona makes no representations about the suitability of this    C
C  software for any purpose. It is provided 'as is' without express    C
C  or implied warranty.                                                C
CCCCCCCCCCCCCCCCCCCCCCCCCCCCCCCCCCCCCCCCCCCCCCCCCCCCCCCCCCCCCCCCCCCCCCCCCC

C  ***********************************************************************
C                       MAIN PROGRAM
C  ***********************************************************************
      IMPLICIT DOUBLE PRECISION (A-H,O-Z), INTEGER*4 (I-N)
      CHARACTER*20 MFNAME, OUTNAME
      CHARACTER*20 matfile(10)
      CHARACTER*62 NAME
C
C  ****  Auxiliary arrays.
      PARAMETER (NEGP=200)
      DIMENSION E_MFP(6)
      PARAMETER (MAX_ENERGY_BINS=60005)
      DIMENSION PROBABILITY(MAX_ENERGY_BINS)
      DIMENSION X(NEGP), Y(NEGP)
      DIMENSION ONE(NEGP), TWO(NEGP), THREE(NEGP), FOUR (NEGP)
C
C  ****  Simulation parameters.
      PARAMETER (MAXMAT=10)
      COMMON/CSIMPA/EABS(3,MAXMAT),C1(MAXMAT),C2(MAXMAT),WCC(MAXMAT),
        WCR(MAXMAT)
C
      DIMENSION EABS0(3,MAXMAT)
      COMMON/CECUTR/ECUTR(MAXMAT)
      COMMON/CSGAWR/ISGAW  ! Controls warning messages from SUMGA.
      COMMON/CERSEC/IERSEC
C
C  ****  Composition data.
      COMMON/COMPOS/STF(MAXMAT,30),ZT(MAXMAT),AT(MAXMAT),RHO(MAXMAT),
        VMOL(MAXMAT),IZ(MAXMAT,30),NELEM(MAXMAT)

C  ****  Penelope energy grid and Rayleigh sampling data:
      PARAMETER (NP=128,NPM1=NP-1)
      COMMON/CGRA03/QRA(NP,MAXMAT),PRA(NP,MAXMAT),DPRA(NP,MAXMAT),
        ARA(NP,MAXMAT),BRA(NP,MAXMAT),PMAX(NEGP,MAXMAT),
        ITLRA(NP,MAXMAT),ITURA(NP,MAXMAT)
      DIMENSION PCO(NP,MAXMAT)
```

```
C
C  ****  Energy grid and interpolation constants for the current energy.
      COMMON/CEGRID/EMIN,EL,EU,ET(NEGP),DLEMP(NEGP),DLEMP1,DLFC,
        XEL,XE,XEK,KE
C
C  ****  Compton scattering.
      PARAMETER (NOCO=512)
      COMMON/CGCO/FCO(MAXMAT,NOCO),UICO(MAXMAT,NOCO),FJ0(MAXMAT,NOCO),
        PTRSH(MAXMAT,NOCO),KZCO(MAXMAT,NOCO),KSCO(MAXMAT,NOCO),
        NOSCCO(MAXMAT)

      WRITE(6,*)" "
      WRITE(6,*)" "
      WRITE(6,*)"          **********************************"
      WRITE(6,*)"          *** MC-GPU_create_material_data ***"
      WRITE(6,*)"          **********************************"
      WRITE(6,*)" "
      WRITE(6,*)" "
      WRITE(6,*)"    Creating a material input file for MC-GPU."
      WRITE(6,*)
     &"    This program reads a PENELOPE 2014 material file and outputs"
      WRITE(6,*)
     & "    a table with photon interaction mean free paths (MFP) and"
      WRITE(6,*)
     & "    data for Rayleigh and Compton interaction sampling."
C
C  ****  Parameters (to tabulate the complete energy range and to switch
C        soft interactions off).
C
C  ****  Material data file.
C
      WRITE(6,'(a)') '  '
      WRITE(6,'(a)') '  -- Enter the energy range to tabulate: '//
     &           ' Emin, Emax (eg, 5000  125000):'
      READ(5,*) EMIN, EMAX
      WRITE(6,'(a)') '  -- Enter the number of energy bins (eg, 8192):'    ! 8192 =
      2^13
      READ(5,*) NBINS
      DE=(EMAX-EMIN)/DBLE(NBINS)
      WRITE(6,'(a,1pe17.10)')
     &       '      - Energy bin width set to (EMAX-EMIN)/NBINS = ',DE
      WRITE(6,'(a)') '  -- Enter the name of the PENELOPE 2014'//
     &                ' material data file (eg, water.mat):'
      READ(5,'(A20)') MFNAME
      WRITE(6,'(a)') '  -- Enter the name of the output data file'//
     &               'for MC-GPU (eg, water.mcgpu)...'
      READ(5,'(A20)') OUTNAME
      WRITE(6,'('' Material data file:  '', A24)') MFNAME
      WRITE(6,'(a)') '  '
      WRITE(6,'(a)') 'Processing material data. Please, wait...'

      ! -- Initializing PENELOPE with the material information:
      !    Tabulate the material tables between the input maximum and minimum
      energies.

      DO M=1,MAXMAT
        EABS(1,M) = EMIN
        EABS(2,M) = EMIN
        EABS(3,M) = EMIN
        C1(M)     = 0.0D0
        C2(M)     = 0.0D0
        WCC(M)    = 0.0D0
        WCR(M)    =-10.0D0
      ENDDO

      matfile(1) = MFNAME
      CALL PEINIT(EMAX,1,6,1,matfile)

      ! -- Re-open the material file and read the material name (2nd line):
      OPEN(11,FILE=MFNAME)
      READ(11,'(A55)') NAME
      READ(11,'(11X,A62)') NAME
      CLOSE(11)
```

```
145
146   C  ****  Calculate photon mean free paths:
147
148         ! Set mat number and particle:
149         M=1                ! Use first material defined in the input material file
150         KPAR = 2           ! Select photons (1=electron, 2=photon, 3=positron)
151
152         ! -- Open output file:
153         OPEN(1, FILE=OUTNAME)
154
155         ! -- Write file header:
156         WRITE(1,'(a)')'#[MATERIAL DEFINITION FOR MC-GPU: interaction'//
157        &       ' mean free path and sampling data from PENELOPE 2014]'
158         WRITE(1,'(a)')'#[MATERIAL NAME]'
159         WRITE(1,1001) NAME
160         format('# ',a)
161         WRITE(1,'(a)')'#[NOMINAL DENSITY (g/cm^3)]'
162         WRITE(1,1002) RHO(M)
163         format('# ',f12.8)
164         WRITE(1,'(a)')'#[NUMBER OF DATA VALUES]'
165         WRITE(1,1003) NBINS
166         format('# ',I6)
167         WRITE(1,'(a)')'#[MEAN FREE PATHS (cm)'//
168        &        ' (ie, average distance between interactions)]'
169         WRITE(1,'(a)') '#[Energy (eV)     | Rayleigh        |'//
170        &                ' Compton         | Photoelectric   |'//
171        &                ' TOTAL (+pair prod) (cm) |'//            !  &  '
       Pair-production | TOTAL (cm) |'//
172        &                ' Rayleigh: max cumul prob F^2]'
173
174   ccccc *** MEAN FREE PATH DATA (and Rayleigh cumulative prob) **********
175
176         WRITE(6,*) "X(IE)        Y(IE)"
177         do IE = 1, NEGP
178          X(IE)=ET(IE)
179          Y(IE)=PMAX(IE,1)
180          WRITE(6,*) X(IE), Y(IE)
181         enddo
182
183         CALL SPLINE(X,Y,ONE,TWO,THREE,FOUR,0.0D0,0.0D0,NEGP)
184
185         do i = 1, NBINS
186
187           E = EMIN + (i-1)*DE             ! Set bin energy
188
189           IF(E.LT.EABS(KPAR,M).OR.E.GT.EMAX) THEN
190             WRITE(6,*) '!!ERROR!! Energy outside the table interval!',
191        &                ' #bin, E = ', i, E
192             STOP 'ERROR!'
193           ENDIF
194
195           E_MFP(1) = E                    ! Store the bin energy
196           E_MFP(2) = PHMFP(E,KPAR,M,1)    ! Store the bin MFPs: (1) Rayleigh
197           E_MFP(3) = PHMFP(E,KPAR,M,2)    ! Store the bin MFPs: (2) Compton
198           E_MFP(4) = PHMFP(E,KPAR,M,3)    ! Store the bin MFPs: (3) photoelectric
199           E_MFP(5) = PHMFP(E,KPAR,M,4)    ! Store the bin MFPs: (4) pair production
200
201           E_MFP(6) = 1.0/E_MFP(2)+1.0/E_MFP(3)+1.0/E_MFP(4)+1.0/E_MFP(5)
202           E_MFP(6) = 1.0/E_MFP(6)         ! Store the bin total MFP
203
204           CALL FINDI(ET,E,NEGP,j)
205           PROBABILITY(i) = ONE(j)+E*(TWO(j)+E*(THREE(j)+E*FOUR(j)))
206
207           write(1,'(6(1x,1pe17.10))') E_MFP(1), E_MFP(2), E_MFP(3),    ! Write MFP
       table to external file
208        &                E_MFP(4), E_MFP(6), PROBABILITY(i)     ! Write the Rayleigh
       cumulative probability for the energy bin
209
210             ! E_MFP(5) --> Pair production MFP is not written bc it is not used in the
                simulation, but it is included in the TOTAL MFP
211
212
213         enddo
```

```
216   ccccc *** RAYLEIGH DATA ************************************************
217
218         ! -- Rayleigh sampling data header:
219         WRITE(1,'(a)')'#[RAYLEIGH INTERACTIONS (RITA sampling '//
220        &              ' of atomic form factor from EPDL database)]'
221         WRITE(1,'(a)')
222        & '#[DATA VALUES TO SAMPLE SQUARED MOLECULAR FORM FACTOR (F^2)]'
223         WRITE(1,1003) NP
224         WRITE(1,'(a)')
225        & '#[SAMPLING DATA FROM COMMON/CGRA/: X, P, A, B, ITL, ITU]'   ! X == momentum
           transfer data value (adaptive grid), tabulated from the minimum to the maximum
           possible momentum transfers
226                                                                       ! P == squared
                                                                          Molecular Form
                                                                          Factor
                                                                          cumulative prob
                                                                          at this X
                                                                          (adaptive grid)
227                                                                       ! A & B == RITA
                                                                          sampling
                                                                          parameters
228                                                                       ! ITL & ITU ==
                                                                          lower and upper
                                                                          limits to speed
                                                                          binary search
229
230         do i = 1, NP
231         !XCO(i,M)=QRA(i,M)*20.6074D0
232           IF(i.EQ.1) THEN
233             PCO(i,M)=0.0D0
234           ENDIF
235           IF(i.EQ.2) THEN
236             PCO(i,M)=DPRA(i,M)+DPRA(i-1,M)
237           ELSE
238             PCO(i,M)=DPRA(i,M)+PCO(i-1,M)
239           ENDIF
240
241           write(1,5555) QRA(i,M), PCO(i,M), ARA(i,M),
242                         BRA(i,M), ITLRA(i,M), ITURA(i,M)
243         enddo
244         format(4(1x,1pe17.10),1x,i4,1x,i4)
245
246
247   ccccc *** COMPTON DATA *************************************************
248
249         ! -- Compton sampling data header:
250         WRITE(1,'(a)')
251        &  '#[COMPTON INTERACTIONS (relativistic impulse model with'//
252        &  ' approximated one-electron analytical profiles)]'
253         WRITE(1,'(a)')'#[NUMBER OF SHELLS]'
254         WRITE(1,1003) NOSCCO(M)
255         WRITE(1,'(a)')'#[SHELL INFORMATION FROM COMMON/CGCO/:'//      ! FCO ==
           equivalent number of electrons in the shell?? (eq. 2.36 penelope 2008)
256        &              ' FCO, UICO, FJ0, KZCO, KSCO]'                  ! UICO == shell
           ionization energy
257                                                                       ! FJ0 ==
                                                                          one-electron
                                                                          shell profile
                                                                          at p_z=0 (eq.
                                                                          2.54, page 72,
                                                                          penelope 2008)
258                                                                       ! KZCO ==
                                                                          element that
                                                                          "owns" the
                                                                          shell??
259                                                                       ! KSCO ==
                                                                          atomic shell
                                                                          number, ie,
                                                                          atomic
                                                                          transition line
260                                                                       ! NOSCCO ==
                                                                          number of
                                                                          shells, after
                                                                          grouping
261         do i = 1, NOSCCO(M)
262           write(1,5107) FCO(M,i), UICO(M,i), FJ0(M,i),
263        &                KZCO(M,i), KSCO(M,i)
264         enddo
265         format(3(1X,E16.8),2(1X,I4))
266
267
268         WRITE(1,'(a)')' '
269         CLOSE(1)
270
271         WRITE(6,'(a)')
272        & '*** Material file correctly generated. Have a nice simulation!'
273         WRITE(6,*)' '
274
275         END
```

11.2.3 Air_5_120keV.mcgpu

Figure 37: Air 5-120 keV material file

```
#[MATERIAL DEFINITION FOR MC-GPU: interaction mean free path and sampling data from
PENELOPE 2014]
#[MATERIAL NAME]
# AIR, DRY (NEAR SEA LEVEL)  (104)
#[NOMINAL DENSITY (g/cm^3)]
#   0.00120479
#[NUMBER OF DATA VALUES]
#  23001
#[MEAN FREE PATHS (cm) (ie, average distance between interactions)]
#[Energy (eV)     | Rayleigh        | Compton         | Photoelectric   | TOTAL
(+pair prod) (cm) | Rayleigh: max cumul prob F^2]
  5.0000000000E+03  1.5383521825E+03  8.8214400008E+03  2.1475099122E+01
  2.1128710234E+01  3.3697163820E-01
  5.0050000000E+03  1.5401633560E+03  8.8156226766E+03  2.1539780758E+01
  2.1191628750E+01  3.3721959472E-01
  5.0100000000E+03  1.5419748502E+03  8.8098149914E+03  2.1604591935E+01
  2.1254669497E+01  3.3746753094E-01
  5.0150000000E+03  1.5438046817E+03  8.8040169199E+03  2.1669532782E+01
  2.1317836015E+01  3.3771542679E-01
  5.0200000000E+03  1.5456456294E+03  8.7982284364E+03  2.1734603426E+01
  2.1381127065E+01  3.3796326216E-01
```

[…]

```
#[RAYLEIGH INTERACTIONS (RITA sampling  of atomic form factor from EPDL database)]
#[DATA VALUES TO SAMPLE SQUARED MOLECULAR FORM FACTOR (F^2)]
#    128
#[SAMPLING DATA FROM COMMON/CGRA/: X, P, A, B, ITL, ITU]
  0.0000000000E+00  2.7555440646E-03 -6.4004091321E-03  5.7900082577E-04    1    4
  1.0561873956E-06  5.4815488904E-03 -5.5002750093E-03 -3.0777036093E-06    3    5
  2.1123747912E-06  1.0844503752E-02 -1.0884079932E-02 -3.7647908999E-06    4    6
  4.2247495824E-06  2.1226352931E-02 -2.1623884185E-02  2.0464725546E-04    5    7
  8.4494991649E-06  3.1175453162E-02 -2.0631249493E-02 -2.7668683039E-04    6    7
  1.2674248747E-05  4.0712482354E-02 -2.0827873675E-02  1.5080196585E-04    6    8
  1.6898998330E-05  4.9868818971E-02 -1.9917169991E-02  1.2285842525E-04    7    9
  2.1123747912E-05  5.8670888394E-02 -1.9197591483E-02 -2.0111762273E-04    8   10
  2.5348497495E-05  7.5266357449E-02 -3.8429153864E-02 -2.5829331890E-05    9   10
  3.3797996659E-05  1.0492119585E-01 -7.1042563969E-02  2.6059866825E-04    9   11
  5.0696994989E-05  1.3066230523E-01 -6.5937329122E-02 -1.6159298318E-04   10   11
  6.7595993319E-05  1.5319976692E-01 -6.2354446443E-02  1.8005411540E-05   10   11
  8.4494991649E-05  1.7310217604E-01 -5.8473669749E-02  2.4570488877E-04   10   11
  1.0139398998E-04  2.0673451058E-01 -1.0388765051E-01  8.3893712754E-04   10   12
  1.3519198664E-04  2.3415718387E-01 -9.2307963964E-02  5.8726992301E-04   11   12
  1.6898998330E-04  2.5702910821E-01 -8.3224261823E-02  9.6154170598E-04   11   12
  2.0278797996E-04  2.7649234534E-01 -7.4465194983E-02  8.1753123540E-04   11   13
  2.3658597662E-04  2.9334142093E-01 -6.7418375037E-02  1.1662130820E-03   12   13
  2.7038397328E-04  3.2137066486E-01 -1.1382074096E-01  3.5726405956E-03   12   13
```

[…]

```
#[COMPTON INTERACTIONS (relativistic impulse model with approximated one-electron
analytical profiles)]
#[NUMBER OF SHELLS]
#     11
#[SHELL INFORMATION FROM COMMON/CGCO/: FCO, UICO, FJ0, KZCO, KSCO]
   0.30037400E-03   0.11260000E+02   0.66924682E+02    6   30
   0.32246090E+01   0.14303508E+02   0.53767140E+02    0   30
   0.15688600E+01   0.20330000E+02   0.92073666E+02    7   30
   0.43083822E+00   0.28496480E+02   0.79406063E+02    0   30
   0.18684440E-01   0.24850000E+03   0.14217622E+02   18    4
   0.93422200E-02   0.25060000E+03   0.14139237E+02   18    3
   0.30037400E-03   0.28800000E+03   0.20977471E+02    6    1
   0.93422200E-02   0.32650000E+03   0.27055428E+02   18    2
   0.15688600E+01   0.40300000E+03   0.17833454E+02    7    1
   0.42149600E+00   0.53800000E+03   0.15510145E+02    8    1
   0.93422200E-02   0.32063000E+04   0.66727076E+01   18    1
```

11.2.4 RQR6.spc

Figure 38: RQR 6 spectrum file

```
#
# Calculation of X-ray spectra - v. 3.5 ********* 2017
# ----------------------------------------------------------------------
# Spectrum #1:
#
# kVp         =  80.0 kV
# Anode angle = 18.0 deg
# Distance    =   72.0 cm
#
# Absorber thickness:
# Beryllium:   8.00 mm
# Aluminium:   3.00 mm
# Copper   :   0.00 mm
# Tin      :   0.00 mm
# Lead     :   0.00 mm
# Water    :   0.00 mm
# PMMA     :   0.00 mm
# Tr.oil   :   0.00 mm
#
# Calculated data:
# ----------------
#
# Photon flux:
# total   :  2.345E+0006 photons/(mA.s.mmý)
# K-X rays:  4.615E+0004 photons/(mA.s.mmý)
# L-X rays not calc.
#
# Mean photon energy:
# Spectrum    :  43.6 keV
# Kerma distr.:  37.6 keV
#
# Half-value layers (Al):
# 1.HVL =   3.02 mmAl
# 2.HVL =   4.38 mmAl
# Half-value layers (Cu):
# 1.HVL =  0.112 mmCu
# 2.HVL =  0.181 mmCu
#
# Kerma in air:  1.197E+0002 æGy/(mA.s) = 7.185E+0000 mGy/(mA.min)
#
# Photon spectrum :
# -----------------
# rel. distribution normalized to 100000 photons
# Energy(eV) / Intensity
# ----------------------
10000   0
11000   0
12000   0
13000   0
14000   1
15000   6
16000   22
17000   60
18000   132
19000   249
20000   414
21000   611
22000   834
23000   1075
24000   1323
25000   1569
26000   1804
27000   2022
28000   2217
29000   2389
30000   2536
31000   2632
32000   2699
33000   2747
34000   2778
35000   2795
36000   2798
37000   2789
```

```
 74   38000   2771
 75   39000   2744
 76   40000   2709
 77   41000   2657
 78   42000   2598
 79   43000   2536
 80   44000   2473
 81   45000   2407
 82   46000   2341
 83   47000   2273
 84   48000   2205
 85   49000   2136
 86   50000   2067
 87   51000   1994
 88   52000   1920
 89   53000   1846
 90   54000   1774
 91   55000   1702
 92   56000   1630
 93   57000   1559
 94   58000   1489
 95   59000   1973
 96   60000   2324
 97   61000   1279
 98   62000   1209
 99   63000   1139
100   64000   1071
101   65000   1003
102   66000   935
103   67000   869
104   68000   1148
105   69000   737
106   70000   746
107   71000   592
108   72000   532
109   73000   472
110   74000   412
111   75000   353
112   76000   293
113   77000   234
114   78000   175
115   79000   116
116   80000   58
117   80000   -1
```

This spectrum is shown in the following plot to visualize it:

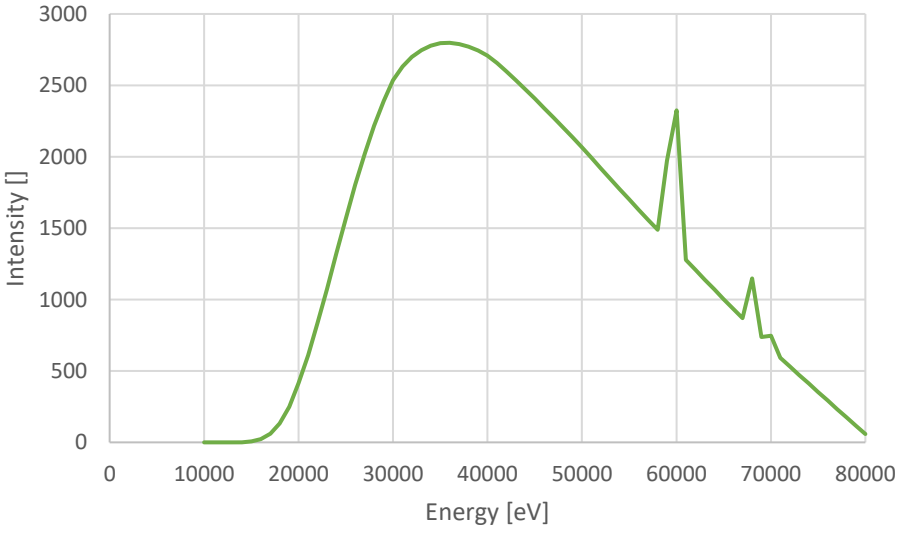

Figure 39: RQR 6 spectrum distribution

11.3 APPENDIX C: SIMULATIONS' RESULTS

SIMULATION 1

SIMULATION 1		
Phantom	Nº Voxels	1 x 1 x 1
	Voxel size (cm^3)	10 x 10 x 10
	Dimensions (cm^3)	10 x 10 x 10
	Material	Dry air (ρ = 0.001205 g/cm^3)
Source	Focal position (cm)	5 -15 5
	Spectrum	Monoenergetic spectra (60 – 120 keV)
	Histories	1.0E9
Detector size (cm^2)		20 x 20
Source-to-detector distance (cm)		30

DOSE (eV/g·hist)	Energy Spectrum (keV)	MC-GPU	NEW MC-GPU	penEasy	Old Difference	New Difference	Old Relative error	New Relative error	Improvement factor
	60	11.61226	11.47738	11.436	0.176	0.042	1.543%	0.364%	4.244
	70	11.54258	11.44943	11.418	0.124	0.031	1.088%	0.273%	3.992
	80	12.22802	12.15716	12.115	0.113	0.042	0.935%	0.350%	2.669
	90	13.34371	13.28865	13.256	0.087	0.032	0.659%	0.244%	2.702
	100	14.75085	14.71027	14.650	0.100	0.060	0.686%	0.409%	1.678
	110	16.36093	16.32939	16.252	0.109	0.077	0.668%	0.474%	1.409
	120	18.08912	18.06191	17.984	0.105	0.078	0.582%	0.431%	1.351
	200		33.94609	33.830		0.116		0.344%	
	300		54.81751	54.566		0.252		0.462%	

ENERGY DEPOSITION (eV/hist)	Energy Spectrum (keV)	MC-GPU	NEW MC-GPU	penEasy	Old Difference	New Difference	Old Relative error	New Relative error	Improvement factor
	60	13.99	13.83	13.780	0.210	0.050	1.523%	0.362%	4.206
	70	13.91	13.80	13.759	0.151	0.041	1.097%	0.297%	3.689
	80	14.73	14.65	14.598	0.132	0.052	0.903%	0.355%	2.544
	90	16.08	16.01	15.974	0.106	0.036	0.664%	0.226%	2.939
	100	17.77	17.73	17.654	0.116	0.076	0.659%	0.432%	1.524
	110	19.71	19.68	19.584	0.126	0.096	0.643%	0.490%	1.313
	120	21.80	21.76	21.671	0.129	0.089	0.594%	0.410%	1.450
	200		40.91	40.765		0.145		0.356%	
	300		66.06	65.752		0.309		0.469%	

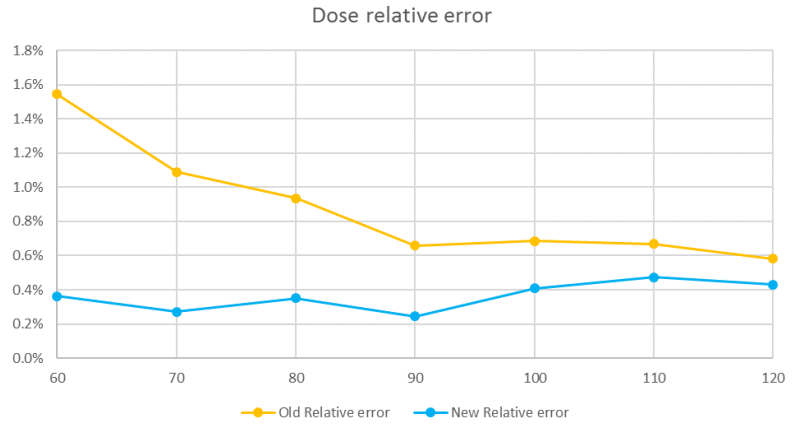

ETSEIB

SIMULATION 2

SIMULATION 2		
Phantom	Nº Voxels	6 x 3 x 6
	Voxel size (cm^3)	5 x 10 x 5
	Dimensions (cm^3)	30 x 30 x 30
	Material	PMMA (ρ = 1.19 g/cm^3)
Source	Focal position (cm)	15 -45 15
	Spectrum	Monoenergetic spectra (60 – 120 keV)
	Histories	1.0E9
Detector size (cm^2)		54 x 54
Source-to-detector distance (cm)		81

	Energy Spectrum (keV)	MC-GPU	NEW MC-GPU	penEasy	Old Difference	Old Relative error	New Difference	New Relative error
DOSE (eV/g·hist)	60	0.808	0.801	0.802	0.0053	0.666%	0.0009	0.116%
	70	0.888	0.882	0.883	0.0049	0.555%	0.0011	0.124%
	80	0.983	0.978	0.979	0.0045	0.456%	0.0011	0.114%
	90	1.090	1.085	1.086	0.0041	0.378%	0.0011	0.100%
	100	1.206	1.201	1.202	0.0038	0.318%	0.0010	0.086%
	110	1.328	1.324	1.325	0.0036	0.273%	0.0010	0.074%
	120	1.456	1.452	1.453	0.0033	0.231%	0.0009	0.065%
	200		2.591	2.592			0.0008	0.030%
	300		4.114	4.115			0.0006	0.015%

	Energy Spectrum (keV)	MC-GPU	NEW MC-GPU	penEasy	Old Difference	Old Relative error	New Difference	New Relative error
ENERGY DEPOSITION (eV/hist)	60	25947.550	25745.970	25776.000	171.550	0.666%	30.030	0.117%
	70	28540.420	28347.670	28382.900	157.520	0.555%	35.230	0.124%
	80	31596.950	31417.570	31453.500	143.450	0.456%	35.930	0.114%
	90	35020.840	34854.070	34888.900	131.940	0.378%	34.830	0.100%
	100	38732.970	38577.050	38610.300	122.670	0.318%	33.250	0.086%
	110	42673.680	42526.050	42557.500	116.180	0.273%	31.450	0.074%
	120	46793.210	46655.240	46685.500	107.710	0.231%	30.260	0.065%
	200		83241.110	83266.300			25.190	0.030%
	300		132191.460	132211.000			19.540	0.015%

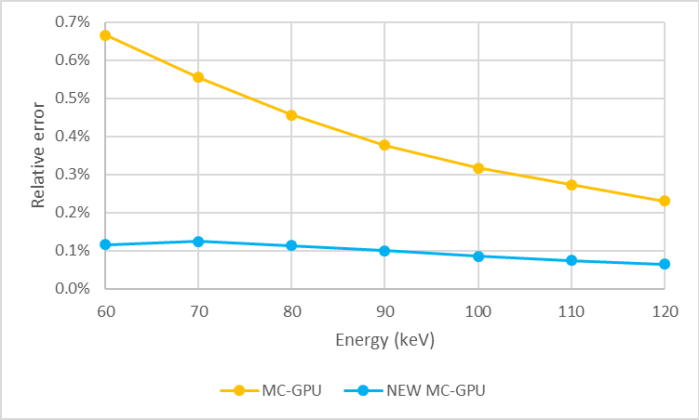

ETSEIB

SIMULATION 3

SIMULATION 3		
Phantom	Nº Voxels	3 x 3 x 3
	Voxel size (cm^3)	10 x 10 x 10
	Dimensions (cm^3)	30 x 30 x 30
	Materials	PMMA and Dry Air (1voxel)
Source	Focal position (cm)	15 -45 15
	Spectrum	N100
	Histories	1006720000
Detector size (cm^2)		54 x 54
Source-to-detector distance (cm)		81

	MC-GPU original	MC-GPU updated	PENELOPE/penEasy	Original Relative Error	Updated Relative Error
Total Energy Absorbed (eV/hist)	32322.85	32144.36	32180.97	0.441%	0.114%
Maximum voxel dose (ev/g·hist)	2.851025	2.831048	2.8371	0.493%	0.212%
Sigma	0.000845	0.000838	0.00060		
Coordinates	(1,0,1)	(1,0,1)	(2,1,2)=(1,0,1)		
PMMA					
Dose ROI (ev/g·hist)	1.057630	1.05179	1.05299	0.441%	0.114%
Sigma	<< 1%	<< 1%			
E dp (ev/hist)	32321.29	32142.82	32179.40	0.441%	0.114%
Sigma	-	-	1.90		
Mass (g)	30560.000010				
Dry Air					
Dose ROI (ev/g·hist)	1.292280	1.28424	1.301278008	0.691%	1.309%
Sigma	0.011590	0.01153			
E dp (ev/hist)	1.56	1.55	1.5680	0.513%	1.150%
Sigma	-	-	0.014		
Mass (g)	1.205				

Real simulation time (s)	49.30	59.72	20357.19

ETSEIB

SIMULATION 4

SIMULATION 4		
Phantom	Nº Voxels	3 x 10 x 3
	Voxel size (cm^3)	10 x 1 x 10
	Dimensions (cm^3)	30 x 10 x 30
	Materials	Skin, Muscle and Bone
Source	Focal position (cm)	15 -30 15
	Spectrum	90 kVp 4 mm Al
	Histories	1006720000
Detector size (cm^2)		50 x 50
Source-to-detector distance (cm)		50

	MC-GPU original	MC-GPU updated	PENELOPE/penEasy	Original Relative Error	Updated Relative Error
Total Energy Absorbed (eV/hist)	30525.70	30415.65	30406.04	0.394%	0.032%
Sigma					
Maximum voxel dose (ev/g·hist)	8.659510	8.687543	8.7034	0.504%	0.182%
Sigma	0.001915	0.001915	0.00290		
Sigma/mean	0.022%	0.022%	0.033%		
Coordinates	(1,3,1)	(1,3,1)	(2,4,2)=(1,3,1)		
E dp Maximum voxel dose (ev/hist)	1602.009384	1607.195447	1610.12	0.504%	0.182%
E deposition (eV/hist)					
1 (Skin)	4066.19	3867.54	3893.75	4.429%	0.673%
2 (Mucle)	6056.99	5983.71	6024.76	0.535%	0.681%
3 (Bone)	19560.43	19715.85	19653.70	0.475%	0.316%
4 (Muscle)	697.48	704.93	693.30	0.603%	1.678%
5 (Skin)	144.62	143.62	140.54	2.906%	2.194%
Dose (eV/g·hist)					
1 (Skin)	4.10727	3.90661	3.93	4.429%	0.673%
2 (Mucle)	3.23557	3.19643	3.22	0.535%	0.681%
3 (Bone)	3.916	3.94712	3.93	0.475%	0.316%
4 (Muscle)	0.24839	0.25104	0.25	0.603%	1.677%
5 (Skin)	0.14608	0.14507	0.14	2.905%	2.194%
E deposition (eV/hist)					
Skin	4210.81	4011.16	4034.29	4.376%	0.573%
Muscle	6754.47	6688.64	6718.06	0.542%	0.438%
Bone	19560.43	19715.85	19653.70	0.475%	0.316%
Dose (eV/g·hist)					
Skin	2.13	2.03	2.04	4.376%	0.573%
Muscle	1.44	1.43	1.44	0.542%	0.438%
Bone	3.92	3.95	3.93	0.475%	0.316%

Real simulation time (s)	43.1	66.43	24704.07

ETSEIB

SIMULATION 5

SIMULATION 5 (Zubal)		
Phantom	Nº Voxels	128 x 128 x 243
	Voxel size (cm^3)	0.4 x 0.4 x 0.4
	Dimensions (cm^3)	51.2 x 51.2 x 97.2
	Materials	Human body materials
Source	Focal position (cm)	25.6 -51.2 48.6
	Spectrum	N100
	Histories	1006720000
Detector size (cm^2)		110 x 110
Source-to-detector distance (cm)		110

Energy dep (eV/hist)	MC-GPU original	MC-GPU updated	Relative difference	PENELOPE/penEasy	Original Relative Error	Updated Relative Error
Air	53.83	53.67	0.297%	53.46	0.701%	0.402%
Muscle	6935.92	6948.03	0.175%	6925.39	0.152%	0.327%
Soft tissue	270.94	272.9	0.723%	270.89	0.020%	0.743%
Bone	7474.56	7339.13	1.812%	7321.86	2.086%	0.236%
Cartilage	44.34	44.3	0.090%	44.45	0.250%	0.340%
Adipose	2.62	2.62	0.000%	2.62	0.162%	0.162%
Blood	497.01	490.56	1.298%	461.23	7.758%	6.360%
Skin	6066.87	5979.67	1.437%	6292.76	3.590%	4.975%
Lung	961.86	967.77	0.614%	931.40	3.270%	3.905%
Glands	5.1	5.07	0.588%	4.97	2.543%	1.940%
Brain	47.17	48.15	2.078%	48.02	1.775%	0.266%
Red Marrow	285.84	289.34	1.224%	288.18	0.813%	0.401%
Liver	1018.19	1018.33	0.014%	1016.94	0.123%	0.137%
Stomach	2140.63	2134.55	0.284%	2124.28	0.770%	0.483%
Water	323.32	322.93	0.121%	321.64	0.521%	0.400%
TOTAL	26128.19	25917.03	0.808%	26108.0977	0.077%	0.732%

Dose (eV/g·hist)	MC-GPU original	MC-GPU updated	Relative difference	PENELOPE/penEasy	Original Relative Error	Updated Relative Error
Air	0.23407	0.23338	0.295%	0.2324	0.701%	0.405%
Muscle	0.27855	0.27903	0.172%	0.2781	0.153%	0.326%
Soft tissue	0.20116	0.20262	0.726%	0.2011	0.019%	0.745%
Bone	0.71376	0.70083	1.812%	0.6992	2.085%	0.236%
Cartilage	0.33987	0.33960	0.079%	0.3408	0.258%	0.338%
Adipose	0.08942	0.08954	0.134%	0.0897	0.320%	0.186%
Blood	0.42861	0.42304	1.300%	0.3977	7.759%	6.358%
Skin	0.32297	0.31833	1.437%	0.3350	3.589%	4.974%
Lung	0.36786	0.37012	0.614%	0.3562	3.269%	3.904%
Glands	0.45867	0.45600	0.582%	0.4471	2.581%	1.984%
Brain	0.03322	0.03391	2.077%	0.0338	1.771%	0.269%
Red Marrow	0.20604	0.20856	1.223%	0.2077	0.812%	0.401%
Liver	0.51752	0.51760	0.015%	0.5169	0.122%	0.137%
Stomach	0.61291	0.61117	0.284%	0.6082	0.770%	0.484%
Water	0.42900	0.42847	0.124%	0.4268	0.522%	0.398%
Maximum dose point	6.125987	5.989736		5.8445		
Sigma	0.002147	0.001928		4.5		
Sigma/mean	0.035%	0.032%		77.00%		
Coordinates	(72,2,116)	(72,15,106)		(91,25,173)		
Real simulation time (s)	87.25	128.32		41570.21		

ETSEIB

	Updated MC-GPU validation								
	PENELOPE/penEasy	Sigma	MAX PenEasy	MIN PenEasy	Superior Relative Error	Relative error	Inferior Relative Error	**Minimum Error**	**Maximum Error**
Air	53.46	0.1	5.35E+01	5.34E+01	0.25%	0.40%	0.55%	0.25%	0.55%
Muscle	6925.39	1.0	6.93E+03	6.92E+03	0.31%	0.33%	0.34%	0.31%	0.34%
Soft tissue	270.89	0.2	2.71E+02	2.71E+02	0.67%	0.74%	0.82%	0.67%	0.82%
Bone	7321.86	1.3	7.32E+03	7.32E+03	0.22%	0.24%	0.25%	0.22%	0.25%
Cartilage	44.45	0.1	4.45E+01	4.44E+01	0.52%	0.34%	0.16%	0.16%	0.52%
Adipose	2.62	0.0	2.64E+00	2.61E+00	0.77%	0.16%	0.45%	0.16%	0.77%
Blood	461.23	0.3	4.61E+02	4.61E+02	6.30%	6.36%	6.42%	6.30%	6.42%
Skin	6292.76	0.9	6.29E+03	6.29E+03	4.99%	4.98%	4.96%	4.96%	4.99%
Lung	931.40	0.4	9.32E+02	9.31E+02	3.86%	3.90%	3.95%	3.86%	3.95%
Glands	4.97	0.0	5.00E+00	4.95E+00	1.43%	1.94%	2.46%	1.43%	2.46%
Brain	48.02	0.1	4.81E+01	4.79E+01	0.07%	0.27%	0.46%	0.07%	0.46%
Red Marrow	288.18	0.2	2.88E+02	2.88E+02	0.33%	0.40%	0.47%	0.33%	0.47%
Liver	1016.94	0.4	1.02E+03	1.02E+03	0.09%	0.14%	0.18%	0.09%	0.18%
Stomach	2124.28	0.6	2.12E+03	2.12E+03	0.45%	0.48%	0.51%	0.45%	0.51%
Water	321.64	0.2	3.22E+02	3.21E+02	0.33%	0.40%	0.47%	0.33%	0.47%

SIMULATION 5 LONG

SIMULATION 5 (Zubal)		
Phantom	Nº Voxels	128 x 128 x 243
	Voxel size (cm^3)	0.4 x 0.4 x 0.4
	Dimensions (cm^3)	51.2 x 51.2 x 97.2
	Materials	Human body materials
Source	Focal position (cm)	25.6 -51.2 48.6
	Spectrum	N100
	Histories MCGPU	1006720000
	Histories penEasy	$2 \cdot 10^{10}$
Detector size (cm^2)		110 x 110
Source-to-detector distance (cm)		110

Energy dep (eV/hist)	MC-GPU original	MC-GPU updated	Relative difference	PENELOPE/penEasy	Original Relative Error	Updated Relative Error
Air	53.83	53.67	0.297%	53.48	0.650%	0.351%
Muscle	6935.92	6948.03	0.175%	6924.55	0.164%	0.339%
Soft tissue	270.94	272.9	0.723%	271.00	0.021%	0.702%
Bone	7474.56	7339.13	1.812%	7321.85	2.086%	0.236%
Cartilage	44.34	44.3	0.090%	44.41	0.163%	0.254%
Adipose	2.62	2.62	0.000%	2.62	0.120%	0.120%
Blood	497.01	490.56	1.298%	461.29	7.744%	6.346%
Skin	6066.87	5979.67	1.437%	6292.37	3.584%	4.970%
Lung	961.86	967.77	0.614%	931.39	3.271%	3.906%
Glands	5.1	5.07	0.588%	4.98	2.428%	1.826%
Brain	47.17	48.15	2.078%	48.03	1.781%	0.260%
Red Marrow	285.84	289.34	1.224%	288.18	0.813%	0.402%
Liver	1018.19	1018.33	0.014%	1017.24	0.093%	0.107%
Stomach	2140.63	2134.55	0.284%	2124.25	0.771%	0.485%
Water	323.32	322.93	0.121%	321.57	0.545%	0.424%
TOTAL	26128.19	25917.03	0.808%	26107.2111	0.080%	0.728%

Maximum dose point (eV/g·hist)	6.125987	5.989736		3.7912		
Sigma	0.002147	0.001928		0.018		
Sigma/mean	0.035%	0.032%		0.475%		
Coordinates	(72,2,116)	(72,15,106)		(65,24,131)		
Real simulation time (s)	87.25	128.32		7.63E+05		

ETSEIB

	Updated MC-GPU validation								
	PENELOPE/penEasy	Sigma	MAX PenEasy	MIN PenEasy	Superior Relative Error	Relative error	Inferior Relative Error	**Minimum Error**	**Maximum Error**
Air	53.48	0.0	5.35E+01	5.35E+01	0.32%	0.35%	0.39%	0.32%	0.39%
Muscle	6924.55	0.2	6.92E+03	6.92E+03	0.34%	0.34%	0.34%	0.34%	0.34%
Soft tissue	271.00	0.0	2.71E+02	2.71E+02	0.69%	0.70%	0.72%	0.69%	0.72%
Bone	7321.85	0.3	7.32E+03	7.32E+03	0.23%	0.24%	0.24%	0.23%	0.24%
Cartilage	44.41	0.0	4.44E+01	4.44E+01	0.29%	0.25%	0.21%	0.21%	0.29%
Adipose	2.62	0.0	2.63E+00	2.62E+00	0.26%	0.12%	0.02%	0.02%	0.26%
Blood	461.29	0.1	4.61E+02	4.61E+02	6.33%	6.35%	6.36%	6.33%	6.36%
Skin	6292.37	0.2	6.29E+03	6.29E+03	4.97%	4.97%	4.97%	4.97%	4.97%
Lung	931.39	0.1	9.31E+02	9.31E+02	3.90%	3.91%	3.92%	3.90%	3.92%
Glands	4.98	0.0	4.98E+00	4.97E+00	1.71%	1.83%	1.94%	1.71%	1.94%
Brain	48.03	0.0	4.80E+01	4.80E+01	0.22%	0.26%	0.30%	0.22%	0.30%
Red Marrow	288.18	0.0	2.88E+02	2.88E+02	0.39%	0.40%	0.42%	0.39%	0.42%
Liver	1017.24	0.1	1.02E+03	1.02E+03	0.10%	0.11%	0.12%	0.10%	0.12%
Stomach	2124.25	0.1	2.12E+03	2.12E+03	0.48%	0.48%	0.49%	0.48%	0.49%
Water	321.57	0.1	3.22E+02	3.22E+02	0.41%	0.42%	0.44%	0.41%	0.44%

SIMULATION 6

SIMULATION 6 (Duke)		
Phantom	Nº Voxels	122 x 62 x 372
	Voxel size (cm^3)	0.5 x 0.5 x 0.5
	Dimensions (cm^3)	61 x 31 x 186
	Materials	Human body materials
Source	Focal position (cm)	30.5 -30.5 130
	Spectra	100 keV monoenergetic and RQR 6
	Histories	1006720000
Detector size (cm^2)		143 x 143
Source-to-detector distance (cm)		71.5

Spectrum: 100 keV monoenergetic

Energy dep (eV/hist)	MC-GPU original	MC-GPU updated	Relative difference	PENELOPE/penEasy	Original Relative Error	Updated Relative Error
Air	44.41	44.29	0.270%	44.27	0.323%	0.052%
Muscle	11959.95	11906.22	0.449%	11914.90	0.378%	0.073%
Soft tissue	1461.58	1454.86	0.460%	1457.04	0.312%	0.150%
Bone	6513.28	6521.7	0.129%	6527.99	0.225%	0.096%
Cartilage	293.2	291.94	0.430%	292.07	0.386%	0.046%
Adipose	3712.12	3682.66	0.794%	3684.46	0.751%	0.049%
Blood	377.72	371.22	1.721%	371.39	1.704%	0.046%
Skin	1610.44	1592.23	1.131%	1592.02	1.157%	0.013%
Lung	1587.82	1581.7	0.385%	1584.38	0.217%	0.169%
TOTAL	27560.52	27446.82	0.413%	27468.5211	0.335%	0.079%

Dose (eV/g·hist)	MC-GPU original	MC-GPU updated	Relative difference	PENELOPE/penEasy	Original Relative Error	Updated Relative Error
Air	0.13024	0.12989	0.269%	0.1298	0.330%	0.061%
Muscle	0.33006	0.32858	0.448%	0.3288	0.377%	0.073%
Soft tissue	0.32366	0.32217	0.460%	0.3226	0.313%	0.149%
Bone	0.82896	0.83003	0.129%	0.8308	0.225%	0.096%
Cartilage	0.18801	0.18720	0.431%	0.1873	0.386%	0.047%
Adipose	0.30844	0.30599	0.794%	0.3061	0.751%	0.050%
Blood	0.31869	0.31321	1.720%	0.3134	1.703%	0.046%
Skin	0.2969	0.29354	1.132%	0.2935	1.158%	0.013%
Lung	0.62977	0.62735	0.384%	0.6284	0.217%	0.168%

Maximum dose point	4.188542	4.000672		4.2011		
Sigma	0.001671	0.001422		2.5		
Sigma/mean	0.040%	0.036%		59.508%		
Coordinates	(40,4,273)	(45,2,256)		(70,1,256)		

Real simulation time (s)	76.25	127.95		42225.31		

ETSEIB

Updated MC-GPU validation									
PENELOPE/penEasy	Sigma	Sigma/Mean	MAX PenEasy	MIN PenEasy	Superior Relative Error	Relative error	Inferior Relative Error	**Minimum Error**	**Maximum Error**
44.27	0.07	0.16%	44.34	44.20	0.11%	0.05%	0.21%	0.05%	0.21%
11914.90	1.40	0.01%	11916.30	11913.50	0.08%	0.07%	0.06%	0.06%	0.08%
1457.04	0.50	0.03%	1457.54	1456.54	0.18%	0.15%	0.12%	0.12%	0.18%
6527.99	1.30	0.02%	6529.29	6526.69	0.12%	0.10%	0.08%	0.08%	0.12%
292.07	0.20	0.07%	292.27	291.87	0.11%	0.05%	0.02%	0.02%	0.11%
3684.46	0.64	0.02%	3685.10	3683.82	0.07%	0.05%	0.03%	0.03%	0.07%
371.39	0.24	0.06%	371.63	371.15	0.11%	0.05%	0.02%	0.02%	0.11%
1592.02	0.44	0.03%	1592.46	1591.58	0.01%	0.01%	0.04%	0.01%	0.04%
1584.38	0.52	0.03%	1584.90	1583.86	0.20%	0.17%	0.14%	0.14%	0.20%

Spectrum: RQR 6

Energy dep (eV/hist)	MC-GPU updated	PENELOPE/penEasy	Updated Relative Error
Air	47.01	47.03	0.040%
Muscle	8217.67	8222.13	0.054%
Soft tissue	622.83	619.28	0.573%
Bone	4965.44	4949.00	0.332%
Cartilage	99.72	98.80	0.929%
Adipose	1994.75	1999.26	0.226%
Blood	126.87	126.47	0.313%
Skin	1445.43	1451.83	0.441%
Lung	743.69	738.77	0.666%
TOTAL	18263.42	18252.5758	0.059%

Dose (eV/g·hist)	MC-GPU updated	PENELOPE/penEasy	Updated Relative Error
Air	0.13787	0.1379	0.029%
Muscle	0.22679	0.2269	0.053%
Soft tissue	0.13792	0.1371	0.572%
Bone	0.63196	0.6299	0.332%
Cartilage	0.06394	0.0634	0.923%
Adipose	0.16574	0.1661	0.228%
Blood	0.10704	0.1067	0.309%
Skin	0.26648	0.2677	0.439%
Lung	0.29497	0.2930	0.667%

Maximum dose point	7.232274	7.3318	1.357%
Sigma	0.001633	0.067	
Sigma/mean	0.02%	0.91%	
Coordinates	(58,5,271)	(58,5,271)	
Real simulation time (s)	112.96	33641.11	

ETSEIB

Updated MC-GPU validation									
PENELOPE/penEasy	Sigma	Sigma/Mean	MAX PenEasy	MIN PenEasy	Superior Relative Error	Relative error	Inferior Relative Error	**Minimum Error**	**Maximum Error**
47.03	0.08	0.16%	47.10	46.95	0.20%	0.04%	0.12%	0.04%	0.20%
8222.13	0.97	0.01%	8223.10	8221.16	0.07%	0.05%	0.04%	0.04%	0.07%
619.28	0.30	0.05%	619.58	618.98	0.52%	0.57%	0.62%	0.52%	0.62%
4949.00	0.87	0.02%	4949.87	4948.13	0.31%	0.33%	0.35%	0.31%	0.35%
98.80	0.12	0.12%	98.92	98.68	0.81%	0.93%	1.05%	0.81%	1.05%
1999.26	0.47	0.02%	1999.73	1998.79	0.25%	0.23%	0.20%	0.20%	0.25%
126.47	0.13	0.10%	126.60	126.34	0.21%	0.31%	0.42%	0.21%	0.42%
1451.83	0.41	0.03%	1452.24	1451.42	0.47%	0.44%	0.41%	0.41%	0.47%
738.77	0.33	0.04%	739.10	738.44	0.62%	0.67%	0.71%	0.62%	0.71%

SIMULATION 6 LONG

SIMULATION 6 (Duke)		
Phantom	Nº Voxels	122 x 62 x 372
	Voxel size (cm^3)	0.5 x 0.5 x 0.5
	Dimensions (cm^3)	61 x 31 x 186
	Materials	Human body materials
Source	Focal position (cm)	30.5 -30.5 130
	Spectra	100 keV monoenergetic
	Histories MC-GPU	1006720000
	Histories penEasy	$1.8 \cdot 10^{10}$
Detector size (cm^2)		143 x 143
Source-to-detector distance (cm)		71.5

Energy dep (eV/hist)	MC-GPU original	MC-GPU updated	Relative difference	PENELOPE/penEasy	Original Relative Error	Updated Relative Error
Air	44.41	44.29	0.270%	44.26	0.328%	0.057%
Muscle	11959.95	11906.22	0.449%	11915.00	0.377%	0.074%
Soft tissue	1461.58	1454.86	0.460%	1456.98	0.316%	0.146%
Bone	6513.28	6521.7	0.129%	6528.23	0.229%	0.100%
Cartilage	293.2	291.94	0.430%	292.19	0.345%	0.086%
Adipose	3712.12	3682.66	0.794%	3685.18	0.731%	0.068%
Blood	377.72	371.22	1.721%	371.37	1.711%	0.040%
Skin	1610.44	1592.23	1.131%	1592.09	1.153%	0.009%
Lung	1587.82	1581.7	0.385%	1584.08	0.236%	0.150%
TOTAL	27560.52	27446.82	0.413%	27469.3837	0.332%	0.082%

Dose (eV/g·hist)	MC-GPU original	MC-GPU updated	Relative difference	PENELOPE/penEasy	Original Relative Error	Updated Relative Error
Air	0.13024	0.12989	0.269%	0.1298	0.336%	0.066%
Muscle	0.33006	0.32858	0.448%	0.3288	0.376%	0.074%
Soft tissue	0.32366	0.32217	0.460%	0.3226	0.317%	0.145%
Bone	0.82896	0.83003	0.129%	0.8309	0.229%	0.100%
Cartilage	0.18801	0.18720	0.431%	0.1874	0.345%	0.087%
Adipose	0.30844	0.30599	0.794%	0.3062	0.731%	0.069%
Blood	0.31869	0.31321	1.720%	0.3133	1.709%	0.039%
Skin	0.2969	0.29354	1.132%	0.2935	1.154%	0.009%
Lung	0.62977	0.62735	0.384%	0.6283	0.236%	0.150%

Maximum dose point	4.188542	4.000672		3.8884	7.719%	2.887%
Sigma	0.001671	0.001422		0.014		
Sigma/mean	0.040%	0.036%		0.360%		
Coordinates	(40,4,273)	(45,2,256)		(58,6,267)		

Real simulation time (s)	76.25	127.95		7.62E+05		

ETSEIB

Updated MC-GPU validation									
PENELOPE/penEasy	Sigma	Sigma/Mean	MAX PenEasy	MIN PenEasy	Superior Relative Error	Relative error	Inferior Relative Error	**Minimum Error**	**Maximum Error**
44.26	0.02	0.04%	44.28	44.25	0.02%	0.06%	0.10%	0.02%	0.10%
11915.00	0.32	0.00%	11915.32	11914.68	0.08%	0.07%	0.07%	0.07%	0.08%
1456.98	0.12	0.01%	1457.10	1456.86	0.15%	0.15%	0.14%	0.14%	0.15%
6528.23	0.30	0.00%	6528.53	6527.93	0.10%	0.10%	0.10%	0.10%	0.10%
292.19	0.05	0.02%	292.24	292.14	0.10%	0.09%	0.07%	0.07%	0.10%
3685.18	0.15	0.00%	3685.33	3685.03	0.07%	0.07%	0.06%	0.06%	0.07%
371.37	0.06	0.02%	371.42	371.31	0.05%	0.04%	0.02%	0.02%	0.05%
1592.09	0.10	0.01%	1592.19	1591.99	0.00%	0.01%	0.02%	0.00%	0.02%
1584.08	0.12	0.01%	1584.20	1583.96	0.16%	0.15%	0.14%	0.14%	0.16%

SIMULATION 7

SIMULATION 7 (Duke Chest)		
Phantom	Nº Voxels	580 x 260 x 300
	Voxel size (cm^3)	0.1 x 0.1 x 0.1
	Dimensions (cm^3)	58 x 26 x 30
	Materials	Human body materials
Source	Focal position (cm)	29 -32.65 15
	Spectra	100 keV monoenergetic and RQRs 6 - 9
	Histories	1006720000
Detector size (cm^2)		122.8 x 61.4
Source-to-detector distance (cm)		68.65

100 keV Monoenergetic											
Energy dep (eV/hist)	MC-GPU	penEasy	Sigma	Sigma/Mean	MAX PenEasy	MIN PenEasy	Sup Relative Error	Relative error	Inf Relative Error	**Min Error**	**Max Error**
Air	20.51	20.48	0.05	0.239%	20.53	20.43	-0.08%	0.16%	0.40%	0.08%	0.40%
Muscle	11084.77	11094.70	1.30	0.012%	11096.00	11093.40	-0.10%	-0.09%	-0.08%	0.08%	0.10%
Soft tissue	1210.71	1211.84	0.45	0.037%	1212.29	1211.39	-0.13%	-0.09%	-0.06%	0.06%	0.13%
Bone	5616	5622.64	1.20	0.021%	5623.84	5621.44	-0.14%	-0.12%	-0.10%	0.10%	0.14%
Cartilage	210.94	211.16	0.17	0.081%	211.33	210.99	-0.19%	-0.10%	-0.02%	0.02%	0.19%
Adipose	2757.97	2758.55	0.54	0.020%	2759.09	2758.01	-0.04%	-0.02%	0.00%	0.00%	0.04%
Blood	501.21	501.71	0.28	0.056%	501.99	501.43	-0.15%	-0.10%	-0.04%	0.04%	0.15%
Skin	1404.08	1404.47	0.41	0.029%	1404.88	1404.06	-0.06%	-0.03%	0.00%	0.00%	0.06%
Lung	2861.56	2866.50	0.70	0.024%	2867.20	2865.80	-0.20%	-0.17%	-0.15%	0.15%	0.20%
TOTAL	25667.74	25692.04						-0.09%			

RQR 6											
Energy dep (eV/hist)	MC-GPU	penEasy	Sigma	Sigma/Mean	MAX PenEasy	MIN PenEasy	Sup Relative Error	Relative error	Inf Relative Error	**Min Error**	**Max Error**
Air	22.51	22.56	0.05	0.231%	22.61	22.50	-0.43%	-0.20%	0.03%	0.03%	0.43%
Muscle	8131.99	8143.86	0.96	0.012%	8144.82	8142.90	-0.16%	-0.15%	-0.13%	0.13%	0.16%
Soft tissue	516.71	512.20	0.27	0.053%	512.47	511.93	0.83%	0.88%	0.93%	0.83%	0.93%
Bone	4766.54	4754.35	0.85	0.018%	4755.20	4753.50	0.24%	0.26%	0.27%	0.24%	0.27%
Cartilage	67	66.26	0.10	0.146%	66.35	66.16	0.97%	1.12%	1.27%	0.97%	1.27%
Adipose	1558.52	1563.26	0.41	0.026%	1563.67	1562.85	-0.33%	-0.30%	-0.28%	0.28%	0.33%
Blood	176.07	175.73	0.16	0.091%	175.89	175.57	0.10%	0.19%	0.29%	0.10%	0.29%
Skin	1339.13	1345.15	0.40	0.030%	1345.55	1344.75	-0.48%	-0.45%	-0.42%	0.42%	0.48%
Lung	1381.05	1372.09	0.45	0.033%	1372.54	1371.64	0.62%	0.65%	0.69%	0.62%	0.69%
TOTAL	17959.54	17955.45						0.02%			

RQR 7											
Energy dep (eV/hist)	MC-GPU	penEasy	Sigma	Sigma/Mean	MAX PenEasy	MIN PenEasy	Sup Relative Error	Relative error	Inf Relative Error	**Min Error**	**Max Error**
Air	21.56	21.53	0.05	0.237%	21.58	21.48	-0.11%	0.12%	0.36%	0.11%	0.36%
Muscle	8205.12	8218.45	0.98	0.012%	8219.43	8217.47	-0.17%	-0.16%	-0.15%	0.15%	0.17%
Soft tissue	562.37	558.34	0.29	0.052%	558.63	558.05	0.67%	0.72%	0.78%	0.67%	0.78%
Bone	4935.12	4925.56	0.89	0.018%	4926.45	4924.67	0.18%	0.19%	0.21%	0.18%	0.21%
Cartilage	76.42	75.86	0.10	0.132%	75.96	75.76	0.61%	0.74%	0.87%	0.61%	0.87%
Adipose	1594.33	1598.77	0.41	0.026%	1599.18	1598.36	-0.30%	-0.28%	-0.25%	0.25%	0.30%
Blood	197.71	197.52	0.17	0.086%	197.69	197.35	0.01%	0.10%	0.18%	0.01%	0.18%
Skin	1299.95	1305.43	0.39	0.030%	1305.82	1305.04	-0.45%	-0.42%	-0.39%	0.39%	0.45%
Lung	1482.04	1474.50	0.47	0.032%	1474.97	1474.03	0.48%	0.51%	0.54%	0.48%	0.54%
TOTAL	18374.64	18375.96						-0.01%			

RQR 8											
Energy dep (eV/hist)	MC-GPU	penEasy	Sigma	Sigma/Mean	MAX PenEasy	MIN PenEasy	Sup Relative Error	Relative error	Inf Relative Error	**Min Error**	**Max Error**
Air	20.86	20.85	0.05	0.245%	20.90	20.79	-0.17%	0.07%	0.32%	0.07%	0.32%
Muscle	8297.4	8310.79	1.00	0.012%	8311.79	8309.79	-0.17%	-0.16%	-0.15%	0.15%	0.17%
Soft tissue	602.24	598.99	0.30	0.050%	599.29	598.69	0.49%	0.54%	0.59%	0.49%	0.59%
Bone	5055.94	5048.93	0.91	0.018%	5049.84	5048.02	0.12%	0.14%	0.16%	0.12%	0.16%
Cartilage	84.82	84.25	0.11	0.131%	84.36	84.14	0.55%	0.68%	0.81%	0.55%	0.81%
Adipose	1635.74	1639.76	0.42	0.026%	1640.18	1639.34	-0.27%	-0.25%	-0.22%	0.22%	0.27%
Blood	216.8	216.39	0.18	0.083%	216.57	216.21	0.11%	0.19%	0.27%	0.11%	0.27%
Skin	1275.27	1279.94	0.39	0.030%	1280.33	1279.55	-0.40%	-0.36%	-0.33%	0.33%	0.40%
Lung	1569.63	1563.09	0.49	0.031%	1563.58	1562.60	0.39%	0.42%	0.45%	0.39%	0.45%
TOTAL	18758.72	18762.98						-0.02%			

RQR 9											
Energy dep (eV/hist)	MC-GPU	penEasy	Sigma	Sigma/Mean	MAX PenEasy	MIN PenEasy	Sup Relative Error	Relative error	Inf Relative Error	**Min Error**	**Max Error**
Air	19.75	19.71	0.05	0.254%	19.76	19.66	-0.03%	0.22%	0.48%	0.03%	0.48%
Muscle	8540.64	8555.52	1.00	0.012%	8556.52	8554.52	-0.19%	-0.17%	-0.16%	0.16%	0.19%
Soft tissue	684.36	681.94	0.32	0.047%	682.26	681.62	0.31%	0.36%	0.40%	0.31%	0.40%
Bone	5277.19	5274.25	0.96	0.018%	5275.21	5273.29	0.04%	0.06%	0.07%	0.04%	0.07%
Cartilage	101.81	101.30	0.12	0.118%	101.42	101.18	0.39%	0.50%	0.62%	0.39%	0.62%
Adipose	1734.27	1737.37	0.43	0.025%	1737.80	1736.94	-0.20%	-0.18%	-0.15%	0.15%	0.20%
Blood	254.63	254.58	0.20	0.079%	254.78	254.38	-0.06%	0.02%	0.10%	0.02%	0.10%
Skin	1238.88	1242.37	0.39	0.031%	1242.76	1241.98	-0.31%	-0.28%	-0.25%	0.25%	0.31%
Lung	1749.36	1745.64	0.52	0.030%	1746.16	1745.12	0.18%	0.21%	0.24%	0.18%	0.24%
TOTAL	19600.89	19612.67						-0.06%			

100 keV Monoenergetic					
Mass (g)	PENEASY Dose	MC-GPU Dose	Dose sigma	Sigma/mean	Relative error
28.7959	0.711149851	0.71235	0.00171	0.240%	0.17%
9933.98468	1.116842874	1.11584	0.00009	0.008%	0.09%
1601.7584	0.756568531	0.75586	0.00023	0.030%	0.09%
1937.78241	2.901584807	2.89816	0.00055	0.019%	0.12%
328.35161	0.643094151	0.64241	0.0005	0.078%	0.11%
2977.92241	0.926333739	0.92614	0.00016	0.017%	0.02%
680.30584	0.737469783	0.73674	0.00036	0.049%	0.10%
1281.94773	1.09557509	1.09527	0.0003	0.027%	0.03%
2521.23637	1.13694219	1.13498	0.00022	0.019%	0.17%

RQR 6					
Mass (g)	PENEASY Dose	MC-GPU Dose	Dose sigma	Sigma/mean	Relative error
28.7959	0.78327123	0.78188	0.00181	0.231%	0.18%
9933.98468	0.819797922	0.8186	0.00009	0.011%	0.15%
1601.7584	0.319771072	0.32259	0.00016	0.050%	0.88%
1937.78241	2.453500442	2.45979	0.00043	0.017%	0.26%
328.35161	0.201786433	0.20405	0.00029	0.142%	1.12%
2977.92241	0.524949876	0.52336	0.00013	0.025%	0.30%
680.30584	0.258307352	0.25881	0.00022	0.085%	0.19%
1281.94773	1.049301753	1.04461	0.0003	0.029%	0.45%
2521.23637	0.544213155	0.54777	0.00016	0.029%	0.65%

RQR 7					
Mass (g)	PENEASY Dose	MC-GPU Dose	Dose sigma	Sigma/mean	Relative error
28.7959	0.747800902	0.74886	0.00178	0.238%	0.14%
9933.98468	0.82730649	0.82596	0.00009	0.011%	0.16%
1601.7584	0.34857629	0.35109	0.00016	0.046%	0.72%
1937.78241	2.541854015	2.54679	0.00044	0.017%	0.19%
328.35161	0.231024602	0.23275	0.00031	0.133%	0.75%
2977.92241	0.536874297	0.53538	0.00013	0.024%	0.28%
680.30584	0.290341473	0.29062	0.00023	0.079%	0.10%
1281.94773	1.01831765	1.01405	0.0003	0.030%	0.42%
2521.23637	0.584832116	0.58782	0.00017	0.029%	0.51%

RQR 8					
Mass (g)	PENEASY Dose	MC-GPU Dose	Dose sigma	Sigma/mean	Relative error
28.7959	0.723891248	0.72445	0.00176	0.243%	0.08%
9933.98468	0.836601854	0.83525	0.00009	0.011%	0.16%
1601.7584	0.373960268	0.37599	0.00017	0.045%	0.54%
1937.78241	2.605519574	2.60914	0.00045	0.017%	0.14%
328.35161	0.256573434	0.25834	0.00033	0.128%	0.69%
2977.92241	0.550638927	0.54929	0.00013	0.024%	0.24%
680.30584	0.318074588	0.31869	0.00024	0.075%	0.19%
1281.94773	0.998433844	0.99479	0.0003	0.030%	0.36%
2521.23637	0.619969638	0.62257	0.00017	0.027%	0.42%

RQR 9					
Mass (g)	PENEASY Dose	MC-GPU Dose	Dose sigma	Sigma/mean	Relative error
28.7959	0.684347424	0.68574	0.00173	0.252%	0.20%
9933.98468	0.861237487	0.85974	0.00009	0.010%	0.17%
1601.7584	0.425743982	0.42726	0.00018	0.042%	0.36%
1937.78241	2.721796819	2.72332	0.00047	0.017%	0.06%
328.35161	0.3085077	0.31006	0.00036	0.116%	0.50%
2977.92241	0.583416812	0.58237	0.00014	0.024%	0.18%
680.30584	0.374208165	0.37429	0.00026	0.069%	0.02%
1281.94773	0.969126877	0.96641	0.00029	0.030%	0.28%
2521.23637	0.692374591	0.69385	0.00018	0.026%	0.21%

Real Simulation Time (s)		
Spectra	MC-GPU	PENEASY
100 keV Monoenergetic	128.54	61326.63
RQR 6	108.12	49790.51
RQR 7	110.86	51640.70
RQR 8	113.65	51355.24
RQR 9	116.13	54053.39

SIMULATION 7 LONG

SIMULATION 7 (Duke Chest)		
Phantom	Nº Voxels	580 x 260 x 300
	Voxel size (cm^3)	0.1 x 0.1 x 0.1
	Dimensions (cm^3)	58 x 26 x 30
	Materials	Human body materials
Source	Focal position (cm)	29 -32.65 15
	Spectra	100 keV monoenergetic
	Histories MC-GPU	1006720000
	Histories penEasy	$1.3 \cdot 10^{10}$
Detector size (cm^2)		122.8 x 61.4
Source-to-detector distance (cm)		68.65

Energy dep (eV/hist)	MC-GPU original	MC-GPU updated	Relative difference	PENELOPE/penEasy	Original Relative Error	Updated Relative Error
Air	20.54	20.51	0.146%	20.50	0.200%	0.053%
Muscle	11138.25	11084.77	0.480%	11094.40	0.395%	0.087%
Soft tissue	1216.29	1210.71	0.459%	1211.75	0.375%	0.086%
Bone	5613.02	5616	0.053%	5622.48	0.168%	0.115%
Cartilage	211.89	210.94	0.448%	211.15	0.351%	0.099%
Adipose	2777.28	2757.97	0.695%	2758.77	0.671%	0.029%
Blood	509.96	501.21	1.716%	501.63	1.660%	0.084%
Skin	1419.75	1404.08	1.104%	1404.41	1.092%	0.023%
Lung	2873.84	2861.56	0.427%	2866.16	0.268%	0.160%
TOTAL	25780.81	25667.74	0.439%	25691.2511	0.349%	0.092%

Dose (eV/g·hist)	MC-GPU original	MC-GPU updated	Relative difference	PENELOPE/penEasy	Original Relative Error	Updated Relative Error
Air	0.71345	0.71235	0.154%	0.7119	0.221%	0.067%
Muscle	1.12123	1.11584	0.481%	1.1168	0.396%	0.087%
Soft tissue	0.75935	0.75586	0.460%	0.7565	0.375%	0.086%
Bone	2.89662	2.89816	0.053%	2.9015	0.168%	0.115%
Cartilage	0.64531	0.64241	0.449%	0.6431	0.350%	0.101%
Adipose	0.93262	0.92614	0.695%	0.9264	0.671%	0.029%
Blood	0.74960	0.73674	1.716%	0.7374	1.659%	0.085%
Skin	1.10749	1.09527	1.103%	1.0955	1.092%	0.024%
Lung	1.13985	1.13498	0.427%	1.1368	0.268%	0.161%

Maximum dose point	173.3247	179.033718	3.294%	24.1286	618.337%	641.998%
Sigma	0.010588	0.010435		24		
Sigma/mean	0.006%	0.006%		99.467%		
Coordinates	(575,126, 220)	(171,36,24)		(179,2,48)		
Real simulation time (s)	89.18	128.02		7.62E+05		

ETSEIB

Updated MC-GPU validation								
PENELOPE/penEasy	Sigma	MAX PenEasy	MIN PenEasy	Superior Relative Error	Relative error	Inferior Relative Error	**Minimum Error**	**Maximum Error**
2.05E+01	0.0	2.05E+01	2.05E+01	0.02%	0.05%	0.12%	0.02%	0.12%
1.11E+04	0.4	1.11E+04	1.11E+04	0.09%	0.09%	0.08%	0.08%	0.09%
1.21E+03	0.1	1.21E+03	1.21E+03	0.10%	0.09%	0.08%	0.08%	0.10%
5.62E+03	0.3	5.62E+03	5.62E+03	0.12%	0.12%	0.11%	0.11%	0.12%
2.11E+02	0.0	2.11E+02	2.11E+02	0.12%	0.10%	0.08%	0.08%	0.12%
2.76E+03	0.2	2.76E+03	2.76E+03	0.03%	0.03%	0.02%	0.02%	0.03%
5.02E+02	0.1	5.02E+02	5.02E+02	0.10%	0.08%	0.07%	0.07%	0.10%
1.40E+03	0.1	1.40E+03	1.40E+03	0.03%	0.02%	0.02%	0.02%	0.03%
2.87E+03	0.2	2.87E+03	2.87E+03	0.17%	0.16%	0.15%	0.15%	0.17%

SIMULATION 8

The main characteristics of the simulations and the results are the following:

SIMULATION 8		
Phantom	Nº Voxels	122 x 62 x 372
	Voxel size (cm^3)	0.5 x 0.5 x 0.5
	Dimensions (cm^3)	61 x 31 x 186
	Materials	Human body materials
Source	Initial focal position (cm)	30.5 -30.5 130
	C-arm radius (cm)	46
	Spectra	RQR 8 (PA) and RQR 9 (AP)
	MC-GPU Beta Simulation time (s)	150
	MC-GPU histories per simulation	1006720000
	Detector size (cm^2)	143 x 143
	Source-to-detector distance (cm)	71.5

Voxels					
x number	122.00	x dim vox	0.50	x dim	61
y number	62.00	y dim vox	0.50	y dim	31
z number	372.00	z dim vox	0.50	z dim	186
Volume	0.13			Total volume	351726

ETSEIB

Energy dep (eV/hist)	MC-GPU 1	MC-GPU 2	MC-GPU Total	MC-GPU Beta	Relative Error
Air	43.7	63.7	107.4	0.00	-
Muscle	8490.1	7102.18	15592.28	15591.80	0.003%
Soft tissue	724.98	928.76	1653.74	1653.79	0.003%
Bone	5356.65	3640.61	8997.26	8997.30	0.000%
Cartilage	122.71	291.97	414.68	415.08	0.096%
Adipose	2116.53	1975.19	4091.72	4091.70	0.000%
Blood	156.65	412.14	568.79	568.91	0.021%
Skin	1389.83	1130.86	2520.69	2521.40	0.028%
Lung	849.45	797.84	1647.29	1647.12	0.010%
TOTAL	19250.61	16343.24	35593.85	35487.10	0.301%

Dose (eV/g·hist)	MC-GPU 1	MC-GPU 2	MC-GPU Total	MC-GPU Beta	Relative Error
Air	0.12815	0.18678	0.31493	0.32	0.174%
Muscle	0.23431	0.19600	0.43031	0.43	0.005%
Soft tissue	0.16054	0.20567	0.36621	0.37	0.003%
Bone	0.68175	0.46335	1.1451	1.15	0.000%
Cartilage	0.07868	0.18722	0.2659	0.27	0.101%
Adipose	0.17586	0.16412	0.33998	0.34	0.000%
Blood	0.13217	0.34773	0.4799	0.48	0.023%
Skin	0.25623	0.20848	0.46471	0.46	0.026%
Lung	0.33691	0.31644	0.65335	0.65	0.009%

Maximum Point	MC-GPU 1	MC-GPU 2	MC-GPU Beta		Relative Error	Relative Error
Edep (eV/hist)	1.688116	1.185994	1.6841	1.1933	-0.238%	0.614%
Dose (eV/g·hist)	6.786396	4.767817	6.770278	4.80E+00	-0.238%	0.614%
Sigma	0.00164	0.001418	0.06	0.05		
Sigma/mean	0.02%	0.03%	0.86%	1.06%		
Coordinates	(58,5,271)	(56,44,265)	(58,5,271)	(56,44,265)		
Material	4	4	4	4		
Voxel mass (g)	0.25	0.25	0.2488	0.2488		

ETSEIB

SIMULATION 9

The main characteristics of the simulations and the results are the following:

SIMULATION 9		
Phantom	Nº Voxels	122 x 62 x 372
	Voxel size (cm^3)	0.5 x 0.5 x 0.5
	Dimensions (cm^3)	61 x 31 x 186
	Materials	Human body materials
Source	Initial focal position (cm)	30.5 -29.5 124
	C-arm radius (cm)	45
	Spectra	RQR 6 and RQR 7
	MC-GPU Beta Simulation time (s)	150
	MC-GPU histories per simulation	1006720000
	Detector size (cm^2)	55 x 55
	Source-to-detector distance (cm)	81

	PA			AP		
Source	30.5	-29.5	124	30.5	60.5	124
Direction	0	1	0	0	-1	0
Detector	55	0	55	55	0	55
Source to detector dis	81			81		
Spectrum	RQR 6			RQR 6		
Nº histories MCGPU	1006720000			1006720000		

PA Reference System						
	RAO 90°			LAO 90°		
Rotation angle	0	0	-90	0	0	90
Direction	0	1	0	0	1	0
Detector	55	0	55	55	0	55
Source to detector dis	81			81		
Spectrum	RQR 6			RQR 6		
Nº histories MCGPU	1006720000			1006720000		
	RAO 45°			LAO 45°		
Rotation angle	0	0	-45	0	0	45
Direction	0	1	0	0	1	0
Detector	55	0	55	55	0	55
Source to detector dis	81			81		
Spectrum	RQR 6			RQR 6		
Nº histories MCGPU	1006720000			1006720000		
	CAUD 45°			CRAN 45°		
Rotation angle	-45	0	0	45	0	0
Direction	0	1	0	0	1	0
Detector	55	0	55	55	0	55
Source to detector dis	81			81		
Spectrum	RQR 7			RQR 7		
Nº histories MCGPU	1006720000			1006720000		

MC-GPU Results

Energy dep (eV/hist)	PA	AP	RAO 90	LAO 90	RAO 45	LAO 45	CAUD 45	CRAN 45	MC-GPU Sum	MC-GPU Average
Air	27.46	61.62	87.93	98.34	44.36	44.00	29.13	34.35	427.19	53.40
Muscle	13488.84	11794.61	11502.33	10201.78	14402.08	13239.53	12040.85	13703.69	100373.71	12546.71
Soft tissue	2435.16	3258.59	920.41	2251.29	1885.85	2660.19	1284.67	1721.39	16417.55	2052.19
Bone	7693.59	4261.25	4623.38	4196.68	6286.11	6661.93	9468.68	9234.10	52425.72	6553.22
Cartilage	177.07	788.51	252.99	214.15	149.94	152.82	148.46	211.84	2095.78	261.97
Adipose	3420.25	4026.97	2503.23	2445.42	3530.87	3791.75	2942.58	4483.96	27145.03	3393.13
Blood	260.80	950.15	414.90	277.90	335.43	279.71	357.24	160.92	3037.05	379.63
Skin	1637.74	1910.23	1859.83	1719.45	2303.53	2136.18	2425.35	2101.56	16093.87	2011.73
Lung	1375.32	1445.02	525.56	626.64	1017.85	1068.25	3047.78	642.93	9749.35	1218.67
TOTAL	**30516.22**	**28496.94**	**22690.57**	**22031.66**	**29956.03**	**30034.37**	**31744.74**	**32294.75**	**227765.25**	**28470.66**

Dose (eV/g·hist)	PA	AP	RAO 90	LAO 90	RAO 45	LAO 45	CAUD 45	CRAN 45	MC-GPU Sum	MC-GPU Average
Air	0.08051	0.18069	0.25785	0.28838	0.13007	0.12902	0.08543	0.10073	1.253	0.157
Muscle	0.37226	0.32550	0.31743	0.28154	0.39746	0.36538	0.33230	0.37819	2.770	0.346
Soft tissue	0.53925	0.72159	0.20382	0.49853	0.41761	0.58908	0.28448	0.38119	3.636	0.454
Bone	0.97918	0.54234	0.58843	0.53412	0.80005	0.84788	1.20510	1.17524	6.672	0.834
Cartilage	0.11355	0.50562	0.16223	0.13732	0.09615	0.09799	0.09520	0.13584	1.344	0.168
Adipose	0.28419	0.33460	0.20799	0.20319	0.29338	0.31506	0.24450	0.37257	2.255	0.282
Blood	0.22005	0.80167	0.35007	0.23448	0.28301	0.23600	0.30141	0.13578	2.562	0.320
Skin	0.30193	0.35217	0.34287	0.31699	0.42467	0.39382	0.44713	0.38744	2.967	0.371
Lung	0.54549	0.57313	0.20845	0.24854	0.40371	0.42370	1.20883	0.25500	3.867	0.483

MC-GPU Beta Results

Energy dep (eV/hist)	PA	AP	RAO 90	LAO 90	RAO 45	LAO 45	CAUD 45	CRAN 45	MC-GPU Beta Sum	MC-GPU Beta Average
Air	27.48	61.59	87.98	98.34	44.43	44.03	29.13	34.35	427.33	0.00
Muscle	13488.41	11794.14	11501.44	10201.92	14401.78	13239.91	12041.74	13702.26	100371.60	12546.45
Soft tissue	2435.46	3258.97	920.29	2251.64	1885.47	2659.74	1284.39	1721.68	16417.64	2052.21
Bone	7693.52	4261.01	4623.40	4196.59	6287.40	6662.19	9469.82	9235.64	52429.57	6553.70
Cartilage	177.02	788.15	253.00	214.01	149.96	152.83	148.58	211.75	2095.30	261.91
Adipose	3420.88	4026.75	2503.30	2445.69	3531.05	3791.36	2942.70	4484.09	27145.81	3393.23
Blood	260.69	950.33	415.02	277.93	335.56	279.83	357.14	160.98	3037.50	379.69
Skin	1637.82	1910.04	1860.02	1719.34	2303.59	2135.61	2425.69	2101.76	16093.87	2011.73
Lung	1375.28	1444.88	525.68	626.38	1017.92	1068.11	3047.57	643.01	9748.84	1218.61
TOTAL	**30489.08**	**28434.26**	**22602.14**	**21933.50**	**29912.74**	**29989.58**	**31717.63**	**32261.18**	**227767.45**	**28417.52**

Dose (eV/g·hist)	PA	AP	RAO 90	LAO 90	RAO 45	LAO 45	CAUD 45	CRAN 45	MC-GPU Sum	MC-GPU Average
Air	0.08059	0.18061	0.25800	0.28837	0.13029	0.12911	0.08542	0.10073	1.253	0.000
Muscle	0.37225	0.32549	0.31741	0.28155	0.39745	0.36539	0.33232	0.37815	2.770	0.346
Soft tissue	0.53931	0.72167	0.20379	0.49861	0.41752	0.58898	0.28442	0.38125	3.636	0.454
Bone	0.97917	0.54231	0.58843	0.53411	0.80021	0.84791	1.20524	1.17544	6.673	0.834
Cartilage	0.11351	0.50539	0.16223	0.13723	0.09616	0.09800	0.09527	0.13578	1.344	0.168
Adipose	0.28424	0.33458	0.20800	0.20321	0.29340	0.31502	0.24451	0.37258	2.256	0.282
Blood	0.21995	0.80183	0.35016	0.23450	0.28313	0.23610	0.30133	0.13583	2.563	0.320
Skin	0.30194	0.35213	0.34291	0.31697	0.42468	0.39372	0.44720	0.38748	2.967	0.371
Lung	0.54547	0.57308	0.20850	0.24844	0.40374	0.42364	1.20875	0.25503	3.867	0.483

Comparison

Energy dep (eV/hist)	PA	AP	RAO 90	LAO 90	RAO 45	LAO 45	CAUD 45	CRAN 45	Relative Error Sum	Relative Error Average
Air	0.08%	-0.05%	0.06%	0.00%	0.16%	0.07%	0.00%	0.00%	0.03%	-100.00%
Muscle	0.00%	0.00%	-0.01%	0.00%	0.00%	0.00%	0.01%	-0.01%	0.00%	0.00%
Soft tissue	0.01%	0.01%	-0.01%	0.02%	-0.02%	-0.02%	-0.02%	0.02%	0.00%	0.00%
Bone	0.00%	-0.01%	0.00%	0.00%	0.02%	0.00%	0.01%	0.02%	0.01%	0.01%
Cartilage	-0.03%	-0.05%	0.00%	-0.07%	0.01%	0.00%	0.08%	-0.04%	-0.02%	-0.02%
Adipose	0.02%	-0.01%	0.00%	0.01%	0.01%	-0.01%	0.00%	0.00%	0.00%	0.00%
Blood	-0.04%	0.02%	0.03%	0.01%	0.04%	0.04%	-0.03%	0.04%	0.01%	0.01%
Skin	0.00%	-0.01%	0.01%	-0.01%	0.00%	-0.03%	0.01%	0.01%	0.00%	0.00%
Lung	0.00%	-0.01%	0.02%	-0.04%	0.01%	-0.01%	-0.01%	0.01%	-0.01%	-0.01%
TOTAL	-0.09%	-0.22%	-0.39%	-0.45%	-0.14%	-0.15%	-0.09%	-0.10%	0.00%	-0.19%

Dose (eV/g·hist)	PA	AP	RAO 90	LAO 90	RAO 45	LAO 45	CAUD 45	CRAN 45	Relative Error Sum	Relative Error Average
Air	0.10%	-0.05%	0.06%	0.00%	0.17%	0.07%	-0.01%	0.00%	0.03%	-100.00%
Muscle	0.00%	0.00%	-0.01%	0.00%	0.00%	0.00%	0.01%	-0.01%	0.00%	0.00%
Soft tissue	0.01%	0.01%	-0.01%	0.02%	-0.02%	-0.02%	-0.02%	0.02%	0.00%	0.00%
Bone	0.00%	-0.01%	0.00%	0.00%	0.02%	0.00%	0.01%	0.02%	0.01%	0.01%
Cartilage	-0.03%	-0.05%	0.00%	-0.07%	0.01%	0.01%	0.08%	-0.04%	-0.02%	-0.02%
Adipose	0.02%	-0.01%	0.00%	0.01%	0.01%	-0.01%	0.00%	0.00%	0.00%	0.00%
Blood	-0.04%	0.02%	0.03%	0.01%	0.04%	0.04%	-0.03%	0.03%	0.01%	0.01%
Skin	0.00%	-0.01%	0.01%	-0.01%	0.00%	-0.03%	0.01%	0.01%	0.00%	0.00%
Lung	0.00%	-0.01%	0.02%	-0.04%	0.01%	-0.01%	-0.01%	0.01%	-0.01%	-0.01%

OTHER SIMULATIONS

PMMA Block

From this simulation the first conclusion can be extracted: the results using the new materials are much more accurate than the old ones and also, the simulation time of the simple layout is significant lower in MC-GPU than PENELOPE/penEasy.

PMMA Block		
Phantom	Nº Voxels	6 x 40 x 6
	Voxel size (cm^3)	5 x 0.5 x 5
	Dimensions (cm^3)	30 x 20 x 30
	Material	PMMA (ρ = 1.19 g/cm^3)
Source	Focal position (cm)	15 -45 15
	Spectrum	80 kVp 2.5 mm Al
	Histories	1.0E9
Detector size (cm^2)		54 x 54
Source-to-detector distance (cm)		81

	MC-GPU original	MC-GPU updated	PENELOPE/penEasy	Original Relative Error	Updated Relative Error
Total Energy Absorbed (eV/hist)	22559.74	22392.43	22391.60	0.751%	0.004%
Sigma			1.20		
Maximum voxel dose (ev/g·hist)	4.140681	4.04893	4.0731	1.659%	0.594%
Sigma	0.001044	0.00103	0.00550		
Coordinates	(2,0,2)	(3,0,2)	(4,1,4)=(3,0,3)		
E dp Maximum voxel dose (ev/hist)					
Dose ROI (ev/g·hist)	1.053210	1.04540	1.04536	0.751%	0.004%
Sigma	3.00E-05	3.00E-05			
Real simulation time (s)	37.96	39.24	18234.91000		

Basic Layers Block

Basic Layers Block		
Phantom	Nº Voxels	3 x 3 x 3
	Voxel size (cm^3)	10 x 10 x 10
	Dimensions (cm^3)	30 x 30 x 30
	Material	Skin, Muscle and Bone
Source	Focal position (cm)	15 -45 15
	Spectrum	90 kVp 4 mm Al
	Histories	1.0E9
Detector size (cm^2)		54 x 54
Source-to-detector distance (cm)		81

	MC-GPU original	MC-GPU updated	PENELOPE/penEasy	Original Relative Error	Updated Relative Error
Total Energy Absorbed (eV/hist)	26668.23	26300.41	26272.96	1.504%	0.104%
Maximum voxel dose (ev/g·hist)	2.726382	2.660662	2.6725	2.015%	0.444%
Sigma	0.000914	0.000896	0.00058		
Sigma/mean	0.0335%	0.0337%	0.0217%		
Coordinates	(1,0,1)	(1,0,1)	(2,1,2)=(1,0,1)		
Real simulation time (s)	56.29	99.88	33140.55		

E deposition (eV/hist)					
Skin	22465.49	21906.97	21965.60	2.276%	0.267%
Muscle	3309.44	3443.18	3391.07	2.407%	1.537%
Bone	893.30	950.25	916.29	2.508%	3.707%
Dose (eV/g·hist)					
Skin	2.269240	2.21283	2.21874	2.276%	0.267%
Muscle	0.353570	0.36786	0.36229	2.408%	1.536%
Bone	0.053650	0.05707	0.05503	2.511%	3.703%

ETSEIB

12. LIST OF TABLES

13. LIST OF FIGURES

14. BIBLIOGRAPHY

The last section of this thesis lists all the books, articles and publications consulted during the project. The bibliography is divided in two categories: the first one includes the most important references used in the learning stage; the second one shows the complementary reading to go into detail of the project and the matter dealt with.

It is important to note that most of the references used are indicated when have been used during the thesis.

14.1 BIBLIOGRAPHICAL REFERENCES

[1] Andreu Badal. MC-GPU v1.3 documentation generated by Doxygen.

[2] Andreu Badal, Fahad Zafar, Han Dong, and Aldo Badano. A real-time radiation dose monitoring system for patients and staff during interventional fluoroscopy using a GPU-accelerated Monte Carlo simulator and an automatic 3D localization system based on a depth camera. SPIE 8668, Medical Imaging 2013: Physics of Medical Imaging, 866828 (19 March 2013); DOI: 10.1117/12.2008031

[3] Andreu Badal and Aldo Badano. Accelerating Monte Carlo simulations of photon transport in a voxelized geometry using a massively parallel graphics processing unit. Medical Physics 36, 4878-4880 (2009); DOI: 10.1118/1.3231824

[4] Josep Sempau, Andreu Badal and Lorenzo Brualla. A PENELOPE-based system for the automated Monte Carlo simulation of clinacs and voxelized geometries-application to far-from-axis fields. Med. Phys 38. Year 2011. PMID: 22047353 DOI: 10.1118/1.3643029

[5] Francesc Salvat. PENELOPE-2014. A Code System for Monte Carlo Simulation of Electron and Photon Transport (Nuclear Energy Agency OECD, 2015). Available at https://www.oecd-nea.org/science/docs/2015/nsc-doc2015-3.pdf

[6] Xavier Ortega Aramburu and Jaume Jorba Bisbal. Radiaciones Ionizantes: Utilización y riesgos vol. I and II. ISBN: 84-8301-170-0

[7] Sara Principi. Doctoral Dissertation. Development of Methodologies for Estimating the Dose to the Eye Lens in Interventional Radiology. Operational Implications of the Eye Lens New Dose Limit.

[8] Glenn F.Knoll. Radiation Detection and Measurement. John Wiley & Sons Inc; 4th Edition. ISBN-10: 0470131489. ISBN-13: 978-0470131480

[9] Frank Herbert Attix. Introduction to radiological physics and radiation dosimetry. Online ISBN: 9783527617135. DOI: 10.1002/9783527617135

[10] ICRP, 2007. The 2007 Recommendations of the International Commission on Radiological Protection. ICRP Publication 103. Ann. ICRP 37 (2-4).

[11] ICRP, 2009. Adult Reference Computational Phantoms. ICRP Publication 110. Ann. ICRP 39 (2).

14.2 FURTHER READING

Vanhavere F., Carinou E., Gualdrini G., Clairand I., Sans Merce M., Ginjaume M., Nikodemova D., Jankowski J., Bordy J-M., Rimpler A., Wach S., Martin P., Struelens L., Krim S., Koukorava C., Ferrari P., Mariotti F., Fantuzzi E., Donadille L., Itié C., Ruiz N., Carnicer A., Fulop M., Domienik J., Brodecki M., Daures J., Barth I., Bilski P. EURADOS Report 2012-02. ORAMED: *Optimization of Radiation Protection of Medical Staff.*

Implications of Medical Low Dose Radiation Exposure. MEDIRAD. NFRP-2016-2017

EU Council Directive 2013/59/EURATOM of 5 December 2013 laying down basic safety standards for protection against the dangers arising from exposure to ionising radiation, and repealing Directives 89/618/Euratom, 90/641/Euratom, 96/29/Euratom, 97/43/Euratom and 2003/122/Euratom. Published in the Official Journal of the European Union.

2017 -2018

MC-GPU HANDBOOK

Version 1.0

MC-GPU USER MANUAL

ÁLVARO MERINO CANETE

UPC | INTE

OUTLINE

MC-GPU DESCRIPTION

MC-GPU is a Monte Carlo simulation code that generates synthetic radiographic images and computed tomography (CT) scans of realistic models of the human anatomy using the computational power of commodity Graphics Processing Unit (GPU) cards. The code implements a massively multi-threaded Monte Carlo simulation algorithm for the transport of x rays in a voxelized geometry. The x ray interaction models and material properties have been adapted from PENELOPE 2006.

MC-GPU was developed using the CUDA programming model from NVIDIA to achieve maximum performance on NVIDIA GPUs. The code can also be compiled with a standard C compiler to be executed in a regular CPU. In a typical medical imaging simulation, the use of GPU computing with MC-GPU has been shown to provide a speed up of between 20 and 40 times, compared to the execution on a single CPU core.

The MC-GPU code has been described in different scientific publications. The main reference of this work, which the users should cite, is the following:

> *Andreu Badal and Aldo Badano, "Accelerating Monte Carlo simulations of photon transport in a voxelized geometry using a massively parallel Graphics Processing Unit", Medical Physics 36, pp. 4878-4880 (2009)*

The main developer of MC-GPU is Andreu Badal, working at the U.S. Food and Drug Administration (Centre for Devices and Radiological Health, Office of Science and - Engineering Laboratories, Division of Imaging and Applied Mathematics). The source code of MC-GPU is free and open software in the public domain, as explained in the Disclaimer section below. The source code of MC-GPU and its auxiliary files are distributed from the website: http://code.google.com/.

PURPOSE

The purpose of this manual is to help the new users to use the MC-GPU code to simulate a real interventional radiology (IR), also known as vascular and interventional radiology (VIR), in order to obtained in the most precise way the dose received by the patient and by the physician during the intervention.

This manual is structured to learn how to use the MC-GPU program in which only the patient is simulated and then learn the extended version (MC-GPU_Beta) in which the physician, hereinafter operator, is also simulated.

It is divided in sections in which the previous and the posterior steps of a simulation, as well as how to run a simulation, are explained.

PREVIOUS KNOWLEDGE

Before carrying out the simulations it is important to have some basic knowledge about the procedure to be simulated, physics, Monte Carlo simulations and practical aspects of the program configuration itself.

Interventional Radiology (IR)

An interventional radiological procedure is any procedure using radiological imaging equipment in order to guide a therapeutic/invasive procedure on a patient. Examples of such procedures include angiography, angioplasty, embolization, biopsy and drainage, dilations and stent placements. Interventional radiology has gained importance in the fields of cardiology and neurology, vascular and non-vascular medicine and often represents an alternative to more hazardous surgery.

Fluoroscopy is predominantly used, which is a way of working in real time. Currently almost exclusively fluoroscopy is used.

Interventional procedures are complex and generally involve the use of long fluoroscopy times. Consequently, there is a potential for high radiation doses to patients and staff as compared to other X-ray examinations.

X-Rays / Equipment

Fluoroscopy or radioscopy is an imaging technique used in medicine to obtain real-time images of the internal structures of patients by using a fluoroscope. The basic fluoroscopic equipment includes an x-ray source designed to give off pulse or continuous radiation and an image intensifier between which the patient is placed. Both elements are mounted on a C-arm.

In its simplest form, a fluoroscope consists of an X-ray source and a fluorescent screen between which the patient is placed. However, modern fluoroscopes couple the screen to an X-ray image intensifier and a CCD video camera, allowing images to be recorded and played back on a monitor.

The use of X-rays, a type of ionizing radiation, requires that the potential risks of a procedure be carefully weighed against the expected benefits to the patient. Although physicians always try to use low doses of radiation during fluoroscopies, the duration of a typical procedure often results in a relatively high absorbed dose to the patient. Recent advances include the digitization of captured images and flat panel detector systems that further reduce the radiation dose for patients.

In operation, when the x-ray source emits x-rays toward the patient, some radiation typically passes through the patient and impinges on the detector. As the radiation passes through the patient, anatomical structures of different densities inside the patient cause intensity variations of the transmitted radiation that goes into the detector which transmits the image to a monitor.

Nowadays, the use of intensifier tubes and modern digital flat panel receptors make it possible to optimize the balance of patient exposure with high image quality so as not to expose the patient to unnecessary radiation levels.

"C-arm" mobile fluoroscopy machines are often colloquially referred to as image intensifiers, however strictly speaking the image intensifier is only one part of the machine (namely the detector).

A fluoroscopy unit generally consists of two units, the X-ray generator, henceforth the source, and image detector on a moveable C-arm, and a separate workstation unit used to store and manipulate the images. The patient is positioned between the two arms, typically on a radiolucent bed. Most systems arranged as c-arms can have the image intensifier positioned above or below the patient (with the x-ray tube below or above respectively).

X-Ray Circuit[1]

The actual circuit of a modern x-ray machine is very complex; the figure shows a simplified diagram of it. Hereby, only the basic aspects of the x-ray tube are considered in this section.

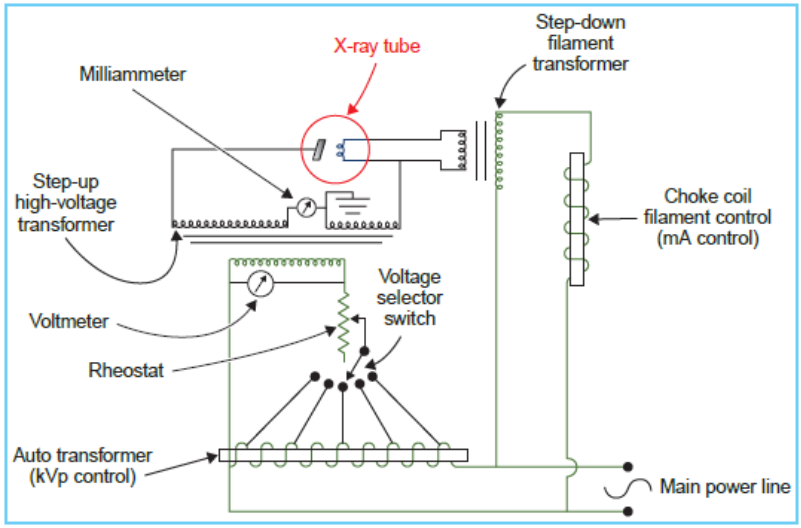

Figure 1: Simplified X-ray circuit

The circuit can be divided into two parts: the high-voltage circuit to provide the accelerating potential for the electrons and the low-voltage circuit to supply heating current to the filament. Since the voltage applied between the cathode and the anode is high enough to accelerate all the electrons across to the target, the filament temperature or filament current controls the tube current (the current in the circuit due to the flow of electrons across the tube) and hence the X-ray intensity.

X-ray tube (Source)

The tube consists of a glass envelope which has been evacuated to high vacuum that converts electrical input power into X-rays. This source of ionizing radiation in contrast to other sources produces X-rays only as long as the tube is energized. A schematic diagram of a conventional x-ray tube is shown below.

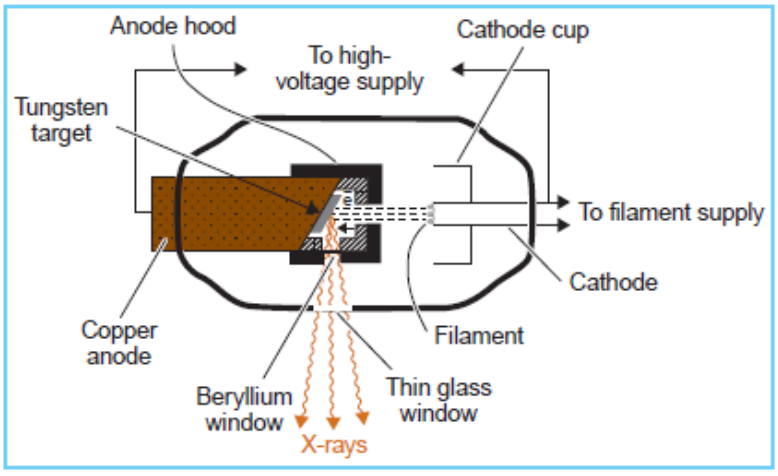

Figure 2: Therapy X-ray tube

The organization is as follow, at one end is a cathode (negative electrode) and at the other an anode (positive electrode), both hermetically sealed in the tube. The cathode is a tungsten filament which when heated

[1] KHAN'S "The physics of radiation therapy".

emits electrons, a phenomenon known as thermionic emission. The anode consists of a thick copper rod, at the end of which is placed a small piece of tungsten target.

When a high voltage is applied between the anode and the cathode, the electrons emitted from the filament are accelerated toward the anode and achieve high velocities before striking the target. The x-rays are produced by the sudden deflection or acceleration of the electron caused by the attractive force of the tungsten nucleus. The physics of x-ray production will be discussing in further sections. The x-ray beam emerges through a thin glass window in the tube envelope. In some tubes, thin beryllium windows are used to reduce inherent filtration of the x-ray beam.

Two types of filtration to generate the desired x-ray spectrum exist: inherent filtration, characteristic of each tube and the added filtration, chosen by the physicians.

In radiation therapy, this conic beam of x-rays is collimated to a desired size. Collimators help to shape the beam of radiation emerging from the machine and can limit the maximum field size of a beam. In our particular case, the resulting beam has a pyramidal shape.

Image intensifier (Detector)

X-ray detectors are devices used to measure the flux, spatial distribution, spectrum, and/or other properties of X-rays.

Detectors can be divided into two major categories: imaging detectors (such as photographic plates and X-ray film (photographic film), now mostly replaced by various digitizing devices like image plates or flat panel detectors) and dose measurement devices.

In this particular case, the detector is an x-ray image intensifier, an image intensifier that converts x-rays into visible light at higher intensity than mere fluorescent screens do. Such intensifiers are used in fluoroscopes to allow low-intensity x-rays to be converted to a conveniently bright visible light output. The device contains a low absorbency/scatter input window, typically aluminium, input fluorescent screen, photocathode, electron optics, output fluorescent screen and output window. These parts are all mounted in a high vacuum environment within glass or more recently, metal/ceramic. By its intensifying effect, it allows the viewer to more easily see the structure of the object being imaged than fluorescent screens alone, whose images are dim. The X-ray II requires lower absorbed doses due to more efficient conversion of x-ray quanta to visible light.

Risks

Patient Risks

Because fluoroscopy involves the use of X-rays, an ionizing radiation, fluoroscopic procedures pose a potential for increasing the patient's risk of radiation-induced cancer. Radiation doses to the patient depend on the size of the patient as well as duration of the procedure. Exposure times vary depending on the procedure being performed. Because of the long duration of some procedures, additionally to the cancer risk and other stochastic radiation effects, deterministic radiation effects have also been observed ranging from mild erythema, equivalent of a sun burn, to more serious burns.

While deterministic radiation effects are a possibility, radiation burns are not typical of standard fluoroscopic procedures. Most procedures sufficiently long in duration to produce radiation burns are part of necessary life-saving operations.

Operator Risks

Some procedures are very complex and they can lead to relatively high doses to the medical staff, henceforth the operators, who stand close to the primary radiation field if they do not protect themselves with the appropriate shield.

Moreover, as the procedures performed in IC/IR require the interventional cardiologists and radiologists to stand close to the patient, who represents the main source of scattered radiation.

From a radiation protection point of view, under-couch (x-ray tube) operation is preferable as it reduces the amount of scattered radiation on operators.

Monte Carlo simulation

Monte Carlo methods are widely used to solve complex physical and mathematical problems, particularly those involving multiple independent variables where more conventional numerical methods would demand formidable amounts of memory and computer time. These methods are applied in radiation transport.

In Monte Carlo simulation of radiation transport, the history (track) of a particle is viewed as a random sequence of free flights that end with an interaction event where the particle changes its direction of movement, loses energy and, occasionally, produces secondary particles.

The Monte Carlo simulation of a given experimental arrangement consists of the numerical generation of random histories.

It distinguishes between a simulation, a Monte Carlo method, and a Monte Carlo simulation: a simulation is a fictitious representation of reality, a Monte Carlo method is a technique that can be used to solve a mathematical or statistical problem, and a Monte Carlo simulation uses repeated sampling to determine the properties of some phenomenon or behaviour.

The seed of the random numbers is a crucial parameter in this kind of simulations because its value modify the results but using the same, the results are identical.

If the number of generated histories is large enough, quantitative information on the transport process may be obtained by simply averaging over the simulated histories. Although the number of simulations achieves more accurate results (lower sigma), it leads to too long simulation times.

Voxelized geometry

In order to carry out realistic simulations, real objects need to go through a voxelization stage is concerned with converting geometric objects from their continuous geometric representation into a set of voxels[2] that best approximates the continuous object. The size of the voxels determines the quality and the accuracy of the simulation and results.

The voxelized geometries used by the MC-GPU use the PENELOPE/PenEasy format. The characterization of each voxel requires two data: material index and density (same material may have different densities in different voxels).

A voxelized geometry is a geometry model in which the object (in this case patient) to be simulated is described in terms of a collection of volume elements or voxel. Each voxel is a rectangular prism with a homogeneous material composition. In the model implemented, all voxels have the same dimensions and they are adjacent, that is, each

[2] A voxel represents a value on a regular grid in three-dimensional space.

voxel has its six faces in contact with those of the closest neighbours, except of course for those voxels located in the periphery of what is called the voxels bounding box.

The coordinate system of the simulated world (reference system) is determined by the input voxelized geometry of the patient. The origin of coordinates is assumed to be located at the lower-back corner of the voxelized volume (in other words left heel), and the axis are located on the vertices of the voxelized volume. This means that the lower-back corner of the first voxel is on the origin and the following voxels are located along the positive X, Y and Z axis (first quadrant).

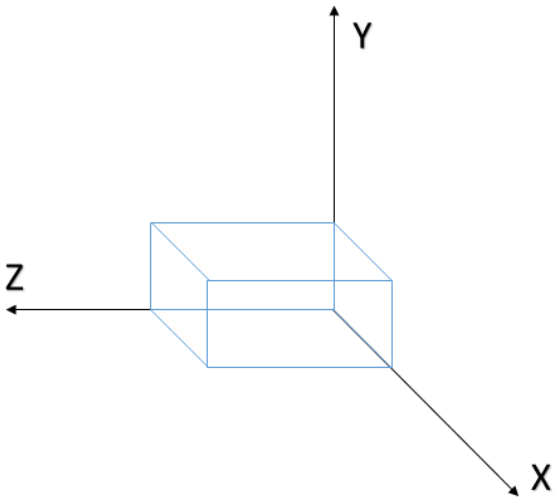

Figure 3: Patient reference system

The reference system (patient system) in this case in which the patient is supposed to be lying is as show the figure.

To distinguish the different organs of the human body the method is to assign a different materials and densities to the voxels which represent them.

For a better visualization, following photo shows the programme axis located in a real cardiovascular X-ray system. The patient is always lying face up on the table. The origin of coordinates is supposed to be in the left heel of the patient.

The photo is taken from the side where de medical staff usually work.

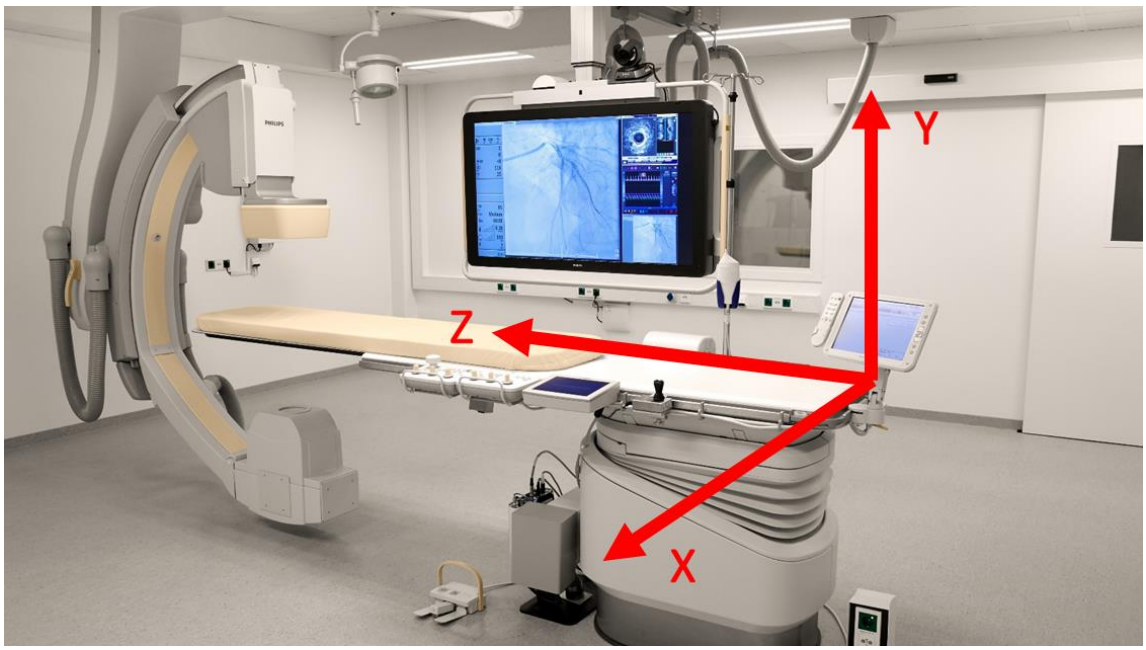

Figure 4: Patient reference system in real X-ray system

Physics

X-Ray

X-radiation is a form of electromagnetic radiation emitted by charged particles (usually electrons) in changing atomic energy levels (called characteristic or fluorescence x-rays) or in slowing down in a Coulomb force field (continuous or Bremsstrahlung x-rays). Most X-rays have a wavelength ranging from 0.01 to 10 nm and energies in the range of 0.1 to 120 keV. Most commonly, the energy ranges of X-rays are now referred in terms of the generating voltage. The range of Diagnostic X-rays is from 20 to 120 kV.

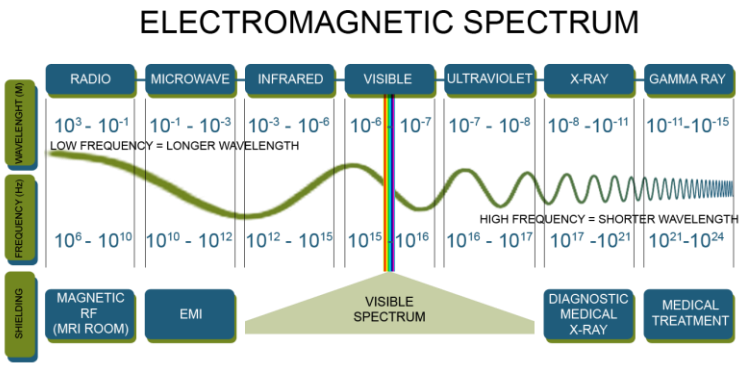

Figure 5: Electromagnetic Spectrum[3]

The relation between the generating voltage (V) and the energy (eV) of the x-rays is difficult to set and depends on the inherent filtration of the X-ray tube and the added filtration.

There are two different mechanisms by which x-rays are produced. One gives rise to bremsstrahlung x-rays and the other characteristic x-rays. Both mechanisms take place if the conditions are accomplished.

Bremsstrahlung

The process of bremsstrahlung (braking radiation) is the result of radiative interaction between a high-speed electron and a nucleus. The electron while passing near a nucleus may be deflected from its path by the action of Coulomb forces of attraction and lose energy as bremsstrahlung, a phenomenon predicted by Maxwell's general theory of electromagnetic radiation. According to this theory, energy is propagated through space by electromagnetic fields. As the electron, with its associated electromagnetic field, passes in the vicinity of a nucleus, it suffers a sudden deflection and acceleration. As a result, a part or all of its energy is dissociated from it and propagates in space as electromagnetic radiation, the x-ray. The mechanism of bremsstrahlung production is illustrated

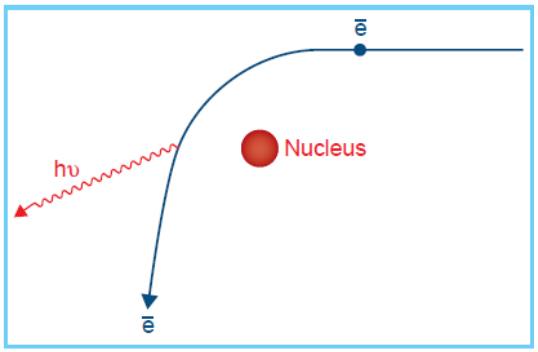

Figure 6: Bremsstrahlung process

[3] http://www.shieldingsystems.com/

Characteristic X-rays

An electron, with kinetic energy E0, may interact with the atoms of the target by ejecting an orbital electron, such as a K, L, or M electron, leaving the atom ionized. The original electron will recede from the collision with energy E0 – ΔE, where ΔE is the energy given to the orbital electron. A part of ΔE is spent in overcoming the binding energy of the electron and the rest is carried by the ejected electron. When a vacancy is created in an orbit, an outer orbital electron will fall down to fill that vacancy. In so doing, the energy is radiated in the form of electromagnetic radiation, x-ray. This is called characteristic radiation. With higher atomic number targets and the transitions involving inner shells such as K and L, the characteristic radiations emitted are of energies high enough to be considered in the x-ray part of the electromagnetic spectrum.

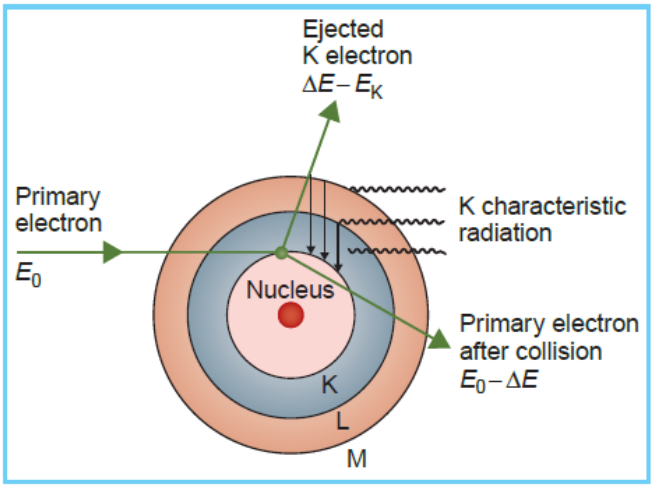

Figure 7: Characteristic x-rays production

It should be noted that, unlike bremsstrahlung, characteristic x-rays are emitted at discrete energies. If the transition involved an electron descending from the L shell to the K shell, then the photon emitted will have energy hv = EK – EL, where EK and EL are the electron-binding energies of the K shell and the L shell, respectively.

The threshold energy that an incident electron must possess in order to first strip an electron from the atom is called critical absorption energy.

The shape of the x-ray energy spectrum is the result of the alternating voltage applied to the tube, multiple bremsstrahlung interactions within the target, and filtration in the beam. However, even if the x-ray tube were to be energized with a constant potential, the x-ray beam would still be heterogeneous in energy because of the multiple bremsstrahlung processes that result indifferent energy photons.

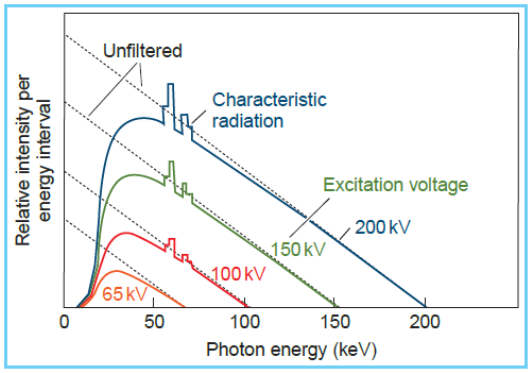

Figure 8: Example of spectral distribution of x-rays

Because of the x-ray beam having a spectral distribution of energies, which depends on voltage, as well as filtration, it is difficult to characterize the beam quality in terms of energy, penetrating power, or degree of beam hardening. A practical rule of thumb is often used which states that the average x-ray energy is approximately one-third of the maximum energy or kVp.

Units and Definitions

Ionizing radiation

Ionization produced by particles is the process by which one or more electrons are liberated in collisions of the particles with atoms or molecules. This can be distinguished from excitation, which is a transfer of electrons to higher energy levels in atoms or molecules and generally requires less energy.

When charged particles have slowed down sufficiently, ionization becomes less likely or impossible, and the particles increasingly dissipate their remaining energy in other processes such as excitation or elastic scattering. Thus, near the end of their range, charged particles that were ionizing can be considered to be non-ionizing.

The term ionizing radiation refers to charged particles (electrons or protons) and uncharged particles (photons or neutrons) that can produce ionizations in a medium or can initiate nuclear or elementary-particle transformations that then result in ionization or the production of ionizing radiation.

Energy

The traditional unit for measurement of radiation energy is the electron volt or eV, defined as the kinetic energy gained by an electron by its acceleration through a potential difference of 1 V. The multiples of kiloelectron volt (keV) and megaelectron volt (MeV) are more common in the measurement of energies for ionizing radiation. The electron volt is a convenient unit when dealing with particulate radiation because the energy gained from an electric field can easily be obtained by multiplying the potential difference by the number of electronic charges carried by the particle

$$1\ eV = 1.602 \cdot 10^{-19}\ J$$

Energy fluence

It is quotient of dR by da, where dR is the radiant energy (energy of particles excluding the rest energy) on a sphere of cross-sectional area da. Its unit is J/m^2 or eV/cm^2.

The use of a sphere of cross-sectional area da expresses in the simplest manner the fact that one considers an area da perpendicular to the direction of each particle.

KERMA (Kinetic Energy Released per unit Mass)

The kerma, K, for ionizing uncharged particles, is the mean energy transferred (sum of the initial kinetic energies of all the charged particles liberated) to charged particles by uncharged ionizing radiation per unit mass. Its unit is gray Gy (J/kg)

Air KERMA

It is of importance in the practical calibration of instruments for photon measurement, where it is used for the traceable calibration of gamma instrument metrology facilities using a "free air" ion chamber to measure air kerma.

The IAEA safety report 16 states "*The quantity air kerma should be used for calibrating the reference photon radiation fields and reference instruments. Radiation protection monitoring instruments should be calibrated in terms of dose equivalent quantities. Area dosimeters or dose parameters should be calibrated in terms of the ambient dose equivalent, H*(10), or the directional dose equivalent, H'(0.07),without any phantom present, i.e. free in air.*"

Conversion coefficients from air kerma in Gy to equivalent dose in Sv are published in the International Commission on Radiological Protection (ICRP) report 74.

Absorbed Dose D

The absorbed dose, D, is the mean energy imparted by ionizing radiation to matter per unit mass. Its unit is gray Gy (J/kg)

Absorbed-Dose Rate $\dot{D}$

It is defined as the increment of absorbed dose in a time interval. Its unit is Gy/s (J/kg·s)

Mean absorbed dose in a tissue or organ, D_T

It is the absorbed dose averaged over the tissue or organ T.

$$D_T = \frac{\varepsilon_T}{m_T}$$

Where ε_T is the mean total energy imparted in a tissue or organ T and m_T is the mass of that tissue or organ.

Equivalent dose, H_T

For a biological material, the probability of radiation effects depends not only on the absorbed dose, but also on the type and energy of the radiation causing the dose.

The dose in a tissue or organ T is given by:

$$H_T = \sum_R w_R \cdot D_{T,R}$$

Where $D_{T,R}$ is the mean absorbed dose from radiation R in a tissue or organ T, and w_R is the radiation weighting factor. Since w_R is dimensionless, the unit for the equivalent dose is the same as for absorbed dose, J/kg, and its special name is sievert (Sv).

The radiation weighting factors are set by International Commission on Radiological Protection (ICRP)

Effective dose, E

As different tissues have different sensitivity to ionizing radiation the effective dose is defined as the tissue-weighted sum of the equivalent doses in all specified tissues and organs of the body, given by the expression

$$E = \sum_T w_T \sum_R w_R \cdot D_{T,R} = \sum_T w_T \cdot H_T$$

where H_T or $w_R \cdot D_{T,R}$ is the equivalent dose in a tissue or organ, T, and w_T is the tissue weighting factor. The unit for the effective dose is the same as for absorbed dose, J/kg, and its special name is sievert (Sv).

The tissue weighting factors are set by International Commission on Radiological Protection (ICRP)

Mass attenuation coefficient

The mass attenuation coefficient of the volume of a material characterizes how easily it can be penetrated by a beam of light or other energy or matter. In addition to visible light, mass attenuation coefficients can be defined for other electromagnetic radiation such as X-rays. The SI unit of mass attenuation coefficient is the square metre per kilogram (m^2/kg). Other common units include cm^2/g (the most common unit for X-ray mass attenuation coefficients). The values of mass attenuation coefficients are dependent upon the absorption and scattering of the incident radiation caused by several different mechanisms.

Photon Interactions

Although a large number of possible interaction mechanisms are known for gamma rays in matter, only four major types play an important role in radiation measurements (figure). All these processes lead to the partial or complete transfer of the photon energy to electron energy. They result in sudden and abrupt changes in the photon history, in that the photon either disappears entirely or is scattered through a significant angle. This behaviour is in marked contrast to the charged particles discussed earlier in this chapter, which slow down gradually through continuous, simultaneous interactions with many absorber atoms.

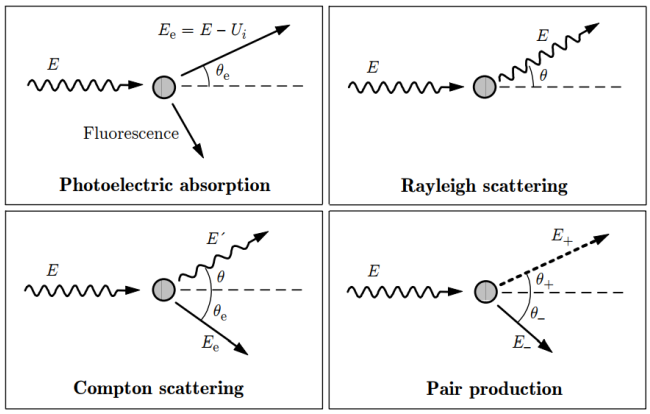

Figure 9: Photon interactions[4]

Photoelectric absorption

In the photoelectric absorption process, a photon undergoes an interaction with an absorber atom in which the photon completely disappears. In its place, an energetic photoelectron is ejected by the atom from one of its bound shells. The interaction is with the atom as a whole and cannot take place with free electrons. For photon of sufficient energy, the most probable origin of the photoelectron is the most tightly bound or K shell of the atom.

In addition to the photoelectron, the interaction also creates an ionized absorber atom with a vacancy in one of its bound shells. This vacancy is quickly filled through capture of a free electron from the medium and/or rearrangement of electrons from other shells of the atom. Therefore, one or more characteristic X-ray photons may also be generated. Although in most cases these X-rays are reabsorbed close to the original site through photoelectric absorption involving less tightly bound shells, their migration and possible escape from radiation detectors can influence their response. In some fraction of the cases, the emission of an Auger electron may substitute for the characteristic X-ray in carrying away the atomic excitation energy. The threshold for ejection of an electron of a given shell is just the ionization energy of the shell.

[4] PENELOPE: A code system for Monte Carlo simulation of electron and photon transport

Compton scattering

The interaction process of Compton scattering takes place between the incident photon and an electron in the absorbing material. It is most often the predominant interaction mechanism for gamma-ray energies typical of radioisotope sources.

In Compton scattering, the incoming photon is deflected through an angle with respect to its original direction. The photon transfers a portion of its energy to the electron (assumed to be initially at rest), which is then known as a recoil electron. Because all angles of scattering are possible, the energy transferred to the electron can vary from zero to a large fraction of the photon energy. This process has a threshold for each shell of bound electrons corresponding to the ionization energy of the shell.

Rayleigh scattering

In addition to Compton scattering, another type of scattering can occur in which the photon interacts coherently with all the electrons of an absorber atom. This coherent scattering or Rayleigh scattering process neither excites nor ionizes the atom, and the photon retains its original energy after the scattering event. Because virtually no energy is transferred, this process is often neglected in basic discussions of interactions.

This term is usually associate to the scattering of light by particles of size much smaller than the wavelength. Its cross section increases rapidly with photon energy. This elastic scattering from atoms has the only cross-section that has no energy threshold.

Pair production

If the photon energy exceeds twice the rest-mass energy of an electron (1.02 MeV), the process of pair production is energetically possible. As a practical matter, the probability of this interaction remains very low until the photon energy approaches several MeV and therefore pair production is predominantly confined to high-energy gamma rays. In the interaction (which must take place in the coulomb field of a nucleus), the photon disappears and is replaced by an electron-positron pair. All the excess energy carried in by the photon above the 1.02 MeV required to create the pair goes into kinetic energy shared by the positron and the electron. Because the positron will subsequently annihilate after slowing down in the absorbing medium, two annihilation photons are normally produced as secondary products of the interaction.

Biological effects of ionizing radiation effect

The biological effects due to an ionizing radiation are divided in two groups:

- **Deterministic Effects**: most of organs and tissues are not affected by the loss of certain number of cells but if the amount of killed cells becomes large, a loss of functional capacity of the tissue will be observed. These reactions that may occur early or late after irradiation are the deterministic effects. The appearance of these effects depends on a threshold dose, below which the effects are null. This limit depends on dose delivery mode and may differ in different persons.
- **Stochastic Effects**: the killing of one or a small number of cells will, in most cases, have no consequences in tissue, but modification in single cells, such as genetic changes or transformations leading ultimately to malignancy, may have serious consequences, this is the case of stochastic effects. The severity of these effects is not dose dependent but the probability increases with the dose.

Extended knowledge

All information presented in the previous sections mean a general overview of the most important concepts need to understand the program but it is only a brief explanation. For

To go deeper and learn more about the subject, the recommended lectures where this information were obtained are the following:

- The Physics Of Radiation Therapy – Faiz M. Khan
- PENELOPE-2014: A Code System for Monte Carlo Simulation of Electron and Photon Transport – Francesc Salvat
- ICRU Report nº 85 Fundamental Quantities and Units for Ionizing Radiation
- ICRP Publication 103: The 2007 Recommendations of the International Commission on Radiological Protection
- Introduction to radiological physics and radiation dosimetry – Frank Herbert Attix
- Radiation Detection and Measurement – Glenn F.Knoll
- Practical Gamma-ray Spectrometry – Gordon R.Gilmore
- Radiaciones ionizantes, Utilización y riesgos I y II – Xavier Ortega y Jaume Jorba (Spanish)
- Documentation given by MC-GPU and penEasy distributors

Simulation tips

A few little advices for creating the plain text inputs:

- The location of all the values in the main input file must be respected. The program needs all the default lines in its adequate position. The only section may increase or decrease its extension is [SECTION MATERIAL FILE LIST] which depends on the voxelized geometry.
- All lines must have the number of values what is expected.
- The space between values in each line must be respected.
- In order to avoid some simulation problems is recommended to respect the space for the minus even for positive values and to type most of the values with one decimal even for integer numbers (except in the [SECTION SIMULATION CONFIG])
- For all the plain text input files the symbol # means a comment and the executables do not read the lines which have it at the beginning.

PRE-SIMULATION INFORMATION

MC-GPU has been developed and tested only in the Linux operating system. A Makefile script is provided to compile the MC-GPU code in Linux. The CUDA libraries and the GNU GCC compiler must be previously installed.

All information need to code compilation are explained in **MC-GPU_v1.3_README.pdf** which is included in the compressed directory which can be downloaded from https://code.google.com/archive/p/mcgpu/downloads.

Once the directory has been decompressed, the user has the necessary libraries to compile the code, some important documentation, the material files library, the gnuplot's scripts and some examples.

All information provided in this handbook henceforth is in case of using the Argos Cluster located into the INTE/SEN facilities (Barcelona) Argos2 server Port 222 where all the libraries and resources need to compile de code are previously installed.

The user just need to compile de code following the instructions collected in the mentioned **MC-GPU_v1.3_README.pdf**.

It is important to highlight that the user needs to have permission to access to this Cluster and its servers and ports.

In order to use the MC-GPU system efficiently some auxiliary tools that are not included in the distribution package will be needed. They are the following:

1. A powerful file manager will also make some tasks considerably easier. To change files from the cluster to the personal computer, WinSCP is recommended. It can be downloaded here: https://winscp.net/eng/download.php
2. An SSH and telnet client which allow you to run simulations in the cluster. In this case the recommendation is Putty
   It can be downloaded here: http://www.putty.org/
3. A plain text editor. A text editor serves to edit plain text (ASCII) files, which do not contain 'implicit' formatting instructions and it is also useful an output text files. The use of Notepad++ is recommended.
   It can be downloaded here: https://notepad-plus-plus.org
4. A graphic program. The recommendation is Gnuplot, a powerful 2D and 3D plotting program, also from the GNU project, that is free and open source.
   It can be downloaded here: http://www.gnuplot.info
5. A graphics program to visualize raw files and volumes. Those files may be read with Octave, Image J, Paraview, Slicer or other programs but the recommendation is ImageJ.
   It can be downloaded here: https://imagej.nih.gov/ij/
6. Spectrum file generator. Spekcal and XCOMP5R (free) are specific programs in this area. This last one is recommended due to it is free and easy to use. However, this program runs only on computers with MS-DOS operating systems, for this reason, a MS-DOS simulator like DOSBOX is need.

GENERAL SCHEME

The scheme shown below gives a general view of the necessary files to run a simulation as well as the process to follow before and after a simulation.

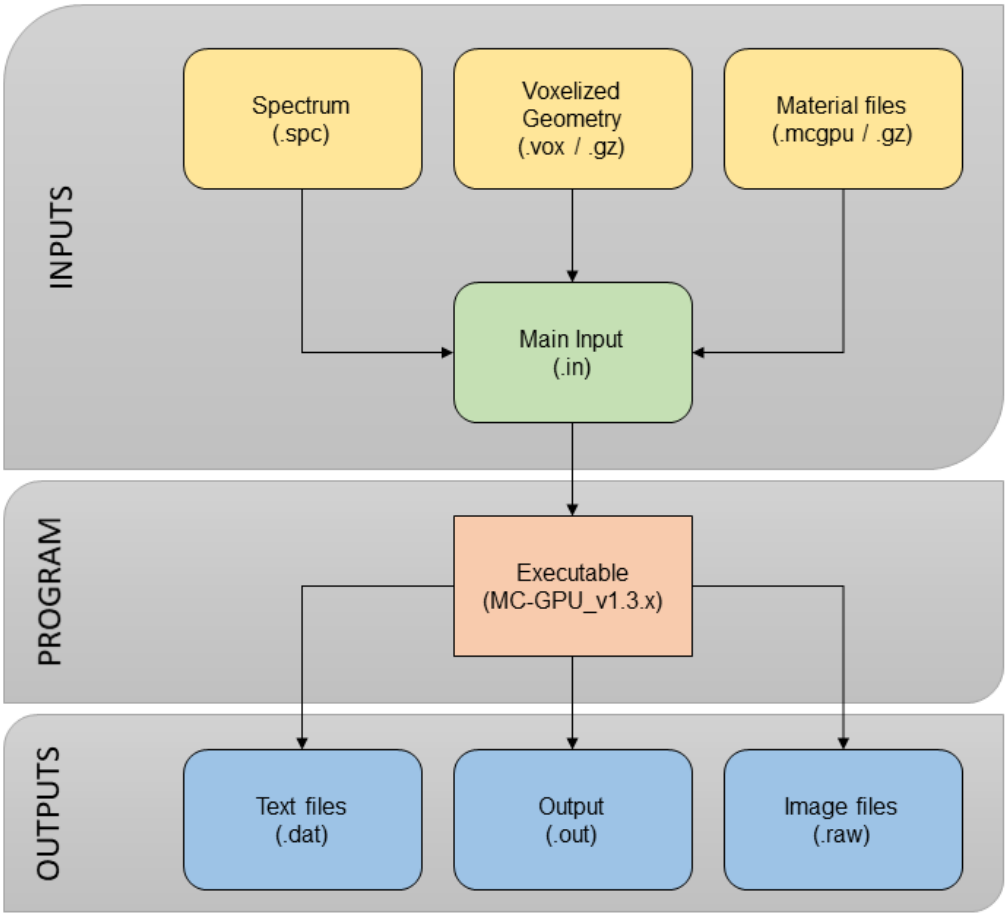

Figure 10: MC-GPU general scheme

It is recommended to have all the inputs (spectrum, geometry, materials and main input file) and the executable in the same directory. In addition, the creation of a directory for each simulation is recommended.

MAIN INPUT FILE SECTIONS

SIMULATION CONFIGURATION SECTION

LINE	NAME	EXAMPLE	DESCRIPTION
1	Total number of histories	1E8	Number of histories[5] to simulate. If it is lower than 1E5, program will take this value as simulation time in seconds. This value set the number of X-rays.
2	Random seed	1234567890	The seed determines the sequence of random numbers utilised during the simulation. Use the same number to compare different simulations
3	GPU number to use when MPI is not used	0	The use of a 0 value avoids MPI runs
4	GPU threads per CUDA block	128	This value must be multiple of 32. Recommended value: 128
5	Simulated histories per GPU thread	100	Recommended value: 100

Note: time simulation depends directly on the total number of histories required.

SOURCE SECTION

The emitted cone beam is computationally collimated to produce a rectangular field on the detector plane, realistic approach, within the azimuthal and polar angles specified by the user.

LINE	NAME	EXAMPLE	DESCRIPTION
1	X-Ray energy spectrum	90keV.spc	This spectrum file is described in Other input files section
2	Source position	15.0 -45.0 15.0	Cartesian coordinates in centimetres of source position origin
3	Source direction cosines	0.0 1.0 0.0	This normal vector determines the direction of the beam
4	Polar and azimuthal apertures for the fan beam	-45.0 -45.0	Angles in degrees that determine the aperture of the pyramid. Input negative to automatically cover the whole detector (recommended)

[5] In Monte Carlo simulation of radiation transport, the history (track) of a particle is viewed as a random sequence of free flights that end with an interaction event where the particle changes its direction of movement, loses energy and, occasionally, produces secondary particles.

IMAGE DETECTOR SECTION

The detector plane is automatically located at the specified distance right in front of the source focal spot, with the collimated cone beam pointing towards the geometric centre of the detector.

LINE	NAME	EXAMPLE	DESCRIPTION
1	Output image file name	mc-gpu_image.dat	Name of the .dat and .raw output files
2	Number of pixels in the detector image	120.0 120.0	Number of pixels in X and Z direction of the detector image
3	Detector image size	120.0 120.0	Width (x-axis) and height (z-axis) in centimetres of the detector image
4	Source-to-detector distance	100.0	Perpendicular distance from point source to detector centre

Note: in order to obtain a good detector image is recommended use a value for number of pixels multiple of the detector image features.

CT SCAN TRAJECTORY SECTION

MC-GPU simulates a single projection image or a full CT scan. The CT is simulated generating many projection images around the static voxelized geometry. The code is limited to perform a simple CT trajectory rotating around the Z axis.

LINE	NAME	EXAMPLE	DESCRIPTION
1	Number of projections	2	Beam must be perpendicular to Z axis and detector. Set to 1 for a single projection
2	Angle between projections	45.0	Angle in degrees between the different projections required. For full CT, 360/n_projections
3	Angles of interest	0.0 3600.0	Projections outside the input interval will be skipped The recommend values are shown
4	Source-to-rotation axis distance	60.0	The rotation radius around the Z axis
5	Vertical translation between projections	0.0	This is use to obtain a helical scan

Note: the results are given separately and jointly

DOSE DEPOSITION SECTION[6]

The tally[7] cards are used to specify what type of information the user wants to gain from the Monte Carlo calculation. This information is requested by the user by using a combination of the following cards. For each answer the fractional standard deviation, relative error, is provided.

LINE	NAME	EXAMPLE	DESCRIPTION
1	Tally material dose	YES	X-ray locally deposited at interaction Options: YES / NO
2	Tally 3D voxel dose	YES	Dose measured separately for each voxel. Options: YES / NO
3	Output voxel dose file name	mc-gpu_dose.dat	Name of the .dat and .raw output files
4	VOXEL DOSE ROI: X-index	1 3	Range in X axis of ROI Xmin Xmax
5	VOXEL DOSE ROI: Y-index	1 1	Range in Y axis of ROI Ymin Ymax
6	VOXEL DOSE ROI: Z-index	1 2	Range in X axis of ROI Zmin Zmax

VOXELIZED GEOMETRY SECTION

In this section the voxelized geometry to simulate is included, there are two different ways of introduce it:

- The name of the file if it is in the same directory of the input
- The name of the path to the file

MATERIAL FILES LIST SECTION

In this section the material files are included, there are two different ways of introduce them:

- The name of the files if they are in the same directory of the input
- The name of the path to the files

Each material must be listed in the adequate position to correspond with the ID number of the material in the voxelized geometry. All must have the same number of bins.

[6] ROI: Region Of Interest
[7] MCNPX User's Manual

OTHER INPUT FILES

The input files explained below are need to run a simulation. They may be in the same directory or in a different one. In this section the files and the way to obtain them are explained.

SPECTRUM FILE

The extension of this spectrum file must be .spc

This file may be generated with a specified program to generate x rays, some advices about XCOMP5R[8] use are explained in this manual, or with a text editor.

Each entry in the spectrum contains two columns, namely, the starting energy[9] (eV) of a channel and its probability, which does not need to be normalized to unity. The list ends whenever a negative probability is found.

Example of 90 keV monoenergetic beam:

# Energy [eV]	Probability
90000.0	1
90000.0	-1

XCOMP5R is a code with which the X-ray spectrum can be calculated for different potentials (20 – 150 kVp), angles of anode (0 – 45 degrees) and focus distances (0 – 1000 cm). Additionally, eight materials may be included as added filtrations of different thicknesses. In addition, the code calculates flux, kerma air, mean energy and HVL.

This code calculates X-ray bremsstrahlung spectra including characteristic K and L fluorescence radiation of tungsten anodes. It can compute 5 x-ray spectra simultaneously (the results of all spectra will be in the same file).

Once the input data is introduced, the program shows the spectra and the information for each input. Printing and saving of the data on a file (ASCII) can be invoked after leaving the graphic screen.

The file obtained needs to change its extension to .spc. Moreover, all information provided at the beginning of the file must be written as a comment (typing a '#' at the beginning of each line as the previous example shows) and at the end of the file a negative value is need. The probabilities do not need to be normalized to one but the energy must be in eV.[10]

Additionally to the main programs, a spectra library is provided in which some spectra used in IR[11] have been created. It is recommended to use them.

---

[8] This program requires a DOS operating system. The recommended DOS emulator is DOSBox (free).

[9] Energy range allowed: 5000 eV – 120000 eV

[10] To change the energies from keV to eV, the recommendation is to use MS Excel or a similar program.

[11] Medical diagnostic X-ray equipment - Radiation conditions for use in the determination of characteristics (IEC 61267:2005)

VOXEL GEOMETRY FILE

The static voxelized geometry file extension must be .vox (penEasy 2008 format), which is a plain text file, but also its compressed form .gz is accepted.

A voxelized geometry is a geometry model in which the object to be simulated is described in terms of a collection of small volume elements. Each voxel is a rectangular prism with a homogeneous material composition. The smaller the voxels, the more accurate the results.

Voxels are assumed to have their sides parallel to the axis of the Cartesian reference frame used for the simulation. The voxels bounding box, the imaginary rectangular box that delimits the set of defined voxels, is implicitly assumed to lie in the first octant of S, that is, in the region {x>0, y>0, z>0}. The voxel with indices (i, j, k) = (1,1,1) has one of its corners at the origin of S. Thus, the coordinates of the centre of each voxel can be inferred from its indices (i, j, k) and the length of the sides.

The voxels are listed with the X index changing first, then the Y index and the Z index last. Blank lines are inserted to separate each X column for different Y, and double blanks to separate XY blocks.

Example of penEasy 2008 voxel geometry file:

```
#
[SECTION VOXELS HEADER v.2008]
3       1       2       NUMBER OF VOXELS IN X, Y, Z
10.0    10.0    15.0    VOXEL SIZE (cm) ALONG X, Y, Z
1                       COLUMN NUMBER WHERE MATERIAL ID IS LOCATED
2                       COLUMN NUMBER WHERE MASS DENSITY IS LOCATED
1                       BLANK LINES AT END OF X, Y-CYCLES (1=YES, 0=NO)
[END OF VXH SECTION]
1 1.50
2 1.50
3 1.50


1 0.50
2 0.50
3 0.50
# END FILE
```

These voxelized geometries may be created with a text editor but it is recommended to use the already detailed and tested ones: Virtual Family[12] and Zubal phantoms[13].

[12] https://www.itis.ethz.ch/virtual-population/virtual-population/vip2/
[13] http://noodle.med.yale.edu/zubal/data.htm

MATERIAL FILES

The material files extension must be .mcgpu, but also the compressed form .gz is accepted. The format of this material files is specific for this program. The material files in this format must be generated with **MC-GPU_create_material_data_2018.x**. In case of using this executable, the materials' data must be .mat format (PENELOPE 2014). Otherwise, the use of the current material files library is recommended.

In this library in which the materials files are, there are also some materials with .mat extension (PENELOPE 2014). If the material required for a simulation is not in this directory, the material will need to be generated with material.exe (PENELOPE 2014) and later convert to .mcgpu with the executable provided. Material.exe of PENELOPE 2014 requires the atomic composition of the materials[14].

Considerations before using the executable: 25005 energy bins as maximum, 5 eV recommended energy steps and when entering the data[15] on screen:

$$\Delta E = \frac{\left(E_{max}^{desired} + \Delta E\right) - E_{min}}{N_{bins}} \qquad E_{max}^{entered} = E_{max}^{requiered} + \Delta E$$

PROGRAM EXECUTION

Initialization

Once the code is compiled, the executable **MC-GPU_v1.3.x** is obtained.

In order to launch a simulation, as shown in the general scheme, few files are need:

- Spectrum file (.spc)
- Voxelized geometry file (.vox)
- Material files (.mcgpu)
- Input file (filename.in)

It is recommended to have all the files in the same directory except the material files.

Launching steps

1. Open the command window
2. Change the directory to the one which have all the files
3. Execute the following command to run the simulation and keep the information reported to the standard output in an external file:

   ./MC-GPU_v1.3.x filename.in | tee filename.out

4. Once the simulation finishes, check few new files appeared in the same directory:
   - Main output file (filename.out)
   - Text files (.dat)
   - Image files (.raw)

[14] The ICRP 110 contains many human organs and tissues with its compositions.

[15] The desired maximum energy will be the last value of energy in the material file and the entered maximum energy is value must be entering on screen.

OUTPUT FILES AND POST PROCESSED

MAIN OUTPUT FILE

This main output file (filename.out) is a text file and it collects all the information of the simulation and it may be divided in two parts.

Most of results are referred per history (x-ray emitted), these values are not normalized but this is not important to compare different simulations.

On the one hand, INITIALIZATION, the result of reading the input files and initialization of the GPUs. On the other hand, MONTE CARLO LOOP: the results of the entire simulation, those are the Dose Tally Reports of the ROI and TOTAL described for each material specified. At the end of this file the total simulation performance is shown. In case of ROI covers all the voxels, the results are the same for both tallies. The two sections are explained below:

VOXEL ROI DOSE TALLY REPORT

- Total energy absorbed inside the dose deposition ROI [keV/history]
- Maximum voxel dose (± 2sigma) [eV/g·hist]
  - Energy deposited in the voxel [eV/hist]
  - Material ID
  - Density [g/cm^3]
  - Voxel mass [g]
  - Voxel coordinates in the reference system
- Table of dose deposited in the different materials inside the input ROI
  - Material ID
  - Dose [eV/g·hist]
  - Twice the standard deviation
  - Relative error
  - Energy deposited [eV/hist]
  - Mass [g]
  - Number of voxels

MATERIALS TOTAL DOSE TALLY REPORT

- Table of dose deposited in each material defined in the input file
  - Material ID
  - Dose [eV/g·hist]
  - Twice the standard deviation
  - Relative error
  - Energy deposited [eV/hist]
  - Mass [g]
  - Number of voxels

Note: Standard deviation is a measure used to quantify the amount of variation or dispersion of a set of data values. A low standard deviation indicates that the data points tend to be close to the mean (expected value) of the set, high accuracy of simulation.

TEXT OUTPUT FILES

The text files obtained after the simulation are separated on the image detector group and the dose group.

Note: The gnuplot's scripts mentioned in this section are only useful if the name of the file is the default, in case of modification in the input file, the gnuplot script must be also modified.

IMAGE DETECTOR TEXT FILES

These files are named **mc-gpu_image.dat_0000** or whatever name the user gave them in the input file. Each number corresponds to the different CT projections.

In order to read all the data obtained, a text editor has to be used. In case of opening the file in this way the features of the projection are shown at the top.

This image is created counting the energy arrived at each pixel of the ideal energy integrating detector. The dimensions of this image are given in the input file.

The text file is organized in four columns: Non-scattered, Compton, Rayleigh and Multi-scattered fluences (eV/cm^2·hist) in each pixel of the image detector.

The format of this file is the same explained for voxelized geometry files: X rows given first, then Y. One blank line separates the different Y.

All particles' fluence values in each pixel at this image detector may be visualized in some figures using the gnuplot script **gnuplot_images_MC-GPU_CT.**

In case of one CT projection is selected, the gnuplot script **gnuplot_images_MC-GPU** shows six different images, corresponding to the signal produced by all particles, x rays that did not interact between the source and the detector (non-scattered), all scattered particles, x rays that suffered a single Compton (inelastic) interaction, a single Rayleigh (elastic) interaction, and multi-scattered x rays.

DOSE TEXT FILE

This file is named **mc-gpu_dose.dat** or whatever name the user gave it in the input file. In order to read the data obtained, a text editor has to be used.

To reduce the memory use and the reporting time this text output reports only the 2D dose (eV/g·hist) and its uncertainty at the Z plane at the level of the source focal spot.

The total dose deposited in each different material is reported to the standard output.

The format of this file is the same explained for voxelized geometry files: X rows given first, then Y, then Z. One blank line separates the different Y, and two blanks the Z values.

Dose values in each voxel at this specific Z plane may be visualized in a figure using the gnuplot script **gnuplot_dose_MC-GPU.**

IMAGE OUTPUT FILES

At the end of the simulation the code reports the tallied 3D dose distribution and the final simulated images in RAW binary form, as 32-bits float values.

The ASCII output mentioned above provide the information required to easily read the RAW binary files with IMAGEJ.

IMAGE DETECTOR RAW FILE

In this section how to open the image raw file with IMAGEJ is explained. The default name of this file is **mc-gpu_image.dat.raw** and it is supposed to be in the same directory of the inputs.

First of all, opening the mc-gpu_image.dat with a text editor the dimensions of the image detector may be read where “Number of pixels in X and Z” is located (see the example).

Example:

Pixel size: 0.333333 x 0.333333 = 0.111111 cm^2

Number of pixels in X and Z: **120** **120**

Then in the IMAGEJ, the file has to be imported *File* > *Import* > *Raw…* and the dimensions of the images must be introduced manually as the figure shows.

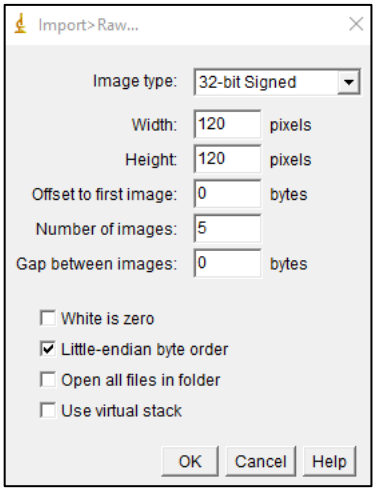

Features:

Image type must be 32-bit signed type.

Width corresponds with the X-axis number of pixels.

Height corresponds with the Z-axis number of pixels.

Number of images corresponds with **5**.

In this way the IMAGEJ shows a collection of five consecutive images corresponding to: total image (scatter + primaries), primary particles, Compton, Rayleigh and multi-scatter.

To visualize these figures in a clearly way a different colour intensity scale may be selected *Image* > *Lookup tables…*

DOSE RAW FILE

In this section how to open the dose raw file with IMAGEJ is explained. The default name of this file is **mc-gpu_dose.dat.raw** and it is supposed to be in the same directory of the inputs.

First of all, opening the mc-gpu_dose.dat with a text editor, the dimensions of the ROI may be read in “the number of voxels in the reported region of interest (ROI)”.

Example:

Voxel size: 5.000000 x 0.500000 x 5.000000 = 12.499999 cm^3

Number of voxels in the reported region of interest (ROI) X, Y and Z:

6 40 6

Coordinates of the ROI inside the voxel volume = X [1,6], Y [1,40], Z [1,6]

Then in the IMAGEJ, the file has to be imported *File* > *Import* > *Raw…* and the dimensions of the images must be introduced manually as the figure shows.

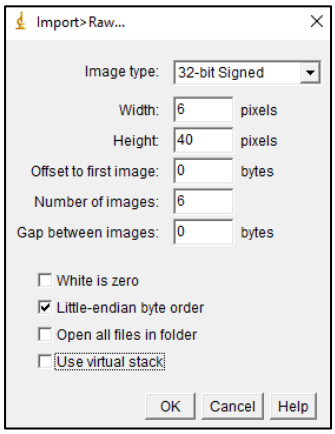

Features:

Image type must be 32-bit signed type.

Width pixels corresponds with the X-axis number of voxels.

Height pixels corresponds with the Y-axis number of voxels.

Number of images corresponds with the Z-axis number of voxels.

IMAGEJ shows a succession of slides along the Z-axis. To visualize the dose in all the voxelized volume, once the image has been imported *Plugins* > *3D* > *Volume viewer.*

OTHER METHODS

These raw files are prepared to open with image visualizer but they also contain the numerical values of doses in each voxel. In this sections three ways to obtain them are explained.

1. A Matlab script called Read Medical Data 3D is able to open these raw files to obtain all the internal information.
2. A Matlab script written in the INTE and provided with the rest of directories. This scripts requires basic information about the voxelized geometry and the files of dose and its sigma in raw format. The problem of this script is that runs slow when the data volume is too much large. It is called **Open_raw.m**
3. IMAGEJ has many useful functions to get information from a raw file, a detailed explanation of how to use of this program is following:

In this section how to obtain the most information about the dose received by the phantom is explained.

First of all, all information of the voxelized geometry must be obtained from the main output file and then use this information to import the dose raw file as it has been explained in previous sections.

Once the raw file has been properly opened, the program shows a Z slide. If the play bottom is press, a succession of slides along the Z-axis are shown.

The colour of each voxels means the dose received by them, to have a better visualization: *Image* > *Lookup Tables* and choose one of them, the most common use is Fire.

At this point the Orthogonal Views may be obtained: *Image* > *Stacks* > *Orthogonal Views.* To change the planes XZ and YZ just click in the XY plane. Also pressing the play bottom, the succession of slides is shown.

To have a three dimensions' idea of the dose received by the voxelized geometry, the plugin may be use: *Plugins* > *3D* > *Volume viewer.* A new window called Volume Viewer is opened and on it the featured may be changed to obtain e better visualization.

On the other hand, to obtain the values of dose in each voxel, instead of opening the Volume Viewer, from the initial stage there are different ways:

1. Once the desired Z slide is selected in the "play bar", *Image* > *Transform* > *Image to Results.* The result is a dose values matrix of each voxel in the selected Z slice. To change the Z slice just close this new window and repeat the process. The values may be saved.
2. Placing the mouse pointer in any voxel the dose and coordinates of the voxel appear in the program main bar.
3. Doing *Image* > *Stacks* > *Plot Z-axis Profile* the mean dose for each Z slice is obtained. And *Image* > *Stacks* > *Statistics* provides the mean, minimum and maximum dose of the whole voxelized geometry.
4. To get rapidly the mean, maximum and minimum dose of a slice, select the slice and *Analyze* > *Measure.* To get more information *Analyze* > *Set Measurements…* and repeat the process.

IMAGEJ this program has many more functions and ways to get the data, to know more about it, it is recommended to read its user guide [16].

[16] https://imagej.nih.gov/ij/docs/guide/index.html

MC-GPU BETA VERSION

MC-GPU BETA DESCRIPTION

This code is an extension of the previous explained code. At this moment, this beta version is not completely validated. Although the main code is the same, few features have been added:

- The inclusion of the operator. In these new simulations a single operator may be added identifying the position of his/her shoulders, head and hip. This simulated operator has his/her own reference system as the figure shows.
- Also, the shield to protect the operator may be simulated.
- This version includes the possibility of run a set of simulations in which the position of the operator, the position of the source (around two axis), the source and the shield change.
- The characterization of the source is more detailed in terms of position and inclination.
- The possibility of use a conversion factor eV/hist to Gray is included.

Note 1: It is important to know and understand the position of axis in both references.

Note 2: The patient reference system (orange) is the same used in the basic MC-GPU code, this is why it is considered the global thus the operator reference system (blue) is just local for him/her and the shield. The coordinates origins are the left heels.

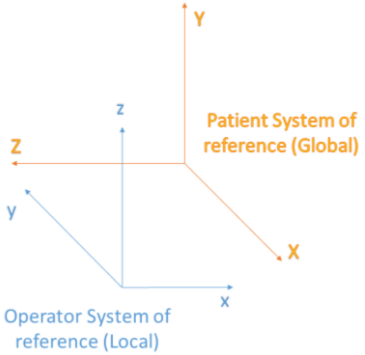

Figure 11: Reference systems

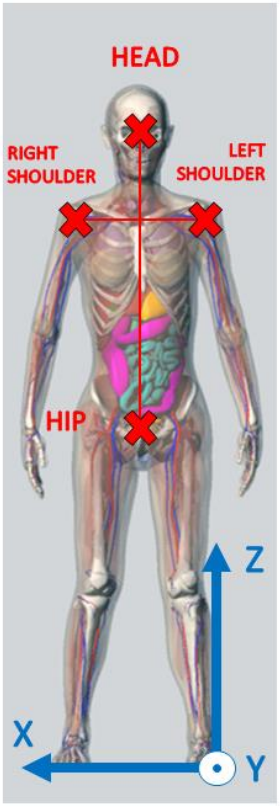

All the environment is generated at the initialization phase and it is referred to the global reference system (patient). The patient may be assumed immobile during the procedure but the position of his/her left heel is need to know.

The operator is located in the work environment with respect to patient axis by these reference points:

- X coordinate: left-right
- Y coordinate: posterior-anterior
- Z coordinate: caudal-cranial

The programme identifies if the operator is facing de patient by the left or right side depending on the shoulders distances to the global coordinates origin.

Figure 12: Operator reference points and axis

For a better visualization, the figure shows both reference systems in a real cardiovascular X-ray system

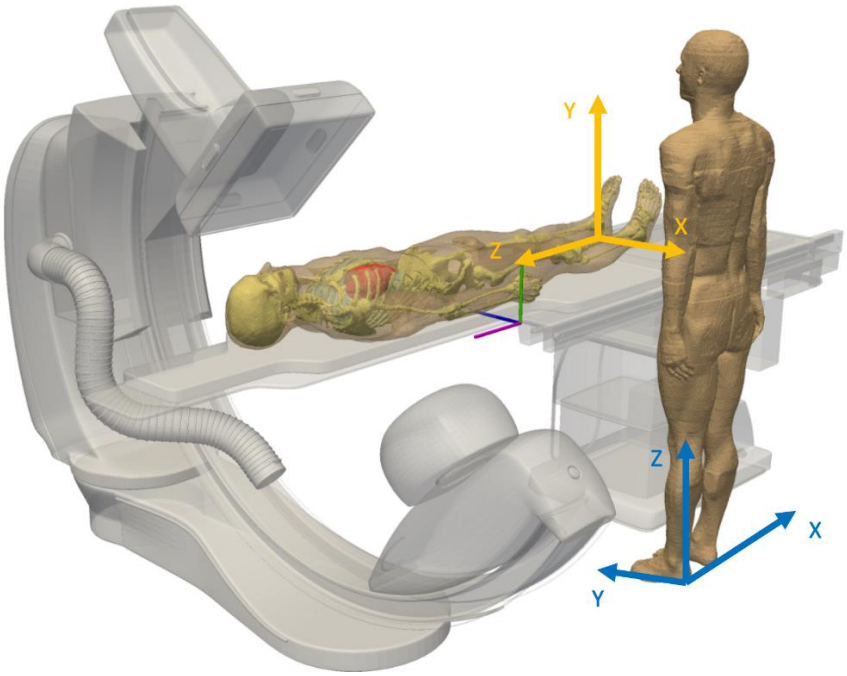

Figure 13: Patient and Operator reference systems in a real X-ray system

PRE-SIMULATION INFORMATION

MC-GPU Beta has been developed and tested only in the Linux operating system. A Makefile script is provided to compile the MC-GPU Beta code in Linux. The CUDA libraries and the GNU GCC compiler must be previously installed.

All information need to code compilation and the executables obtained are explained in **readme_MCGPU_virtual_dosimeter__BETA_2014-12-22.txt**

In this manual the use of the program without the Kinect camera is explained, the executables need are the following:

- **MCGPU_virtual_dosimeter__BETA_2014-12-22.x** Main simulation program. Waits for LCM messages from the source and the operator tracking modules.
- **trigger_operator_and_source_command_line.x** Command line utility to replace both the operator tracking and the source trigger for non-real time use and validation studies. All data is given in the corresponding input file.

GENERAL SCHEME

The scheme shown below gives a general view of the necessary files to run a simulation as well as the process to follow during the simulation.

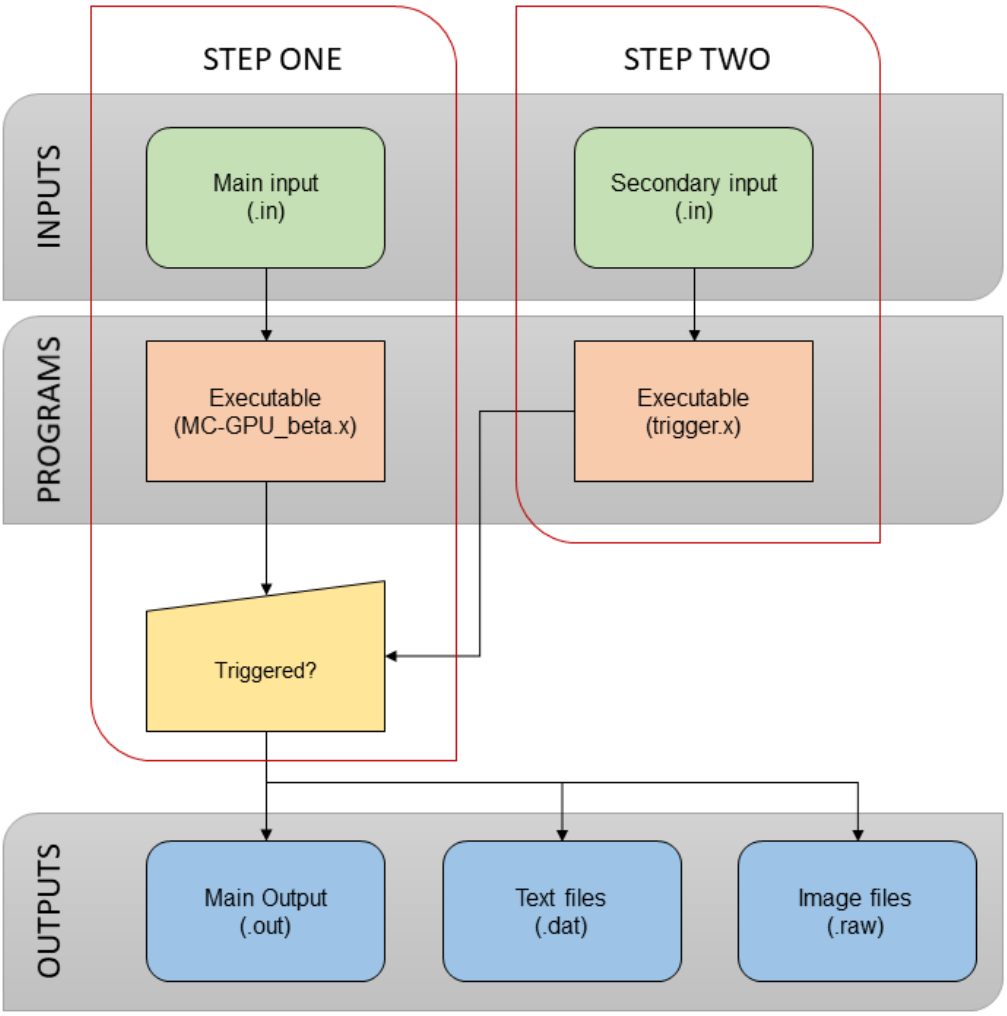

Figure 14: MC-GPU_Beta general scheme

It is recommended to have all the inputs (spectrum, geometry, materials and main and secondary input files) and the executables in the same directory. In addition, the creation of a directory for each simulation is recommended.

In contrast to the other program, to run a simulation in this new one two steps are necessary.

INPUT FILES

In this program the spectrum, material and voxelized geometry files are also needed although they do not appear in the scheme to simplify it.

MAIN INPUT FILE

The main input file is called **source.in**.

This main input file is similar to the mentioned for MC-GPU. It needs a spectrum, material and voxelized geometry files. This new main input file just has an additional section before the voxelized geometry file section.

A main difference in the input file is the use of seconds as regulator of the simulation, the simulation time in seconds value is included in the first line of SIMULATION CONFIGURATION SECTION.

SECTION OPERATOR DOSE

LINE	NAME	EXAMPLE	DESCRIPTION
1	Patient Voxels Scaling Factors	1.0 1.0 1.0	Scaling factor for the patient voxelized geometry for the axis X, Y and Z
2	Operator Voxels Scaling Factors	1.0 1.0 1.0	Scaling factor for the operator voxelized geometry for the axis X, Y and Z
3	Maximum number elements PSF[17]	65.0E6	Select depending on number of histories and available GPU memory

This section is important because the program set the voxelized geometry for both patient and operator, this is why the scaling factors are important in the most probable case of they have different dimensions.

The maximum number elements PSF is important because it will be the source term of the operator calculations. The larger this value, the longer the simulation but also more accurate.

[17] The state of all particles entering the specified DETECTION MATERIAL is written to the file indicated in the PSF field. More precisely, the variables written are, in the quoted order, kpar, e, x, y, z, u, v, w, wght, dn, ilb(1), ilb(2), ilb(3), ilb(4) and ilb(5).

SECONDARY INPUT FILE

The secondary input file is called **operator.in**.

This input file is completely new of this program. It is composed by three sections block which may be repeated as many times as desired simulations. The three sections of each block are explained below.

OPERATOR DATA SECTION

The four points needed to refer to the operator are very important. From these values the program creates a virtual cross to position the worker. All the Cartesian coordinates (x,y,z) introduced in this section must be in the **patient reference system.**

LINE	NAME	EXAMPLE	DESCRIPTION
1	Head	100.0 71.2 93.3	Operator head.
2	Left Shoulder	100.0 31.2 113.3	Operator left shoulder
3	Right Shoulder	100.0 31.2 73.3	Operator right shoulder
4	Hip	100.0 0.0 93.3	Operator hip

SOURCE DATA SECTION

This section allows the user to determine the position of the source (in the global reference system) and its energy spectrum as in the main input file. It additionally includes the possibility of rotate the source around the Z (craneo-caudal) and X (lateral) axis.[18]

LINE	NAME	EXAMPLE	DESCRIPTION
1	Source position	25.6 -30.0 48.6	Cartesian coordinates in centimetres of source position origin
2	Source aperture	-45.0 -45.0	Angles in degrees that determine the aperture of the pyramid. Input negative to automatically cover the whole detector (recommended)
3	C-arm radius	30	Distance in centimetres from source origin to rotation axis.
4	Source rotations	20.0 20.0	Angle in degrees around X and Z axis from the original position.[19]
5	Conversion factor	1	Conversion factor $\frac{eV}{hist} \rightarrow Gy$
6	Energy spectrum	90kVp_4.0mmAl.spc	Name of the spectrum file

[18] These rotation angles are referred to the patient reference system.
[19] The sign of the rotation angles is positive following the right-hand rule.

SHIELD SECTION

The use of shielding to protect the workers against scattered X-rays is an operator decision even its use is recommended. In interventional radiology there are two types of shielding: the sheet shield (for legs) and the ceiling shield (for upper parts).

In this section the characteristics of the shield may be included. All the coordinates and angles are referred to **operator reference system.**

LINE	NAME	EXAMPLE	DESCRIPTION
1	Rotation	0 0 0	Euler angles Rx, Ry, Rz in degrees.
2	Translation	0 0 0	Cartesian coordinates in centimetres from operator origin.
3	Dimensions	0 0 0	Width (along x axis) in cm Thickness (along y axis) in cm Height (along z axis) in cm Input 0 thickness to remove shield
4	Attenuation coefficient at mean energy [20]	0	Attenuation coefficient at mean energy [1/cm]. This is to determine the material of the shielding.

The previous example shows how the shield may be eliminated of the simulation.

Note: the most extended shielding material is lead.

PROGRAM EXECUTION

The MC-GPU Beta program is thought to simulate a complete medical intervention. Usually in this kind of intervention a large number of different position of source, energy spectrum and time take place.

For this reason, MC-GPU Beta is able to simulate the different steps in a real medical intervention characterizing them in block in the secondary input file.

The execution is sequential, this means that once the simulation for patient is done, the PSF generated is used to operator simulation. This sequence is run as many times as blocks in the secondary main. Due to divers factors influence in the conversion factor, each one has its own.

After the entire simulation the results of dose for patient and worker are expected.

As mentioned before, the execution of this program has two parts described following:

[20] Values may be found at https://www.nist.gov/pml/x-ray-mass-attenuation-coefficients

STEP ONE

Initialization

In order to launch a simulation, few files are need:

- Spectrum file (.spc)
- Voxelized geometry file (.vox)
- Material files (.mcgpu)
- Main Input file (initialinput.in)
- **MCGPU_virtual_dosimeter__BETA_2014-12-22.x**

It is recommended to have all the files in the same directory except the material files.

Launching steps

1. Open a command window
2. Change the directory to the one which have all the files
3. Execute the following command to run the simulation and keep the information reported to the standard output in an external file:

   ./MCGPU_virtual_dosimeter__BETA_2014-12-22.x initialinput.in | tee filename.out

4. Program waits for LCM messages from the source and the operator tracking modules. (Go to step two).

STEP TWO

Initialization

In order to launch a simulation, few files are need:

- Spectrum files (.spc)
- Secondary Input file (secondaryinput.in)
- **trigger_operator_and_source_command_line.x**

It is recommended to have all the files in the same directory except the material files.

Launching steps

1. Open a new command window (do not close the previous)
2. Change the directory to the one which have all the files
3. Execute the following command:

   ./trigger_operator_and_source_command_line.x secondaryinput.in

Once the simulations finish, check few new files appeared in the same directory:

- Output file (filename.out)
- Text files (.dat) for both operator and patient
- Image files (.raw and .dat) for both operator and patient

OUTPUT FILES

The files resulted of the simulations may be classified in different ways. In this section all outputs are described briefly so that it is recommended read the output section for MC-GPU where the explanations are more detailed.

MAIN OUTPUT FILE

This main output file (**filename.out**) is a text file and it collects all the information of the simulation and it may be divided in few parts. This file is unique for patient and operator.

1. First part of the text file shows the results of the initialization.
2. Second part reports the results of the different simulations; these reports are repeated as many times as simulations (blocks in the secondary input file).
    - Patient Report
        - Voxel ROI dose tally report
        - Materials total dose tally report
    - Operator Report
        - Voxel ROI dose tally report
        - Materials total dose tally report
3. Third part: these two finals reports only appear once, in them the averaged results are shown.
    - Final Report: Average Patient Voxel Dose
    - Final Report: Average Operator Voxel Dose

All the results are organized in tables, which are explained in the MC-GPU outputs section.

Note: In the third part the column of energy deposition is the average of all the energy deposited in all the different projection and the dose is the result of divide these average energies and the mass of each material.

TEXT OUTPUT FILES

All files included in this section have an extension .dat that is a plain text extension. To read this kind of files, a text editor is need. The files obtained after the simulation are separated for patient and for operator.

IMAGE DETECTOR TEXT FILES

The files **mc-gpu_image.dat** and **mc-gpu_image.dat_operator** are images created counting the energy arriving at each pixel: ideal energy integrating detector. The values in the tables may be read opening the files with a text editor. Otherwise, to visualize the images the recommendation is to use the provided gnuplot script gnuplot_images_MC-GPU_patient-operator.

DOSE TEXT FILES

The doses in each voxel are in the **mc-gpu_dose.dat_TOTAL** (patient) and mc-**gpu_dose.dat_operator_TOTAL** (operator) files. To reduce the memory use and the reporting time these text outputs report only the 2D dose at the Z plane at the level of the source focal spot. The files with similar names give the voxel dose for each simulation

The most important files except the main output file are named **dose_deposited_ROI_patient.dat** and **dose_deposited_ROI_operator.dat**. These text files have a table in which each line below reports the material doses for a different irradiation event, computed adding the energy deposited in every voxel inside the input ROI. Also the average energy deposition for each event and the scaling factors are shown. In them, how to visualize the files in GNUPLOT is described.[21]

IMAGE OUTPUT FILES

At the end of the simulation the code reports the tallied 3D dose distribution and the final simulated images in RAW binary form, as 32-bits float values. To visualize this kind of files IMAGEJ is recommended. The files obtained after the simulation are separated for patient and for operator.

The ASCII output mentioned above provide the information required to easily read the RAW binary files with IMAGEJ.

IMAGE DETECTOR RAW FILES

The files **mc-gpu_image.dat_0001.raw** and **mc-gpu_image.dat_operator_0001.raw** are images created counting the energy arriving at each pixel: ideal energy integrating detector. To visualize the images, the recommendation is to use of IMAGEJ (the use of this programs has already been explained).

DOSE RAW FILES

The 3D dose deposition is reported in binary form in the .raw files **mc-gpu_dose.dat_TOTAL.raw** and **mc-gpu_dose.dat_operator_TOTAL.raw.** To visualize the images, the recommendation is to use of IMAGEJ (the use of this programs has already been explained).

Note: Depending on the type of simulation, the name and number of the resulting files are different. This is why the gnuplot directory has many gnuplot scripts to view the outputs. The recommendation is to open these scripts with a text editor to understand what they are and if it was necessary, change them.

[21] The averaged values are referenced with the material 999. It is important to know that the total average dose is not a physical magnitude because is computed as the quotient between the sum energy deposited and the total mass of the phantom.